UNCLASSIFIED

AD 249 386

Reproduced
by the
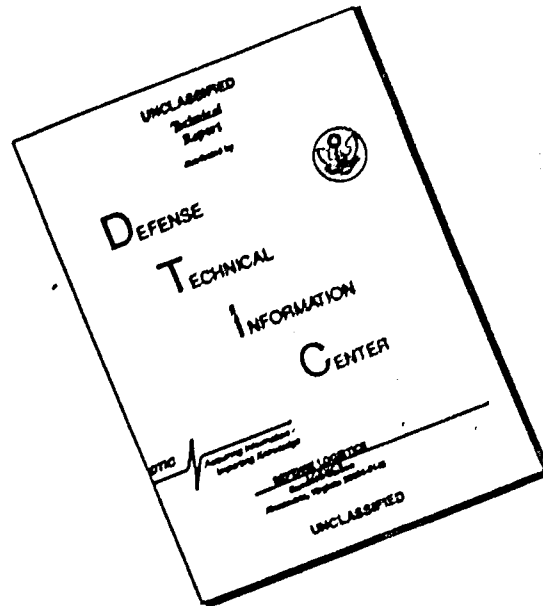
ARMED SERVICES TECHNICAL INFORMATION AGENCY
ARLINGTON HALL STATION
ARLINGTON 12, VIRGINIA

DISCLAIMER NOTICE

UNCLASSIFIED
Technical
Report

DEFENSE

TECHNICAL

INFORMATION

CENTER

UNCLASSIFIED

THIS DOCUMENT IS BEST QUALITY AVAILABLE. THE COPY FURNISHED TO DTIC CONTAINED A SIGNIFICANT NUMBER OF PAGES WHICH DO NOT REPRODUCE LEGIBLY.

A SYSTEMS ANALYSIS VIEW OF LONGITUDINAL FLYING QUALITIES

Duane T. McRuer

Irving L. Ashkenas

C. L. Guerre

Systems Technology, Inc.

JANUARY 1960

WRIGHT AIR DEVELOPMENT DIVISION

A SYSTEMS ANALYSIS VIEW OF LONGITUDINAL FLYING QUALITIES

Duane T. McRuer
Irving L. Ashkenas
C. L. Guerre

Systems Technology, Inc.

JANUARY 1960

WRIGHT AIR DEVELOPMENT DIVISION
AIR RESEARCH AND DEVELOPMENT COMMAND
UNITED STATES AIR FORCE
WRIGHT-PATTERSON AIR FORCE BASE, OHIO

ABSTRACT

The application of servo analysis methods to the study of handling qualities problems provides a unifying framework for requirements which hitherto were apparently diverse and unrelated. The technique is also effective in delineating possible difficulties, and solutions thereto, for the as yet experimentally unexplored regions associated with modern and future vehicles and environments. The research reported is a study of longitudinal handling qualities, in this servo context, which makes substantial progress toward evolving an analytic method for specifying handling qualities requirements. Criteria and procedures are established for estimating both pilot dynamic behavior and opinion. Vehicle-pilot system studies utilizing this pilot model predict the influence of variations in the magnitude and/or the relative location of the poles and zeros in the vehicle transfer function. Where experimental observations on such influences exist, they appear to be reasonably consistent with the analytical predictions. Where they do not, the predictions identify new parameters of possible significance and serve as an interim basis for design and a guide to future testing.

PUBLICATION REVIEW

This report has been reviewed and is approved.

FOR THE COMMANDER:

C. B. WESTBROOK
Chief, Aero-Space Mechanics Branch
Flight Control Laboratory

TABLE OF CONTENTS

LIST OF TABLES

a_z Normal acceleration at the center of gravity

A Amplitude ratio (db)

A_h Numerator polynomial coefficient in complete vertical acceleration transfer function

A_θ Numerator polynomial coefficient in complete pitch angle transfer function

A_θ' Numerator polynomial coefficient in long period pitch rate transfer function

A_u' Numerator polynomial coefficient in long period velocity transfer function

$A_{z\delta}$ Normal acceleration/elevator deflection transfer function

B_θ Numerator polynomial coefficient in complete pitch transfer function

c Mean aerodynamic chord; pilot's output

C_D Total drag coefficient, $\text{drag}/\frac{1}{2}\rho U_o^2 S$

C_{D_α} Drag coefficient variation with angle of attack, $\partial C_D/\partial \alpha$

C_{D_o} Profile drag coefficient

C_{D_u} Nondimensional variation of C_D with speed, $U_o \partial C_D/2\partial u$

C_L Lift coefficient, $nW/\frac{1}{2}\rho U_o^2 S$

C_{L_α} Lift-curve slope, $\partial C_L/\partial \alpha$

C_{L_δ} Control surface lift effectiveness, $\partial C_L/\partial \delta$

C_{L_u} Nondimensional variation of C_L with speed, $U_o \partial C_L/2\partial u$

C_M Pitching moment coefficient, $\text{pitching moment}/\frac{1}{2}\rho U_o^2 S c$

C_{M_α} Pitching moment coefficient variation with angle of attack, $\partial C_M/\partial \alpha$

C_{M_δ} Control surface pitch effectiveness, $\partial C_M/\partial \delta$

C_{M_q} Pitch damping coefficient, $\partial C_M/\partial(qc/2U_o)$

C_θ Numerator polynomial coefficient in complete pitch transfer function

db Decibel

F_s, F_p	Stick force
$\overline{F}_p$	Average stick force
g	Acceleration due to gravity
h	Altitude
I_y	Pitching moment of inertia
$i(t)$	Input (forcing function)
j	$\sqrt{-1}$
$j\omega$	Imaginary portion of the complex variable $\sigma + j\omega$
K_c	Controlled element gain
K_h	Gain of short period normal acceleration transfer function
K_p	Pilot gain
K_θ	Gain of short period pitch attitude transfer function
K_θ'	Gain of long period attitude transfer function
$K_{\theta_{sp}}$	Gain corresponding to short period breakpoint of θ_δ transfer function
K_u'	Gain of long period speed transfer function
m	Mass
M	Mach number; pitching acceleration due to externally applied torques
M_α	$U_o M_w$
$M_{\dot\alpha}$	$U_o M_{\dot w}$
M_δ	$\rho S U_o^2 c\ C_{M_\delta}/2I_y$
M_q	$\rho S U_o o^2\ C_{M_q}/4I_y$
M_u	$\rho S U_o c\ C_{M_u}/I_y$
M_w	$\rho S U_o c\ C_{M_\alpha}/2I_y$
$M_{\dot w}$	$\rho S o^2\ C_{M_{\dot\alpha}}/4I_y$
n	Vertical load factor
n_c	Pilot's output remnant

r	System output
s	Laplace transform variable, $\sigma + j\omega$
S	Wing area
T_{CL_1}, T_{CL_2}	Closed loop time constants
T_{h_1}, T_{h_2}, T_{h_3}	Normal acceleration transfer function numerator time constants
T_I	Pilot generated lag time constant
T_L	Pilot generated lead time constant
T_N	First order time constant approximating pilot's neuromuscular lags
T_{p_1}, T_{p_2}	Time constants associated with decoupled phugoid mode
T_{s_1}, T_{s_2}	Time constants associated with decoupled short period mode
T_{θ_1}, T_{θ_2}	Pitch attitude transfer function numerator time constants
T_{u_1}	Velocity transfer function numerator time constant
u	Linear perturbed velocity along the X-axis
U_o	Linear steady state velocity along the X-axis
U_δ	Airspeed/elevator deflection transfer function
W	Airplane weight
X_α	$U_o X_w$
X_u	$\rho S U_o (-C_D - C_{D_u})/m$
X_w	$\rho S U_o (C_L - C_{D_\alpha})/2m$
x_t	Distance from airplane c.g. to tailplane center of pressure
x_{ac}	Distance from airplane c.g. to aerodynamic center, measured positive forward
Y_c	Controlled element transfer function
Y_p	Pilot's linear describing function
Z_δ	$\rho S U_o^2 (-C_{L_\delta})/2m$
Z_u	$\rho S U_o (-C_L - C_{L_u})/m$
Z_w	$\rho S U_o (-C_{L_\alpha} - C_D)/2m$

α	Instantaneous angle of attack, w/U_o under no wind conditions
δ, δ_e	Control surface (elevator) angular deflection
ϵ	Error (pilot's stimulus)
ζ	Damping ratio
ζ_{CL}	Closed loop damping ratio
ζ_h	Damping ratio of second order numerator term in vertical acceleration transfer function
ζ_p	Damping ratio of phugoid oscillation
ζ_{sp}	Damping ratio of short period oscillation
θ	Pitch angle
θ_δ	Pitch attitude/elevator deflection transfer function
μ	Log ω
ρ	Mass density of air; linear correlation coefficient
σ	Real part of Laplace transform variable $\sigma + j\omega$
τ	Pilot's reaction time delay
φ	Phase angle
φ_M	Phase margin
ω_c	System gain crossover frequency
ω_{co}	Cutoff frequency
ω_{CL}	Closed loop undamped natural frequency
$\equiv$	Identically equal to
$\doteq$	Approximately equal to
$|\ |$	Magnitude, or absolute value
$\ll$	Much less than
∂	Partial derivative
$\angle$	Phase angle

INTRODUCTION

The work reported here was undertaken in furtherance of an Air Force program founded upon the premise that vehicle dynamic handling qualities depend to a large extent on the action of the pilot as a control element in the pilot-vehicle closed loop system. To this end, previous studies have concentrated on the development of an adequate mathematical description of the pilot's activities in such circumstances (References 1-4). The present investigation is part of a continuing effort to apply such mathematical models and to correlate the resulting closed loop system implications with present "conventional" handling qualities flight research data. The ultimate purpose is to derive a systems-oriented theory which will allow the prediction of vehicle handling qualities from a knowledge of the pilot's performance in the loop. Such a theory has long been desired because it would

1. Focus attention upon and explain the correlations which exist between subjective pilot opinion and performance factors of the airframe-pilot system.

2. Form a foundation for the insights required to determine airframe characteristics (and/or assess configuration changes) which offer possible improvement in flying qualities.

3. Provide a basis for deriving handling qualities criteria for configurations which have novel dynamic characteristics.

4. Provide a unifying structure for the large amount of dynamic data which have previously been treated as unconnected.

To a large extent, the present report provides such a structure for control aspects of the airframe longitudinal axis; Reference 5 performs a similar function for the lateral axis.

The development of dynamic handling quality requirements from servo analysis of pilot-airframe combinations presupposes the practical existence of a reasonably linear closed loop system which involves airframe, control system, and human components. Such a complete system, for longitudinal airframe control where the pilot uses elevator alone, is shown in Figure 1. This diagram depicts conventional stability augmenters, stick force producers, feedforwards, etc., as separate transfer blocks. Closing these inner loops allows the entire block of components within the bracket to be considered as an "equivalent airframe" which relates the motion quantities controlled by the pilot to his output. Figure 1 also shows airframe motions fed back to the "display" (which can range in complexity from a single instrument to the presented visual field) and airframe forces and moments fed back directly to the pilot.

Restriction of the present study to situations compatible with available human dynamic data immediately requires the neglect of all but visual inputs to the pilot. This compromise is not serious in tasks requiring only moderate deviations from straight and level flight. Reference 4, for example, shows

that the pilot describing function does not differ in form for fixed-base
(which, by definition, involve only visual inputs) or airborne tasks with
similar controlled element dynamics. The numerical values for the describing
function in the airborne condition do, however, exhibit an increased pilot
reaction time and a lowered gain relative to the fixed base tests. Reference 6,
using opinion as a measure, demonstrates that only slight differences exist
between rotating and fixed-base simulators. These and other experimental
findings lead to the conclusion that fixed-base data can be extrapolated, with
reasonable validity, to many flight situations.

Where large accelerations are involved, the results developed must be used
with somewhat more caution. In this regard, comparisons of performance meas-
ures between fixed-base and centrifuge simulators (Reference 7) indicate that,
up to a steady state level of about 2-1/2 g, the differences were significant
statistically but small practically. Acceleration tended to improve perform-
ance if it was an important cue in the simulated task (e.g., coordination),
and to degrade performance where the acceleration cues were distracting (e.g.,
in tracking). In any event, restriction of the present study to visual inputs
alone focuses attention upon the pilot and airframe systems shown in Figure 2.
It will be noted here that acceleration inputs can still be important although
they must be, in the present context, detected visually. The "display" can
still be considered to cover a wide variety of possible types, although its
form is restricted to be of a general compensatory nature (i.e., the signals
seen by the pilot are functions of an error, or difference between system input
and output).

The body of the report starts in Chapter II with a general review of the
status of the pilot as a dynamic element in a man-machine system. This status
report presents the mathematical model of the pilot in a general, literal form
and gives a set of general "rules" for the adjustment of the model's parameters.
The information summarized can be used to estimate pilot dynamic behavior in
a given control situation. This is followed, in Chapter III, by a detailed
discussion of experimental results on pilot describing function characteristics
obtained during the course of the fixed-base simulations of Reference 3. At
the outset these data are divided into two categories, one where overall closed
loop system dynamic performance is nearly constant (not a strong function of
the controlled element) and the other where the controlled element is so diffi-
cult that the closed loop is dominated by the system input. In the situations
where overall system dynamic performance is held nearly constant, interpreta-
tion of the data allows the subjective pilot opinion ratings to be correlated
with the dynamic performance factors (describing function parameters) used to
characterize the pilot's actions. As a consequence of these correlations
approximate predictions of opinion can be made on the basis of estimated pilot
dynamic behavior. Further, the general adjustment "rules" of Chapter II become
more specific.

With the framework established in Chapters II and III it is possible, given
a set of "controlled element" dynamics (display plus equivalent vehicle), to

    1. Make an estimate of the adopted pilot describing function.

    2. From the adopted describing function, and/or its closed
        loop system consequences, estimate the pilot opinion rela-
        tive to a particular "good" control situation.

FIGURE 1

COMPLETE LONGITUDINAL AIRCRAFT CONTROL SYSTEM
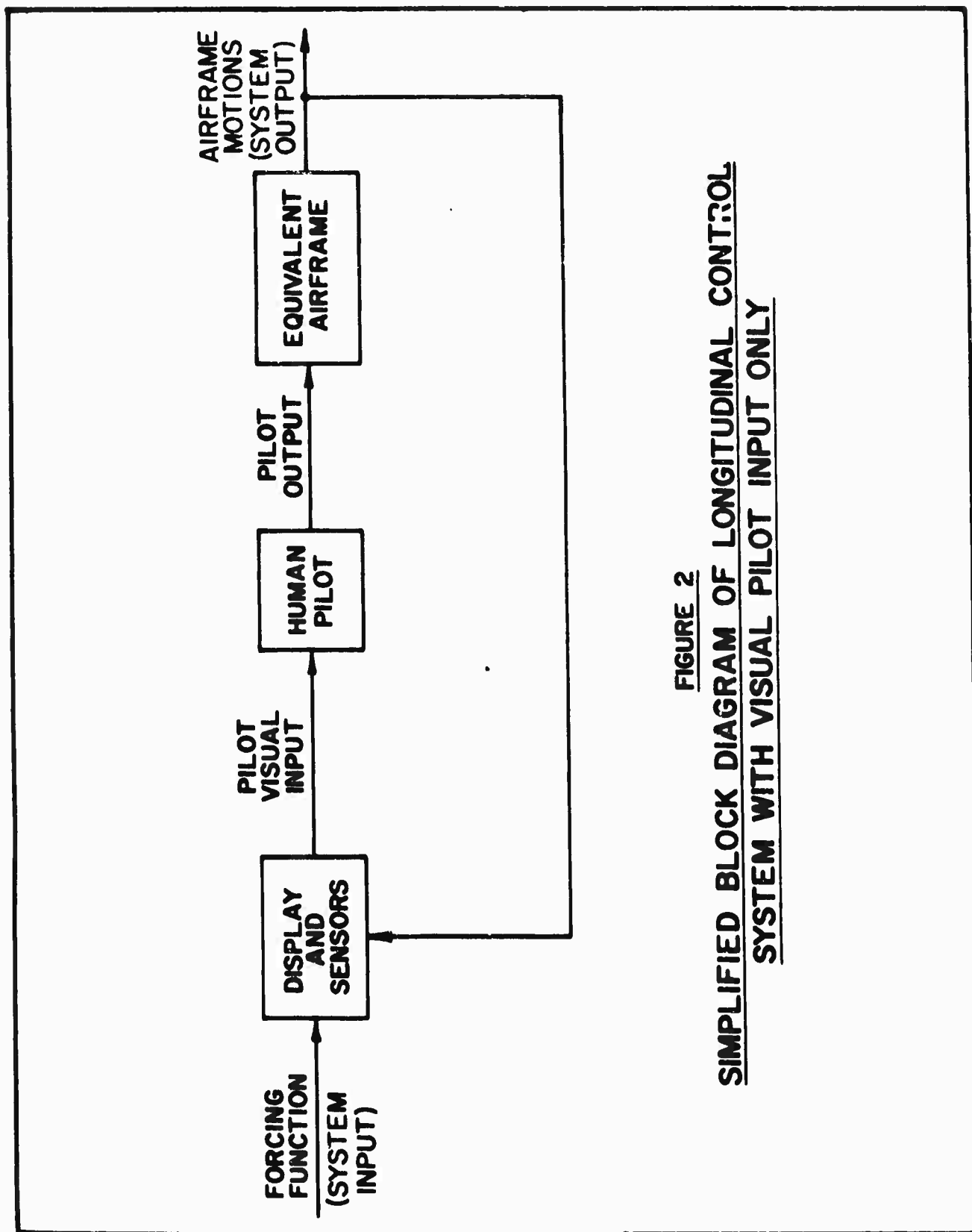
FIGURE 2

**SIMPLIFIED BLOCK DIAGRAM OF LONGITUDINAL CONTROL
SYSTEM WITH VISUAL PILOT INPUT ONLY**

This model of dynamics and opinion is applied in Chapter IV to the control of the longitudinal short period. As a point of departure, the form of pilot describing function, with associated opinion, is estimated for a variety of short period damping ratios and undamped natural frequencies. Opinion boundaries are then established on the basis of these estimates. These predicted boundaries are then compared and correlated with experimental opinions, obtained in fixed-base simulators and variable stability aircraft, with most gratifying results. In the final sections of Chapter IV consideration is centered on those short period characteristics which have not received the detailed experimental attention given to damping ratio and undamped natural frequency. The treatment in these sections is based on the use of the general describing function pilot model and generic airframe transfer functions; and these are combined in a series of system surveys. The generic system analyses performed predict a variety of potential problem areas for future craft. Attention is also given to the problem of marginal controllability, and initial predictions are made and presented.

Chapter V utilizes a treatment similar to that of Chapter IV to cover the control of longitudinal long period motions. While human describing function data directly applicable to this situation are not available, the use of the general pilot model in generic system surveys allows gross predictions which are compatible with the applicable limited handling qualities experiments.

Chapter VI summarizes the conclusions of the analyses detailed in the previous chapters, and defines some aspects of both "good" and "intolerable" airframes when viewed in terms of the servo analysis approach.

CHAPTER II

SUMMARY OF PILOT DYNAMIC CAPABILITIES IN CLOSED LOOP COMPENSATORY TASKS

Human capabilities as a dynamic element in a control system are most succinctly expressed in servo engineering terms, i.e., as catalogs of transfer characteristics which constitute the repertory of pilot dynamic response. Many measurements of human response to visual inputs have been made over the past two decades. These were primarily conducted in ground simulators (References 1-3, 8-16), although one set (Reference 4) was obtained in flight. For each set of data the measurements obtained define two quantities which, taken together, describe the total human dynamic behavior. These are:

1. A quasi-linear random-input describing function which characterizes that portion of the pilot's output linearly correlated with the forcing function.

2. A "remnant" which includes all of the pilot's output which is not linearly correlated with the system forcing function.

The principal measurement situations considered in the studies referenced above corresponded to a single feedback loop arranged in the "compensatory" system of Figure 2. More limited measurements were taken in two-dimensional tasks (still compensatory) and one set (Reference 15) in a single-dimensional "pursuit" situation (illustrated in Figure 3). A summary of pertinent facts relating to these experiments is given in Table I.
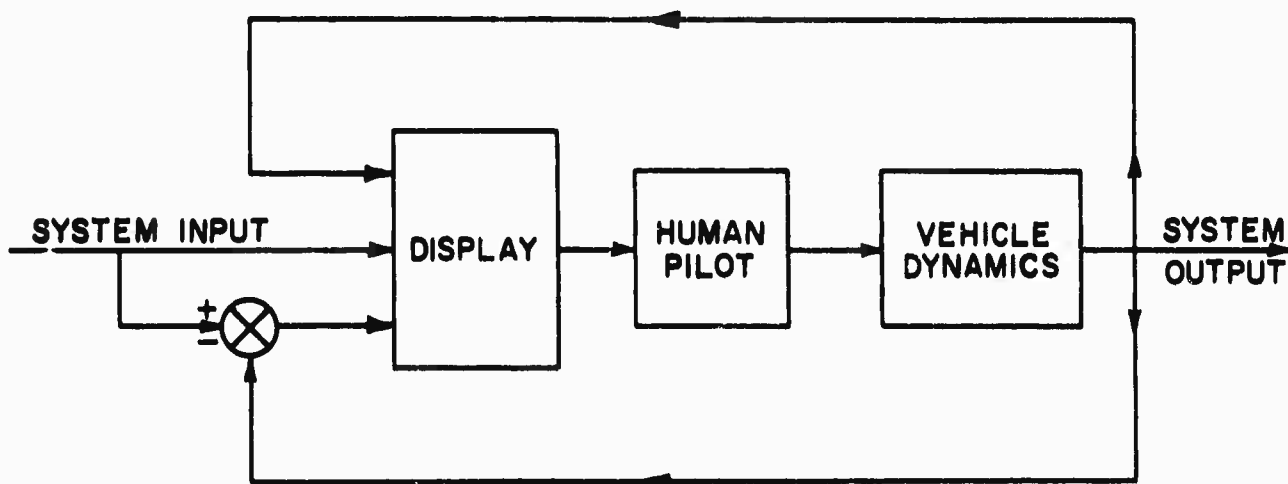
Figure 3

Pursuit System

TABLE I

SUMMARY OF EXPERIMENTS IN HUMAN RESPONSE

Investigator	No. of Random Appearing Forcing Function Types Investigated	No. of Controlled Element Types Investigated	Manual Control Device	Remarks
Tustin (Ref. 11)	2	2	Spade grip, spring restraint	Simulated tank gun turret tracking. Single-dimensional input.
Russell (Ref. 12)	2	11	Handwheel, no restraint	Single-dimensional input.
Goodyear (Ref. 13, 14)	2	2	Aircraft control stick	Simulated control of aircraft pitch axis in both stationary and pitching simulator. Single-dimensional input.
Krendel, et al (Ref. 1, 2)	3	3	Aircraft control stick	Simulated control of aircraft lateral and longitudinal axes in tail-chase, with and without airframe dynamics. Two-dimensional input.
Elkind (Ref. 15)	20	1	Pencil-like "pip trapper", no restraint	Single-dimensional input.
Seckel, et al (Ref. 4)	2	2	Aircraft control stick	Stabilization of aircraft lateral and longitudinal axes in both flight and fixed base simulator. Two-dimensional input.
Hall (Ref. 3)	1	20	Aircraft control wheel	Stabilization of various aircraft longitudinal dynamics while also controlling a fixed set of lateral characteristics. Two-dimensional input.

The block diagram of Figure 2 is shown in modified form in Figure 4 with the pilot represented by his describing function plus remnant, the dynamics of the display, control system, and vehicle lumped into a "controlled element," and the system input modified (if necessary) into an equivalent forcing function.
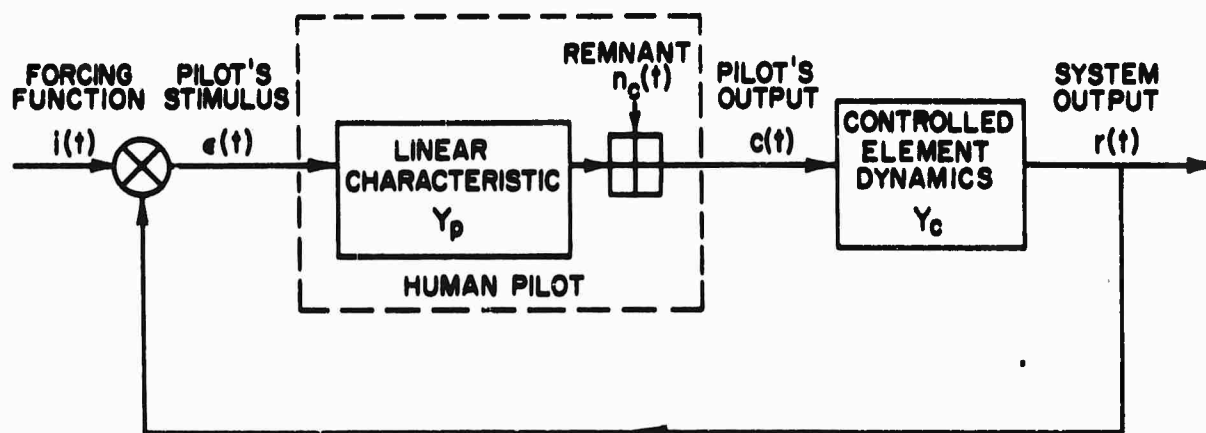
Figure 4

Equivalent Block Diagram of Compensatory System

Human characteristics measured in such situations depend upon the other system elements, i.e., the controlled element dynamics and the forcing function. In actual measurement situations this dependence, although basic, is obscured by the limited frequency range (bandwidtn) and the run-to-run variability, within and between subjects, of the measurements. For averaged data, however, it is possible to show (Reference 2) that a fairly simple analytic describing function form is adequate to describe human behavior for a given controlled element and forcing function. When these describing functions for all experiments are generalized, a servo model of human operation and adaptation (in compensatory tasks with random appearing forcing functions) is obtained. This model is a dynamic description of pilot capabilities in such situations and consists of two elements:

1. A generalized describing function form.

2. A series of "adjustment rules" which specify how to "set" the parameters in the generalized describing function so that it becomes an approximate model of pilot behavior for the particular situation considered.

FIGURE 5

PHASE MARGINS OBSERVED FOR 0db CROSSOVERS WITHIN THE DATA REGION
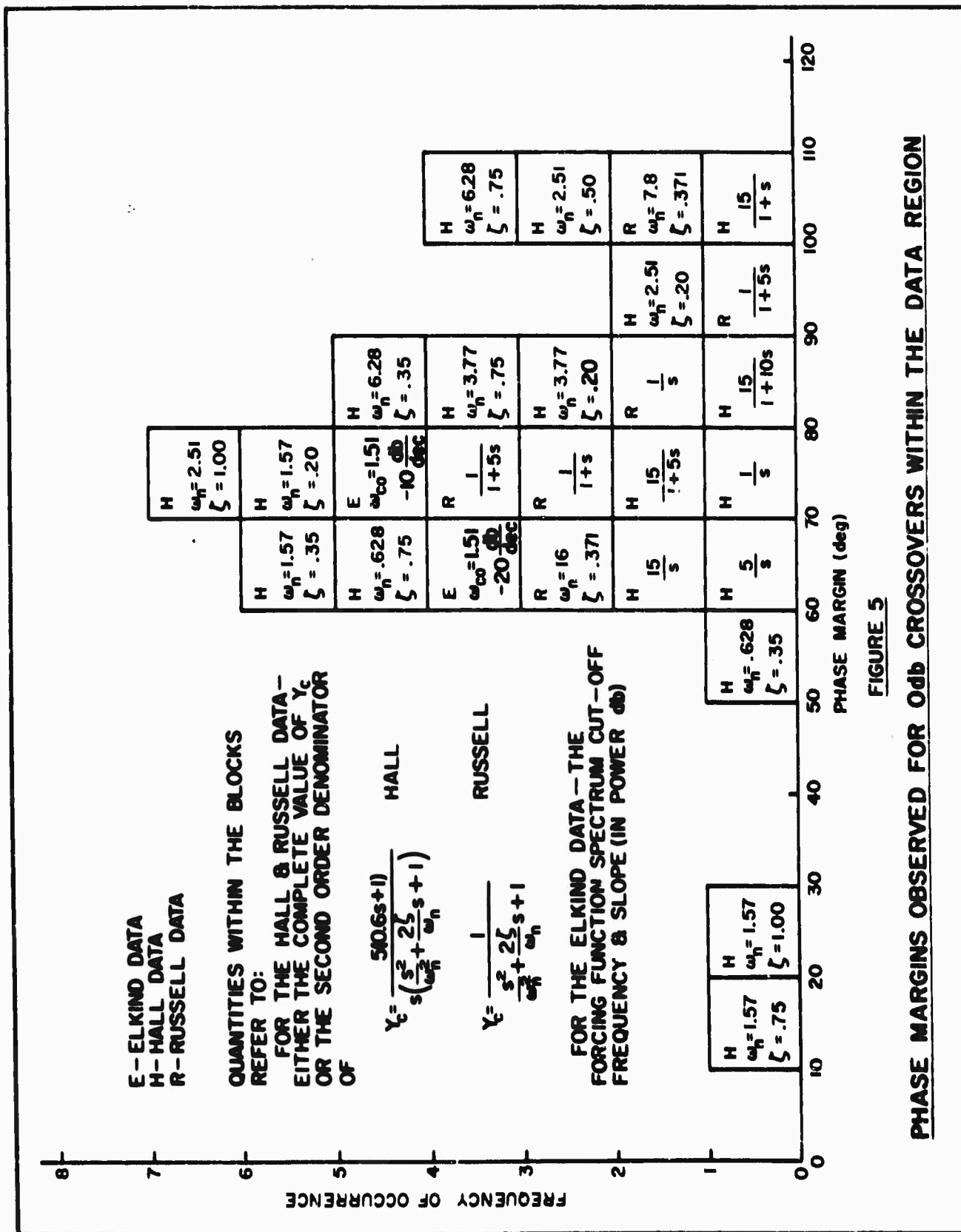
The general form approximating the human being's describing function for one- and two-dimensional compensatory control tasks is given by

$$Y_p = \frac{K_p e^{-\tau s} (T_L s + 1)}{(T_I s + 1)(T_N s + 1)} \tag{1}$$

where $\quad\tau\quad$ is the reaction time delay

$\qquad T_N\quad$ corresponds to neuromuscular lags $\qquad\Bigg\}$ Not adjustable by pilot

$\dfrac{T_L s + 1}{T_I s + 1}$ is the pilot's equalization characteristic

$\qquad K_p\quad$ is the pilot gain

The restriction of pilot equalizer form to one including only a single lead is not strictly precise, since for some isolated instances there is evidence that a second lead term may be generated (References 2, 3, 14). When using human pilot analytical models for rough estimates of pilot capability, however, the form of Eq. (1) is preferred for both simplicity and conservatism.

The adjustment rules are not so simply stated as the describing function general form since they depend intimately upon interactions with the other elements of the man-machine system, i.e., the forcing function and controlled element. In general, the adjustments can be divided artificially into two categories — adaptation and optimalization. Broadly speaking, adaptation is the selection by the pilot of a specific form (lag-lead, lead-lag, pure lead, pure lag, or unity) for the equalization characteristics, and optimalization is the adjustment of both the gain and the selected equalization parameters to satisfy some internally generated criteria. The adaptation process is fairly well understood, being essentially the selection of a form which is compatible with good low frequency, closed loop system response and general system stability. The internal criteria used for the optimalizing process are not known, but some insight into their practical consequences can be obtained by an examination of past human operator data. Figure 5 presents all available data on system phase margins for pilot-plus-controlled-element combinations (the difference between open loop system phase and -180 degrees, at the frequency where open loop gain is unity) for those experiments where measured data points exist in the gain crossover region. These results indicate that the describing function parameters, after initial adaptation of pilot equalization form, ordinarily are adjusted so that the system phase margin is between 60 and 110 degrees.[*]

---

[*]The phase margins noted here are higher than those given in Reference 2 where 0 to 30 degrees was suggested on the basis of extrapolations to crossover. The availability of more data (Reference 3) spanning the crossover region accounts for the change.
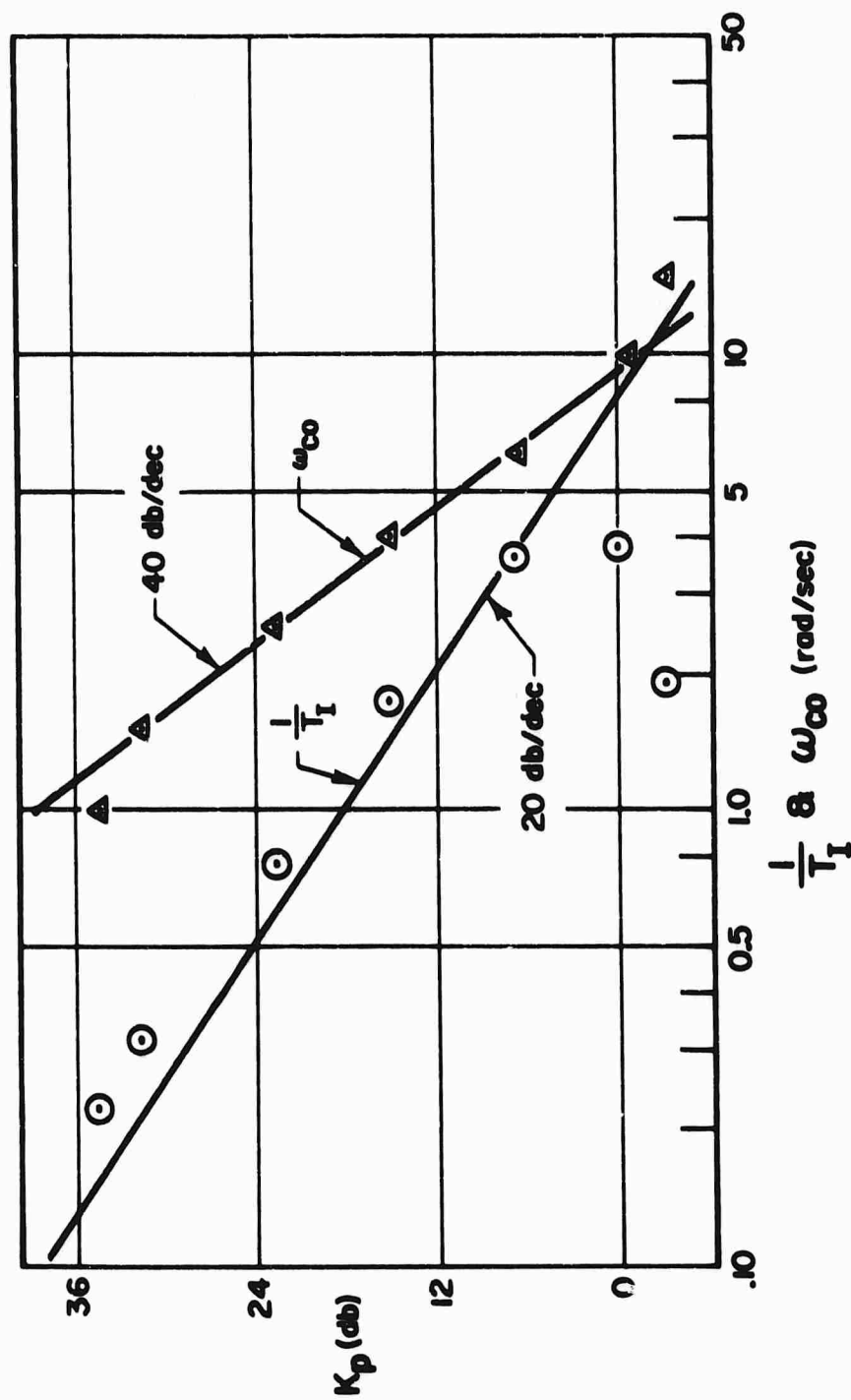
FIGURE 6
VARIATION OF PILOT GAIN AND ASSOCIATED TIME-CONSTANT
WITH CUTOFF FREQUENCY OF RECTANGULAR FORCING FUNCTION SPECTRA

The optimalizing characteristic is best illustrated by referring to one of Elkind's experiments using a compensatory system with a unity-gain controlled element (no dynamics)(Reference 2 or 15). The experiment used forcing function spectra which were rectangular in shape and covered a frequency band from zero to the cutoff frequency, ω_{co}. The cutoff frequency was an experimental variable, and seven values in the range from 1.0 to 15.0 radians/second were available. Human describing function data for experiments performed with each of the available forcing function spectra were curve-fitted with the simple expression

$$Y_p \doteq \frac{K_p e^{-\tau s}}{T_I s + 1} \tag{2}$$

The gains and time constants derived from these fits provide the data for Figure 6 which shows that the describing function adjustments were given approximately by

$$\frac{K_p}{T_I} \doteq 8.2 \ (\text{for } \omega_{oo} < 6 \ \text{rad/sec})$$

$$K_p \doteq \frac{87}{\omega_{oo}^2} \tag{3}$$

Thus: 1. The pilot gain was inversely proportional to the square of the forcing function cutoff frequency (or bandwidth).

2. The system crossover frequency ($\omega_c \doteq K_p/T_I$) was independent of forcing function frequency, provided $\omega_c > \omega_{oo}$.

3. For high cutoff frequencies, the closed loop dynamic characteristics were dominated by the fact that $\omega_c < \omega_{oo}$ and deteriorated accordingly.

The results reviewed above are compatible with other cases although the value of the constant crossover frequency is not the same as cited above since this value depends upon the controlled element dynamics. The optimalizing behavior illustrated here, in the adjustment of K_p and T_I as functions of ω_{oo}, has been shown (Reference 2) to have consequences roughly similar to those obtained using the conventional servo synthesis criteria of minimizing the rms error.

From the discussion above, and other information which is contained in Reference 2, the known adjustment rules for the human operator describing function of Eq. (1) can be summarized as follows:

1. The human adapts the form of his equalizing characteristics to achieve stable control.

2. The human adapts the form of his equalizing characteristics to achieve a good low frequency, closed loop system response to the forcing function. A low frequency lag (T_I) is generated when both of the following conditions apply:

   a. The lag would improve the system low frequency characteristics.

b. The controlled element characteristics are such that the introduction of the low frequency lag will not result in higher frequency destabilizing effects which are incapable of being overcome by a single first order lead (T_L).

3. After good low frequency characteristics are assured, within the above conditions, lead is generated when the controlled element characteristics multiplied by the $e^{-\tau s}$ term of Y_p are such that a lead term would be essential to retain high frequency system stability.

4. After initial adaptation of equalizing characteristic form, the describing function parameters are adjusted so that

    a. System phase margin lies between 60 and 110 degrees.

    b. Closed loop, low frequency performance in operating on the forcing function is optimum in some sense analogous to that of minimizing the rms error.

There is a great similarity between the rules given above and those useful in conventional servo design, particularly as regards selection of equalization, phase margin, and the minimization of rms error. It can be stated, therefore, that the adjustments of the variable parameters in the human describing function are similar to those a servo engineer would select for the same control situation. The controller "black box" available to the servo analyst must, of course, be limited in possible function to that of the general human describing function given in Eq. (1), with allowable adjustments in T_L, T_I, and K_p.

Eq. (1), as adjusted by the above rules, applies quite well to all situations where the system crossover frequency, estimated by application of the model, is greater than the cutoff frequency of the system forcing f nction. When this is not the case the system exhibits degraded closed loop dynamic performance, the pilot becomes much more nonlinear than usual, and he may attempt to overcome the condition, $\omega_c < \omega_{co}$, by generating higher order leads.*

Th describing function and the adjustment "rules" appear to be independent of the type of manual manipulative device, at least over the range covered in Table I**, and to apply to airborne situations in straight and level flight, as shown in Reference 4. However, for the particular flight situation studied the values of τ were greater by about 0.15 seconds and the longitudinal pilot gains were less by about half than those observed on the analogous fixed simulator.

---

*There are very few experimental data for which $\omega_c < \omega_{co}$ for low pass inputs. They consist only of the two Elkind conditions (for ω_{co} = 10.0 and 15.0 rad/sec) and four of Hall's configurations.

**The remnant term, however, is not independent of the manipulative device.

The model of human operations in closed loop tasks summarized above provides the essential tool required for a general manual control theory. Its proper application to a given control situation, defined by the controlled element dynamics and the forcing function power spectra, results in a prediction of pilot and system closed loop behavior. Accordingly, the model is directly useful in defining vehicle dynamics which are difficult or impossible to control (e.g., closed loop unstable). It also provides the basis for assessing the effects of changes in the control situation on pilot behavior. Examples of its use in such applications are given in Reference 5 and the present report.

In that it describes certain kinds of human behavior in mechanistic terms, this pilot dynamic model is the logical culmination of extensive efforts in the field of man-machine systems. But, the human is a unique system component in more ways than can be characterized by the simple servo model — his equivalent "black box" contains also a computer of unusual prowess and a loudspeaker of often exceptional power. In other words, the human pilot is a vocal adaptive controller. Indeed, in much of handling qualities research the vocal, or opinion, aspect of the human has been the only "measure" of complete system operation. Since such a "measure" appears, on the whole, to be surprisingly objective, it is essential, in a complete theory of handling qualities, to connect pilot opinion with pilot and system behavior. If this can be accomplished, then the analyst will be able not only to predict how a pilot behaves in various control situations, but also to estimate the associated opinion variations. Initial efforts in attaining this goal constitute the subject of the next chapter.

PILOT OPINION AS INFLUENCED BY CLOSED LOOP SYSTEM AND PILOT DYNAMICS

A. FACTORS INVOLVED IN PILOT OPINION

In spite of the occasional unreliability of opinion polls, pilot opinion has long been, and promises to remain, a critical element in assessing vehicle manual control configurations. In fact skilled pilots can deliver highly selective, representative, and reliable relative measures of system behavior. These judgments, as gathered and used in handling quality research, do not exhibit the extreme variability common to opinion polls because:

1. A tightly constrained situation is imposed upon the pilot by vehicle dynamics, forcing function, and assigned tasks.

2. The subjects are generally members of a highly restricted and skilled population.

3. The ratings given are ordinarily relative assessments which differentiate between several dynamic configurations possessing similar general characteristics.

For these reasons pilot opinion, as a subjective expression of the overall suitability of a pilot-airframe system, has always been considered to rest strongly upon objective factors. From the standpoint of man-machine system dynamics these objective factors can be divided into three categories:

1. Vehicle dynamic characteristics in response to open loop commands.

2. Closed loop pilot-airframe system dynamic characteristics, i.e., what the closed loop system is doing.

3. Pilot dynamic characteristics as an operating entity in the closed loop situation, i.e., what the pilot is doing.

While the first category cannot be neglected, the latter two are of primary interest in a systems analysis view of handling qualities.

Ideally it would be preferable to separate the effects of closed loop and pilot dynamic characteristics on opinion by performing tests where the closed loop dynamics were held constant while pilot characteristics varied and vice versa. Unfortunately the adaptability of the pilot and the complexity of the dynamic situations makes such a test program extremely difficult to implement except for very simple cases. However, it is possible, as developed below, to achieve at least part of the desired independence by carefully selecting and grouping existing data.

The most pertinent measures of closed loop dynamic characteristics are the poles and zeros of the closed loop transfer function. While the closed loop system may have many poles, it is ordinarily possible to approximate the essential pilot-vehicle system dynamics, for conditions where the system is essentially acting as a low pass filter on a low pass input, by

1. A single first order mode, or

2. A single second order mode, or

3. One first order plus one second order mode.

When the first case applies, the open loop crossover frequency, ω_c, is an excellent approximation to the dominant closed loop root. For the second case, phase margin plus crossover frequency serve to define the dominant closed loop mode. Since the pilot tends to adjust in such a way that phase margin is constant, the closed loop dynamics for pilot-airframe systems which fall into cases 1 and 2 above are quite well measured by the crossover frequency alone. For the third case, crossover frequency is usually a fair measure of the first order mode, but additional information, such as undamped natural frequency and damping ratio, is required to define the closed loop second order mode.

From the above discussion it is apparent that the open loop crossover frequency is an excellent measure of closed loop dynamic characteristics in general, although it may require supplementation to cover the third possibility completely. Accordingly, if data were available for a series of systems in which crossover frequency and the other closed loop dynamic measures were substantially constant, then closed loop dynamic performance could also be considered constant. The systems which possessed these characteristics would then form a set where closed loop dynamics could be eliminated as a factor which generates pilot opinion differences. The principal objective opinion factors remaining would, consequently, have to be due to differences in pilot dynamic characteristics. If pilot describing function data were available, opinion could be correlated with these describing function parameters. This process, assuming correlation existed, would thereby allow an estimate of that portion of the pilot's opinion which is based upon his dynamic characteristics. Data which can be used to perform precisely this sort of correlation are presented and analyzed in succeeding sections.

Unfortunately, the influence of closed loop dynamic performance upon opinion is not quite as clear-cut as is that of the pilot's dynamic characteristics. Part of the closed loop characteristic of interest is, as was previously mentioned, suitably defined by the crossover frequency, ω_c. According to the pilot adjustment "rules" of Chapter II, this parameter will ordinarily be such that the overall system possesses "good" low frequency response to the forcing function. This requires $\omega_c > \omega_{co}$, and the pilot would be expected to adjust accordingly; if such an adjustment were impossible, his opinion of the system would be degraded. Available data, subsequently presented, support this conjecture.

In those cases where a minimum description of the closed loop system requires both a first and second order mode, the crossover frequency is not sufficient to define completely the total system dynamic performance. The simplest supplementary measure is the damping ratio of the closed loop second order mode. As discussed thoroughly in the last section of this chapter, this parameter can be estimated from some of the available data although the procedures involved are fairly tedious. The adjustment rules imply that the pilot should attempt to place the damping ratio within a small range which is consistent with a nearly minimum system rms error. When this adjustment is not achieved, opinion is usually degraded.

With this rather long introduction as a guide, the actual data and correlations can now be presented. Before the correlations are attempted a short description

of the experiments of Reference 3 is given in the next section since their data form the major basis for the development of the theory.

B. GENERAL DESCRIPTION OF THE HALL EXPERIMENTS

The Hall experiments were performed in a mockup simulating the cockpit controls of a Navion airplane. Two pilot test subjects performed two-dimensional (lateral and longitudinal) tracking tasks with random appearing forcing functions which had Gaussian amplitude distributions. The lateral dynamics were those of a Navion aircraft in a cruise configuration while the longitudinal controlled element characteristics were varied over a wide range of transfer function forms. Three two-minute runs per subject were performed for each transfer function. The forcing functions used in both control axes had a spectral form obtained by passing essentially white noise through a third order binomial filter with a break frequency of one radian/second. The pilot's compensatory display indicated the horizon and a roll-resolved target on an inside-out basis.

For each of the controlled element configurations, extensive data were taken on pilot and pilot-airframe system behavior. These included pilot describing functions and linear correlations, power spectra of output, error, and remnant, probability distributions of output, computations of mean absolute tracking error, and pilot opinion.

The pilot opinion scale was evolved by the two subjects. Their definitions were (quoted from Reference 3):

"Good (G)	Aircraft response very suitable for the given tracking task.
Acceptable (A)	Possessed of satisfactory flying qualities, but less easy to control than a "good" configuration; aircraft response either faster or slower than that which the pilot visualizes as most desirable.
Poor (P)	Possessing characteristics which require considerable concentration to accomplish the given tracking task; configurations are either quite touchy, unresponsive, or poorly damped.
Unacceptable (U)	Quite unsuitable.

The subjects differed only between P and U. Pilot II tended to classify aircraft which were unsuitable for the given tracking task, but could conceivably be flown, as P, reserving U for configurations which he considered as unsafe to fly under any circumstances, while Pilot I tended to classify all configurations with which tracking was very difficult as U."

With the exception of the noted differences in P and U ratings, it should be emphasized that the rating system was based solely on tracking tasks.

The four-adjective scale as actually used in assessing all of Hall's configurations resulted in 10 different ratings because of the use of plus ("somewhat more than") and minus ("somewhat less than") qualifications. For plotting

purposes, therefore, a numerical scale which roughly follows that suggested in Reference 21 has been assigned as follows:

Numerical Rating	Adjective Rating
1	G +
2	G
3	G -
4	A +
5	A
6	A -
7	P +
8	P
9	P -
10	U

Development of the other Hall data parameters is not considered necessary here. A complete discussion is contained in Reference 3, and the details of the data used in the developments to follow are presented in context with the arguments which they support.

C. DEPENDENCE OF OPINION UPON PILOT-ADOPTED DYNAMIC CHARACTERISTICS

Turning now to the correlation effort, consider the general pilot model previously discussed. Three fundamental opinion factors are present. These are:

1. Value of gain, K_p.

2. Value of lag inverse time constant, $1/T_I$; alternatively, the frequency position of the lag.

3. Value of lead inverse time constant, $1/T_L$, and the possibility that a second lead term may be generated; alternatively, the order and frequency position of the lead.

The data used to determine the effect of each of these factors upon opinion have been selected from the total available data by considering conditions where, insofar as possible, the remaining factors and the closed loop dynamics are essentially constant.

1. Effect of Pilot Gain on Opinion

The Hall configurations illustrating the effects of gain variations are of the transfer function form

$$Y_c = \frac{K_c}{s} \tag{4}$$

Pertinent data for this set of configurations are presented in Table II. These have already been fairly thoroughly explored, in the present context, in Reference 5 and only the highlights of this exploration will be presented here.

TABLE II

SUMMARY TABLE OF HALL K_c/s CONFIGURATIONS

Configuration K_c (Deg/In)	Opinion Rating			Average Stick Force, $\bar{F}_p$ (Lb)			Mean Absolute Tracking Error, (Deg)		
	Pilot I	Pilot II	Average	Pilot I	Pilot II	Average	Pilot I	Pilot II	Average
35	9	6.5	7.75	.44	.36	.40	.85	.81	.83
25	7	6	6.5	.65	.59	.62	.65	.86	.76
15	2	5	3.5	.71	.97	.84	.76	.79	.78
10	3	2	2.5	1.45	1.95	1.70	.77	.63	.70
5	4	2	3	2.28	3.04	2.66	.75	.67	.71
1	10	5	7.5	7.9	6.5	7.2	.84	.73	.79

In Reference 5 it is shown that the equalization form adopted by the pilot for these configurations is a simple gain. This follows the "rules" postulated in the foregoing Section A. The data show that pilot gain, K_p, is adjusted so that the total open loop gain and, consequently, the crossover frequency remain approximately constant with changes in controlled element gain, K_c. The actual relationship is $K_p K_c = \omega_c \doteq 1.2$. This implies that the closed loop system dynamics are essentially constant. Further evidence is supplied by the measured tracking errors which are about the same for all values of K_c (or K_p). On the basis of these and other observations it is apparent that the pilot's objective opinion can <u>only</u> be influenced by the value of K_p he adopts since this is the only remaining variable. Accordingly, pilot rating is plotted versus pilot gain to yield a measure of the influence of this particular parameter on opinion. This plot is repeated here as Figure 7.

This figure shows an "optimum" pilot gain for highest opinion and indicates that either increasing or decreasing this gain results in a lowered opinion. When the pilot gain is too high or too low, corresponding to a controlled element gain which is too low or too high, the pilot considers the response "too sluggish" or "too sensitive." His opinion, in either situation, is degraded considerably from the optimum gain case. Nevertheless, there is a fairly broad gain band associated with acceptable and good opinions (region G-A in Figure 7).[*]

---

[*]It should be noted that the <u>level</u> of pilot gains considered optimum is <u>not</u> a universal constant, but instead depends on the manipulative device and possibly the axis being controlled. The present instance cites data for longitudinal control with a wheel. Much of the engineering psychology literature on optimum "control ratios" is directly pertinent to this same subject.
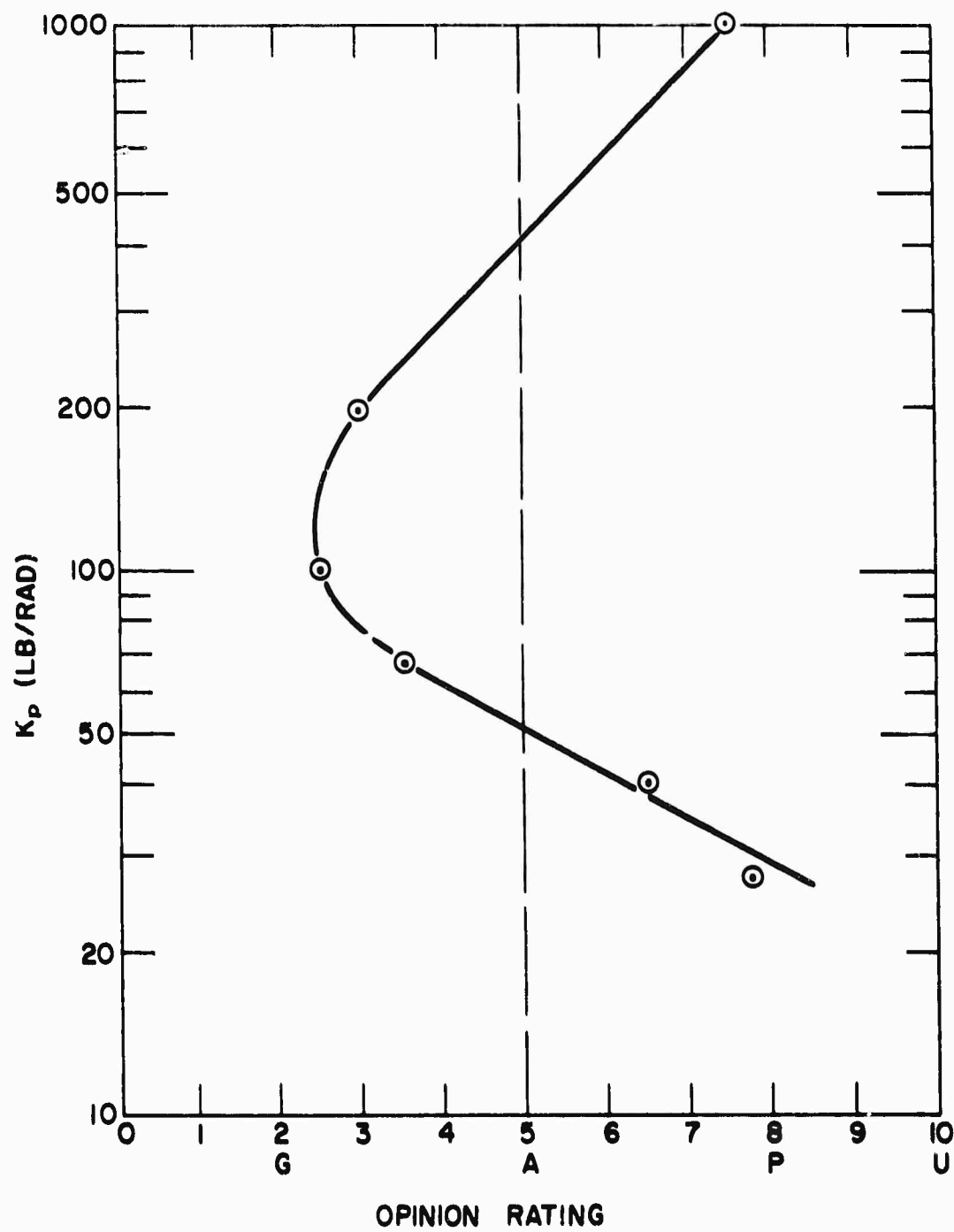
FIGURE 7
PILOT GAIN VERSUS OPINION RATING

2. Effect of Pilot Lead on Opinion

The effects of pilot-adopted lead equalization on opinion have been determined by analyzing and correlating the Hall short period results. The controlled element for this set of tests had the form

$$Y_c = \frac{5(0.6s + 1)}{s\left[\left(\frac{s}{\omega_n}\right)^2 + 2\left(\frac{\zeta}{\omega_n}\right)s + 1\right]} \tag{5}$$

The gain and lead time constant were held constant throughout the experiments, while the undamped natural frequency and damping ratio were varied. Hall gathered pilot response and performance-measure data for a total of 20 different ζ and ω_n configurations. For seven of these, however, the data are incomplete in that pilot describing function and spectral data exist for only one or the other of the two subjects tested. Only the 13 configurations which were completely documented are considered here since two-pilot averages are desirable to increase the significance of the conclusions derived.

Table III summarizes the opinion ratings and performance-measure data for each pilot separately and as averages. A consistent difference in performance, as measured by the mean absolute tracking error, appears to exist between the two pilots. This difference can be summarized concisely by noting that the average $|\epsilon|$ for all configurations is .955 for Pilot I and .760 for Pilot II.

TABLE III

SUMMARY TABLE OF HALL SHORT PERIOD CONFIGURATIONS

Configuration		Opinion Rating			Average Stick Force, $\bar{F}_p$ (Lb)			Mean Absolute Tracking Error, $|\bar{\epsilon}|$ (Deg)		
ω_n	ζ	Pilot I	Pilot II	Average	Pilot I	Pilot II	Average	Pilot I	Pilot II	Average
.63	.35	10	10	10	7.7	8.24	7.97	1.48	1.52	1.50
.63	.75	10	9.5	9.75	6.33	6.88	6.61	1.14	1.46	1.30
1.57	.2	10	10	10	6.5	4.81	5.66	1.30	1.04	1.17
1.57	.35	7	8	7.5	5.24	6.68	5.96	.93	.93	.93
1.57	.75	3	2	2.5	5.67	5.82	5.75	.78	.65	.72
1.57	1.0	6	3	4.5	4.65	3.93	4.29	.90	.77	.84
2.51	.2	10	10	10	2.7	1.71	2.21	1.21	.80	1.01
2.51	.5	2	6	4	2.20	2.76	2.48	.97	.76	.87
2.51	1.0	3	1	2	2.82	2.82	2.82	.85	.64	.75
3.77	.2	5.5	8	6.75	2.15	2.33	2.24	.84	.82	.83
3.77	.75	3	2	2.5	2.44	2.40	2.42	.72	.65	.69
6.28	.75	4	2	3	2.02	1.96	1.99	.68	.76	.72
6.28	.35	7	7	7	1.93	2.03	1.98	.80	.74	.77
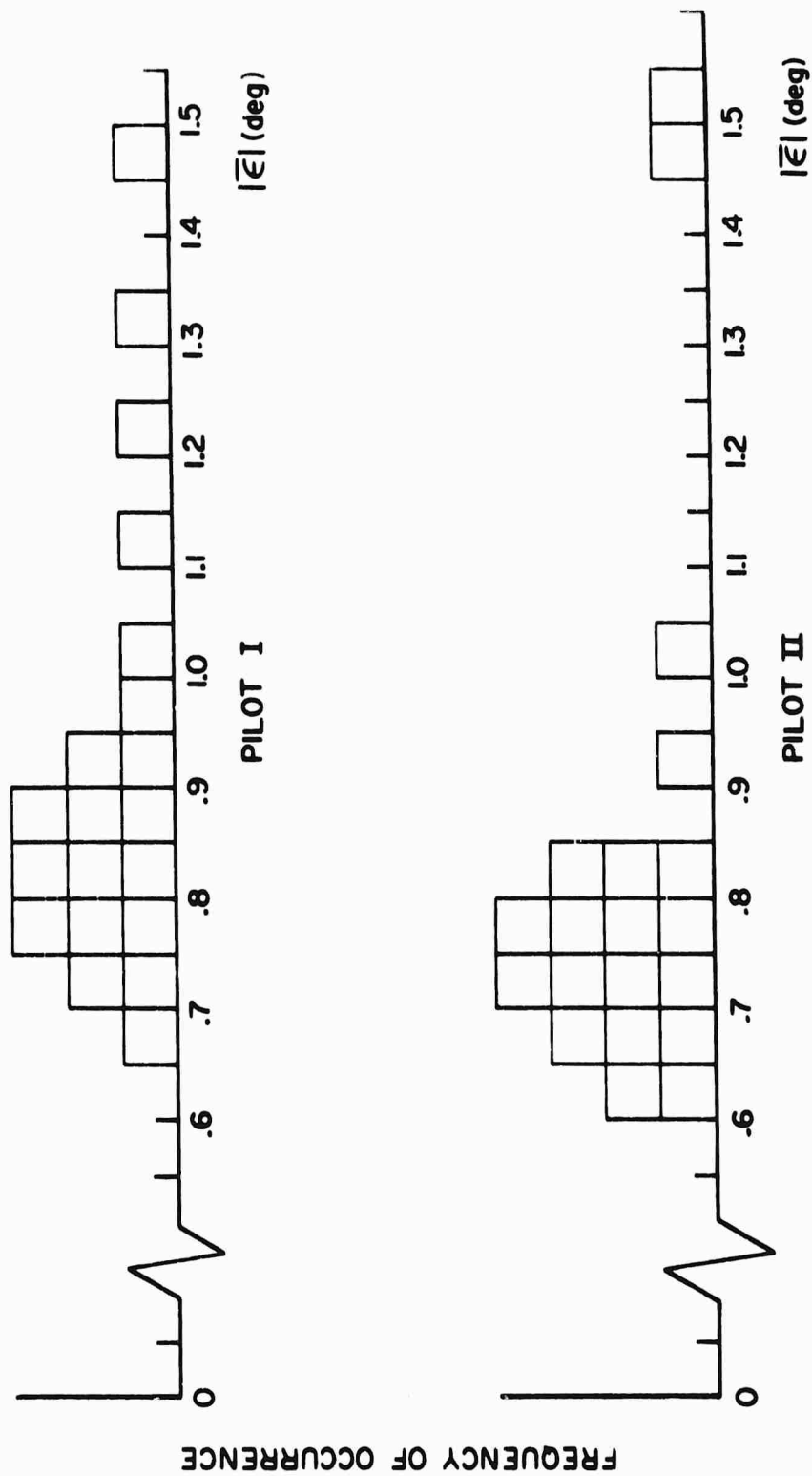
FIGURE 8
MEAN ABSOLUTE ERROR DISTRIBUTIONS FOR BOTH PILOTS —
SHORT PERIOD CONFIGURATIONS

Another indication of a basic difference between the pilots is the error frequency distribution for all configurations, shown in Figure 8. Pilot differences such as these are not atypical (Reference 2) although they do point up the desirability of using only two-pilot averages to obtain the most significant and meaningful results.

The averaged describing functions and linear correlations (ρ) are presented in Figures 9-11, arranged in groups according to both opinion and describing function form. The significance of these groupings will be explained in a later section. Adding these data points to controlled element Bode plots for the corresponding configurations gives system open loop ($Y_p Y_c$) Bodes in the frequency band between 0.5 and 4.0 radians/second. Table IV summarizes open loop system data obtained from such plots (which are not presented).

TABLE IV

TWO-PILOT-AVERAGED FREQUENCY RESPONSE DATA

Configuration		Pilot Gain, K_p or $\|Y_p\|_{\omega \to 0}$ [*]		0 db Crossover Frequency	Phase Margin	Gain Margin
ω_n	ζ	(db)	(Lb/Rad)	(Rad/Sec)	(Deg)	(db)
.63	.35	-21	76	.99	50	12
.63	.75	-16	135	.67	65	1.5
1.57	.2	-20	86	.53	74	3
1.57	.35	-17	120	2.1	65	5
1.57	.75	-10.5	254	1.9	12	1
1.57	1.0	-7	380	1.3	26	7
2.51	.2	-16	135	.77	98	0
2.51	.5	-16	135	1.05	100	4
2.51	1.0	-10	269	1.4	71	14
3.77	.2	-14	170	1.2	80	1
3.77	.75	-12	215	1.7	80	10
6.28	.75	-8	339	1.2	100	1
6.28	.35	-14	170	1.25	83	1

[*]Note that pilot gain, K_p, may be given in units of lb/rad or in/deg. The conversion factor is the aircraft's stick gearing constant, 15 lb/in for the Hall experiments.

As to the interpretation of these data, an examination reveals, at the outset, that they may be divided into two mutually exclusive sets. These sets are defined by the relative values of the crossover frequency, ω_c, and the forcing function cutoff frequency, ω_{co}, and the two sets correspond to conditions where either $\omega_c < \omega_{co}$ or $\omega_c > \omega_{co}$.[*]

When ω_c is less than ω_{co}, poor closed loop performance and poor opinion rating are to be expected. These expectations are corroborated by the error and opinion data of Table III. As will be discussed later, opinion factors other than closed loop performance may also be significant in the ratings for this set, but these will not alter the fact that the $\omega_c < \omega_{co}$ condition is invariably connected with poor opinion and poor closed loop performance.

For the second data set, the gain crossover frequency, ω_c, is always greater than ω_{co}. The actual crossover frequencies for these configurations are confined to the band between 1.05 and 2.1 radians/second. The mean value of ω_c is 1.45 radians/second with a standard deviation of 0.34 radians/second. These data, therefore, form a set in which ω_c is roughly constant and larger than the forcing function cutoff frequency. Accordingly, both closed loop dynamics and system performance measures are expected to be roughly constant. The mean absolute errors (from Table III) for this set, plotted versus opinion in Figure 12, are in approximate accord with this anticipation. Thus, for the data in this group, closed loop dynamics should not be more than a minor factor in the differences in pilot opinion of the various configurations. These differences should depend largely on objective factors associated with pilot dynamic characteristics.

Since an approximate correlation of pilot gain with opinion has already been discussed, K_p is the first pilot dynamic characteristic which should be considered. The data of Table IV, however, indicate that K_p values for the set $\omega_c > \omega_{co}$ are all confined to the good-acceptable region of Figure 7. The differences in gain between configurations in this set should then have only a small, easily corrected influence on pilot opinion differences.[**]

With both closed loop dynamics and performance, and pilot gain, eliminated as major opinion factors for this set, the large opinion differences must be predominantly dependent upon the pilot's equalizing characteristics. From the data of Figures 9-11, these characteristics appear to involve the generation of high frequency lead. Thus, at long last, the data have been grouped and categorized to a point where the effects of pilot lead on opinion can be treated as a separate factor.

Various attempts have been made to correlate the lead equalization factor with opinion, most with only indifferent success. The most suitable measure found involves the parameter $(T_L \, dA/d\mu)$, where $1/T_L$ corresponds to the apparent lead break frequency and $dA/d\mu$ is the slope of the high frequency amplitude ratio, $d|Y_p|/d \log \omega$, in db/decade. It was necessary to use amplitude data only since the phase data are very badly scattered and contaminated with pilot reaction-time delay effect. Despite the scatter of the basic data and the

---

[*]Recall that $\omega_{co} = 1.0$ rad/sec in these experiments.

[**]In Figure 13, points corrected via Table IV and Figure 7 are shown flagged.

FIGURE 9

AVERAGE PILOT DESCRIBING FUNCTIONS & LINEAR CORRELATION
COEFFICIENTS FOR "GOOD" & "ACCEPTABLE" SHORT PERIODS

FIGURE 10

AVERAGE PILOT DESCRIBING FUNCTIONS &
LINEAR CORRELATION COEFFICIENTS FOR
"POOR" SHORT PERIODS

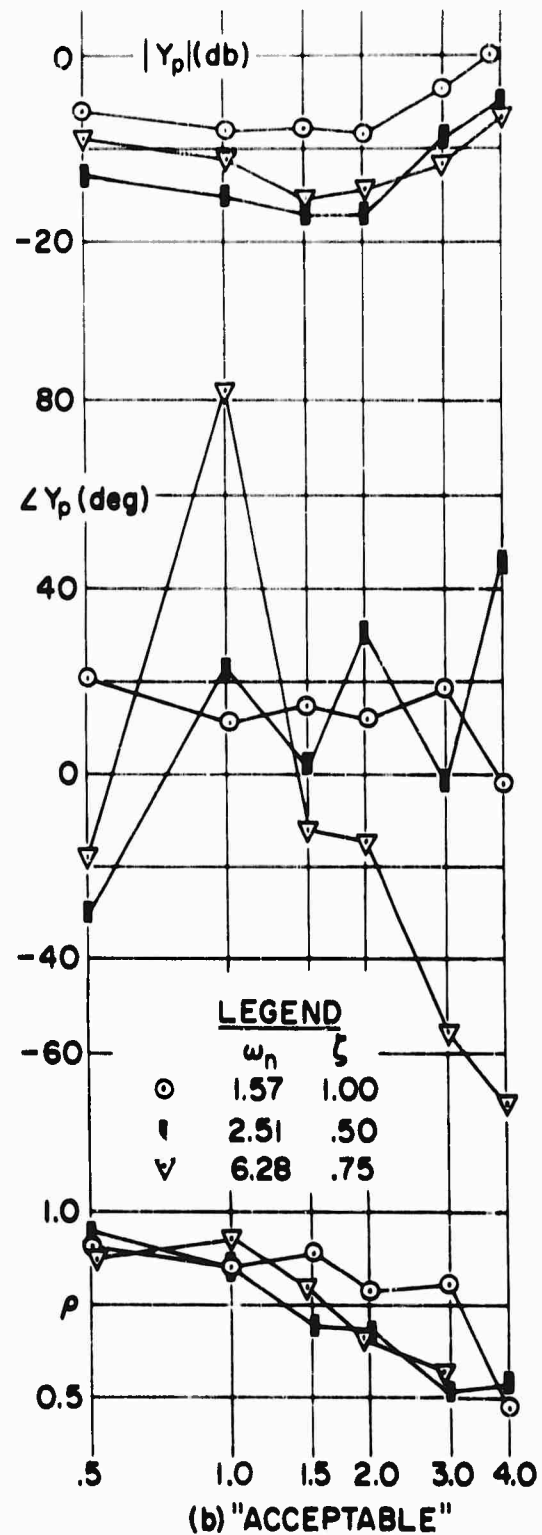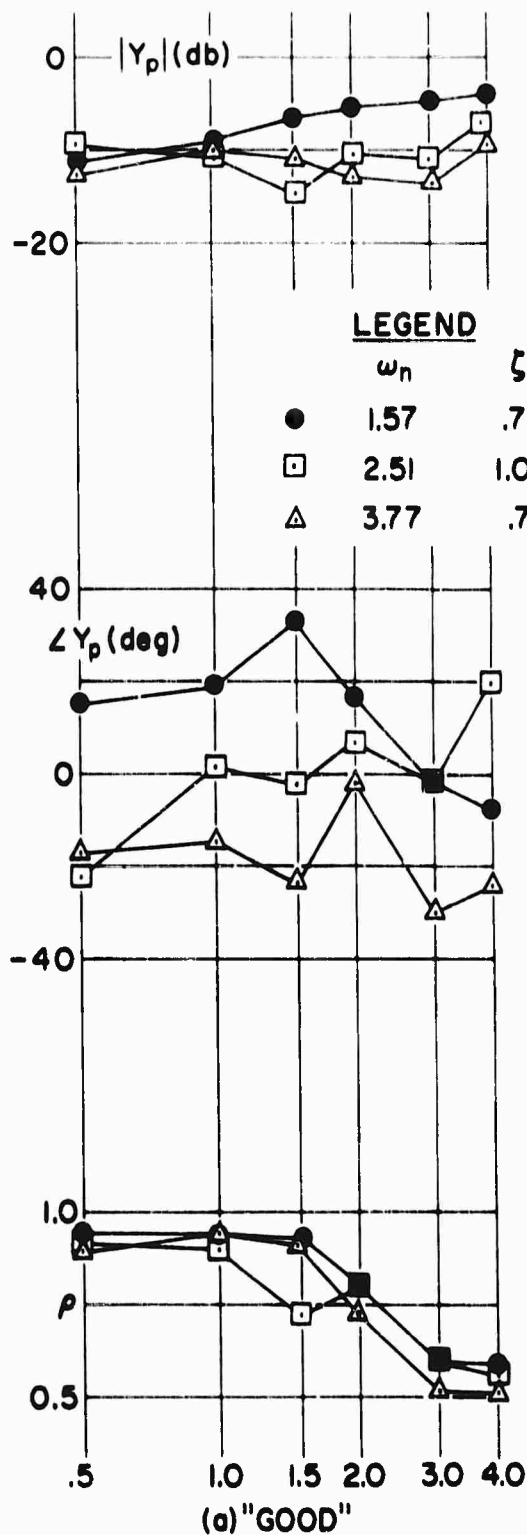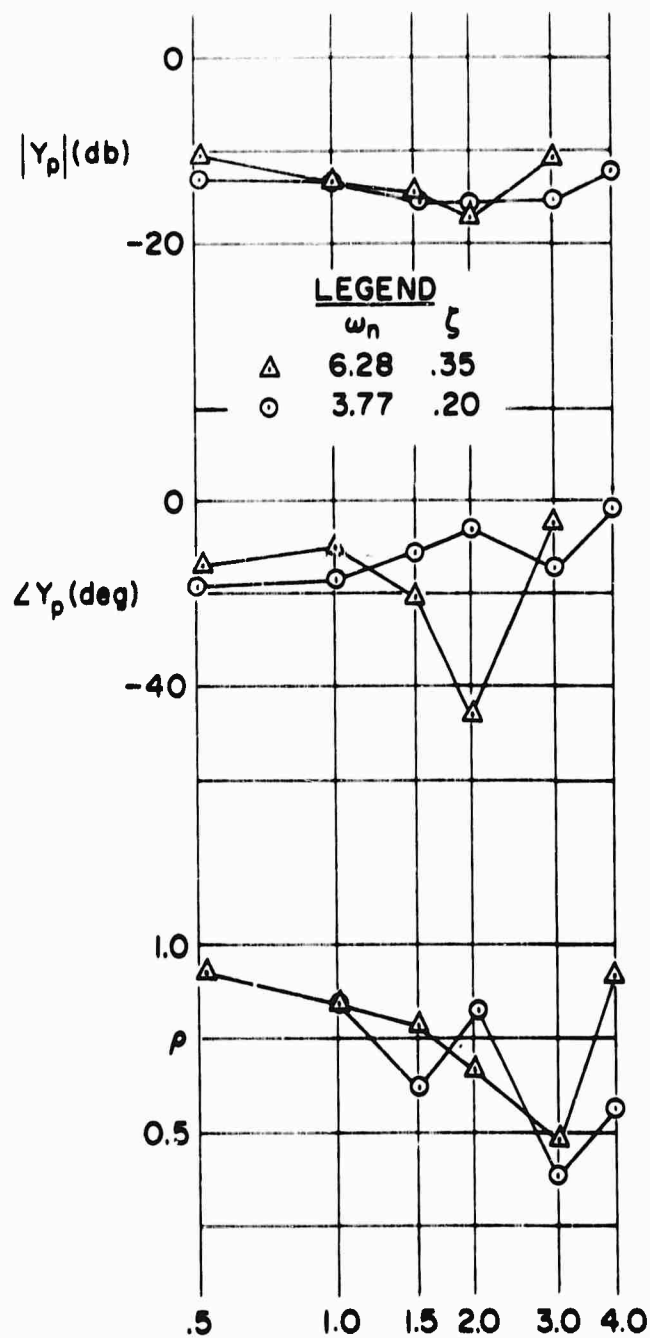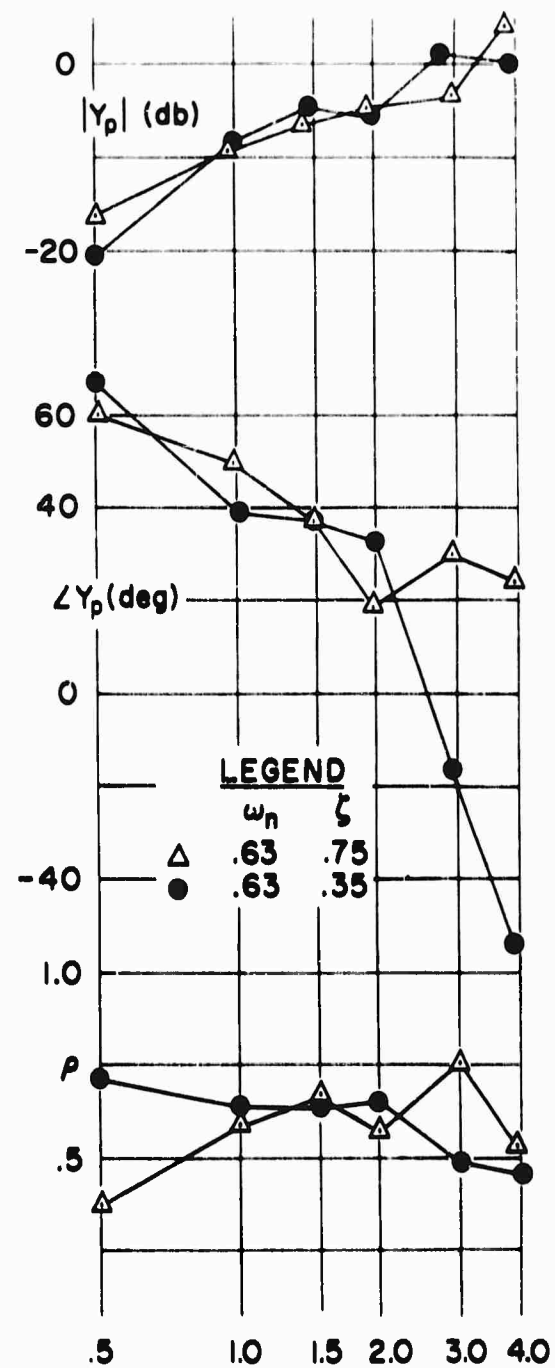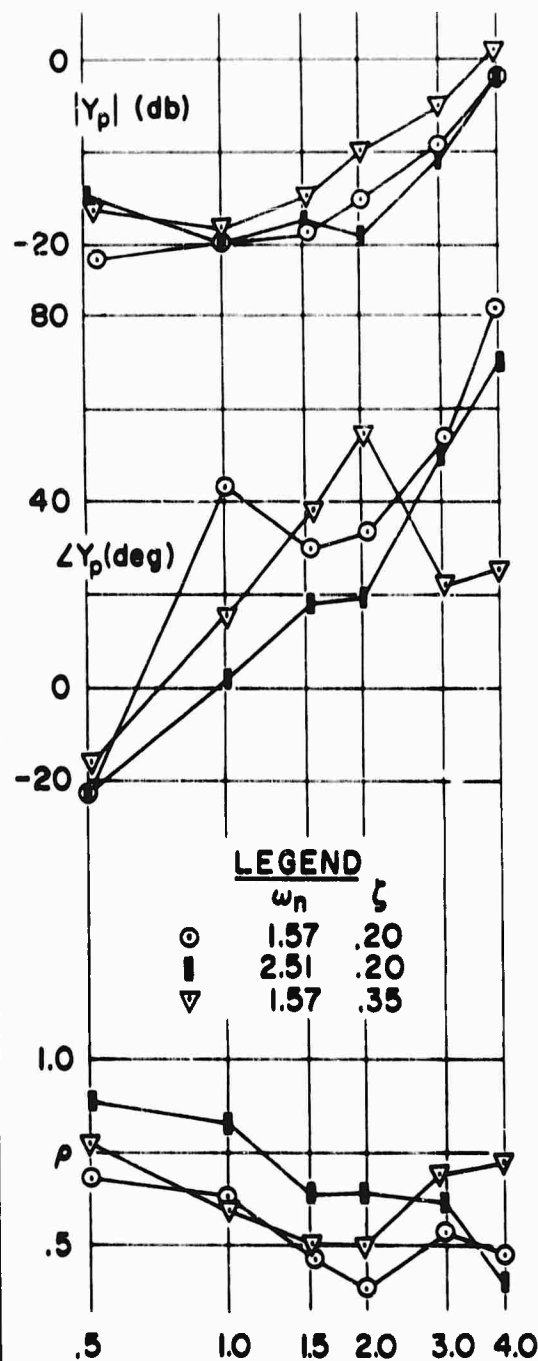FIGURE 11

AVERAGE PILOT DESCRIBING FUNCTIONS & LINEAR
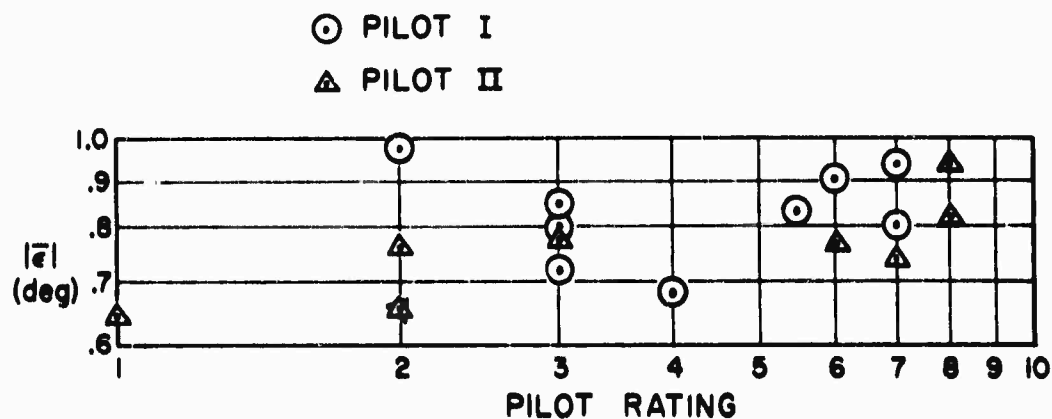CORRELATION COEFFICIENTS FOR "UNACCEPTABLE" SHORT PERIODS

FIGURE 12
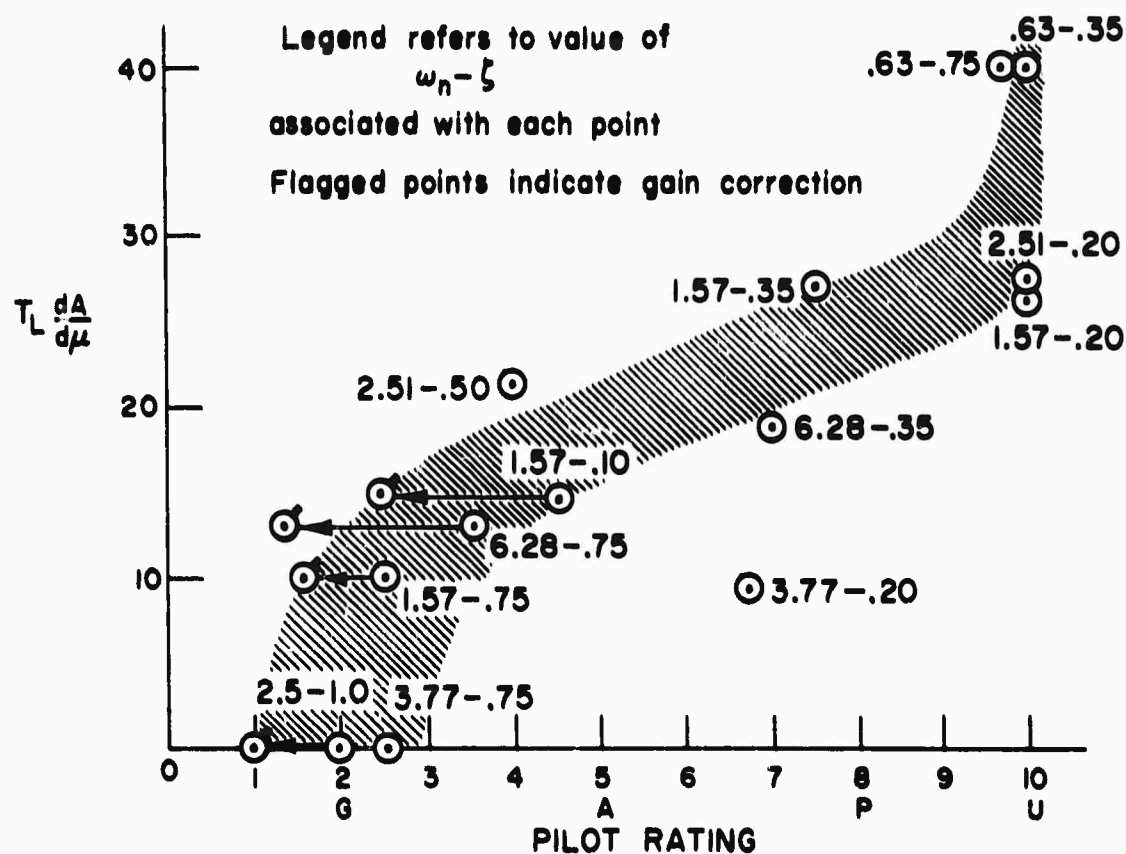VARIATION OF MEAN ERROR WITH PILOT OPINION RATING

FIGURE 13
VARIATION OF PILOT OPINION RATING WITH $T_L \frac{dA}{d\mu}$

difficulty of accurately determining the break frequency, a plot of this function, $(T_L \, dA/d\mu)$, versus opinion rating exhibits a reasonable trend (Figure 13). It can be seen that the best opinion occurs when the pilot equalization approaches a pure gain form, and that opinion degrades as the lead break frequency decreases (T_L increases) and/or the amplitude slope increases. This slope may be considered a measure of the separation between the lead and the unintentional (e.g., neuromuscular) lag break-frequencies. It also takes into account the occasional presence of higher order leads.

It should be noted that the cases corresponding to $\omega_c < \omega_{co}$ are included in Figure 13 (pilot rating $\doteq$ 10) and, in general, follow the trend established by all the other ($\omega_c \doteq$ constant) cases. It is difficult, therefore, to say whether the unacceptable opinion attached to the $\omega_c < \omega_{co}$ cases is due to the poor closed loop system performance, as originally postulated, or to the high degree of pilot lead adopted. Either reason appears sufficient by itself to account for the observed opinion rating. In addition the situation appears somewhat further confused when nonlinear pilot behavior is considered, as outlined below.

The Hall data show that, as pilot lead increases, the pilot tends to operate in an increasingly nonlinear manner. Some indication of the degree of nonlinearity is indicated by the remnant spectrum and the correlation coefficient. With only one system input and no internally generated noise, large remnant power and low correlation coefficient would imply a high degree of pilot nonlinearity. Another indication is the pilot output distribution, which, for a linear system with a Gaussian input, should also be Gaussian. Several histograms, each representing the pilot output distribution for one of the several runs taken for a given configuration, are shown in Figure 14. Two histograms are presented for each configuration to demonstrate the variability of the pilots. In Figure 14(a) the distributions are similar to that for a square wave, indicating highly nonlinear behavior. These distributions are consistent with the assertion that the pilot tends to operate as a relay controller in this low opinion case. Figure 14(b), a better-opinion configuration, represents a transition phase between highly nonlinear and linear operation. Figure 14(c) shows a quasi-Gaussian distribution indicating a relatively high degree of linearity although the configuration has an unacceptable opinion rating. Figure 14(d), for the highest rated configuration, also shows quasi-Gaussian distributions. Here the pilot was operating as a nearly pure gain controller, although the distributions are not purely Gaussian.

In general it appears that nonlinear operation is associated with low opinion, although the converse is not true. The fact that low opinion is also associated with strenuous lead generating efforts on the pilot's part raises some doubt as to the really basic opinion factor. In a practical sense, however, such doubts do not seriously detract from the efficacy of the analysis approach used here. Consider, for example, that a given system has been analyzed on a linear basis and shown to require the adoption of appreciable (possibly second order) pilot lead; then, according to Figure 13, the pilot will be extremely dissatisfied with the configuration. The basic source of this dissatisfaction could be the appreciable lead required, or it could possibly be because

1. The pilot, besides adopting lead, also becomes nonlinear and therefore works much harder than indicated by the linear analysis. This "works harder" comment reflects

the fact that the available data indicate an increase in average stick forces as the pilot becomes more nonlinear.

2. In spite of his efforts, ω_c is less than ω_{co}, so poor closed loop performance colors the pilot's opinion.

Regardless of which effect or combination of effects predominates in influencing pilot opinion, the linear analysis will nevertheless serve as a basis for estimating the pilot's level of dissatisfaction. It should be carefully noted that this statement relies for its validity on the observation, based upon <u>all</u> available data, that nonlinear operation or attempts to force $\omega_c > \omega_{co}$ always involve extreme equalizing efforts on the part of the pilot.

3. Effect of Pilot Lag on Opinion

The effect of pilot lag on opinion can be illustrated by considering the Hall data for $Y_c = K_c$ and $Y_c = K_c/s$. For these controlled elements, two-pilot-averaged describing functions, with $K_c = 5$, are shown in Figure 15. The open loop $Y_p Y_c$ describing function plots, particularly the more reliable amplitude ratio points, are nearly identical for the two configurations. However, the lag characteristic for the $Y_c = K_c$ configuration is pilot induced, whereas that for $Y_c = K_c/s$ is due to the controlled element. Thus, the pilot characteristic changes from the form $Y_p = K_p e^{-\tau s}/(T_I s + 1)$ to $Y_p = K_p e^{-\tau s}$. The averaged opinion for the former is rated at 6.0 while the latter is rated at 3.0. The major portion, if not all, of this opinion difference must be considered to be the result of the pilot-adopted lag since all other opinion factors are about the same for the two cases.

Other existing data, although insufficient for complete verification, indicate that pilot-induced lag effects may be classified in a manner identical to the lead effects. That is, opinion is degraded as the lag break frequency is reduced and/or the accompanying change in slope is increased.

D. ADDITIONAL CLOSED LOOP INFLUENCES UPON PILOT OPINION AND ADAPTATION

Having established the general dependence of opinion on pilot dynamic parameters for essentially constant closed loop dynamics and performance, it is now pertinent to examine the closed loop implications of the data. The first approximate measure of closed loop dynamics, the crossover frequency, has already been extensively discussed in the previous sections of this chapter. The net conclusion of this discussion was that configurations involving $\omega_c < \omega_{co}$ were always associated with poor opinion, but whether the condition $\omega_c < \omega_{co}$ was, of itself, the basic cause for poor opinion could not be definitely established. Also, conditions involving $\omega_c > \omega_{co}$ were shown to have roughly constant closed loop dynamics, and observed opinion variations were then attributed to other factors. Consequently the status of ω_c relative to pilot opinion appears to be such that $\omega_c > \omega_{co}$ is a necessary, but not sufficient, condition for the existence of good opinion and $\omega_c < \omega_{co}$ is a sufficient, but not necessary, condition for poor opinion.

Another closed loop dynamics factor suggested previously is the damping ratio of the second order mode for closed loops whose minimal dynamic description demands a third order system. Consideration of this factor is the principal topic of this section, and such consideration will take the form of an

PILOT I   PILOT II

(a) OUTPUT DISTRIBUTIONS FOR $\omega_n = 0.63, \zeta = 0.35$

wheel travel

(b) OUTPUT DISTRIBUTIONS FOR $\omega_n = 1.57, \zeta = 0.35$

(c) OUTPUT DISTRIBUTIONS FOR $\omega_n = 2.51, \zeta = 0.2$

(d) OUTPUT DISTRIBUTIONS FOR $\omega_n = 2.51, \zeta = 1.0$
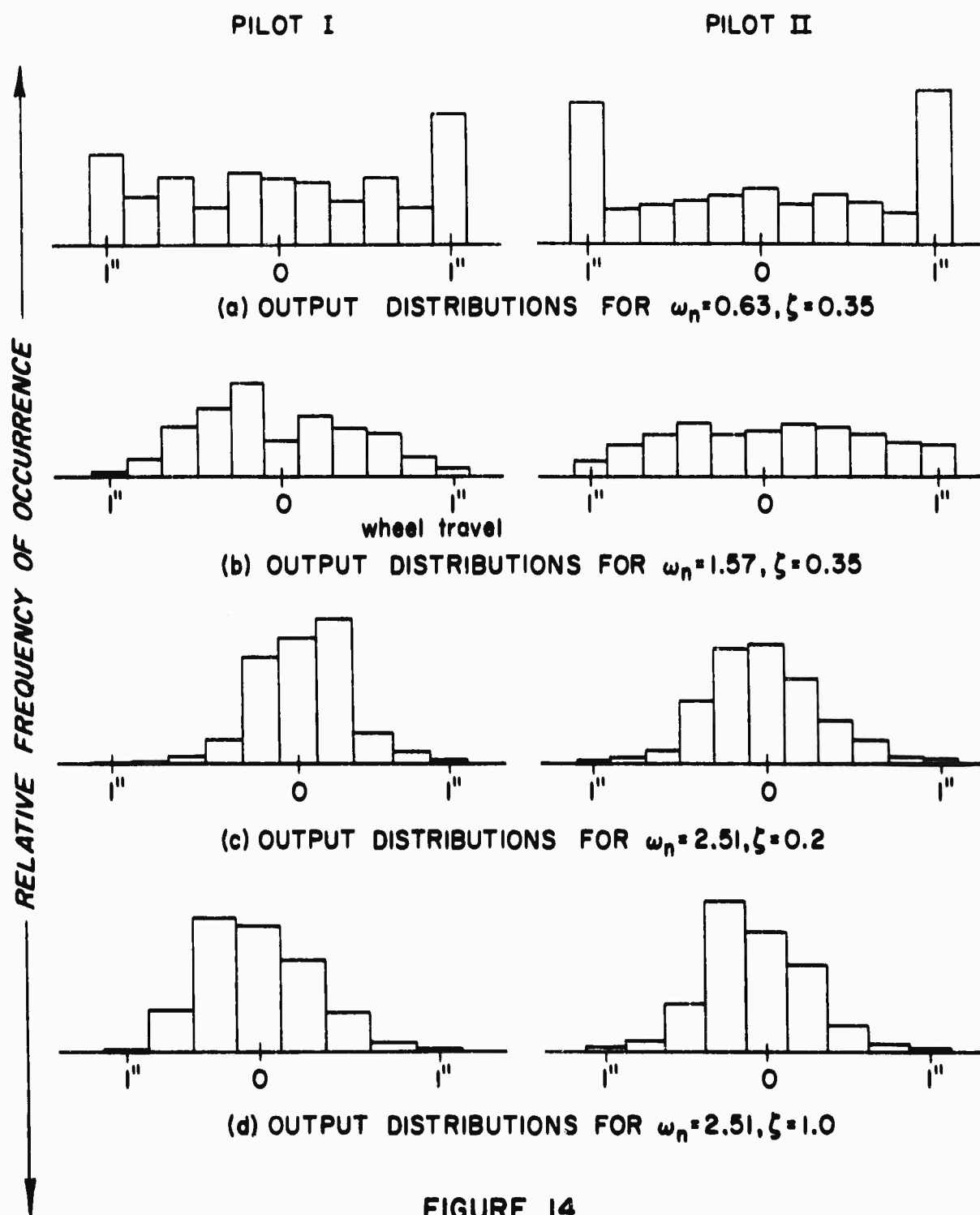
FIGURE 14
PILOT OUTPUT DISTRIBUTIONS FOR SELECTED
SHORT PERIOD CONFIGURATIONS

RELATIVE FREQUENCY OF OCCURRENCE

examination basically directed, as noted in the introduction to this chapter, at determining the closed loop characteristics considered desirable by the pilot.

As a first step in the study, consider that the pilot's equalizing characteristics are nil; that is [see Eq. (1)],

$$Y_p = K_p \frac{e^{-\tau s}}{T_N s + 1} \tag{6}$$

In the low frequency regions of interest the neuromuscular lag time constant, T_N, can be eliminated by changing τ to an "effective" value (Reference 2) which is typically, and consistent with the Hall describing function data, about 0.2. Thus,

$$Y_p \doteq K_p e^{-0.2s} \doteq K_p \frac{(-0.1s + 1)}{(0.1s + 1)} \,^* \tag{7}$$

and the complete open loop transfer function may be written [see Eq. (5)]

$$Y_p Y_c = -5K_p \frac{(0.1s - 1)(0.6s + 1)}{s(0.1s + 1)\left[\left(\frac{s}{\omega_n}\right)^2 + 2\left(\frac{\zeta}{\omega_n}\right)s + 1\right]} \tag{8}$$

The root locus plot for the open loop transfer function of Eq. (8), with unity feedback as in the block diagram of Figure 2, is shown in Figure 16 for $\omega_n = 3.77$, $\zeta = 0.75$. Because of the negative sign of the effective open loop gain, the locus is defined by the zero-degree rather than the customary 180-degree criterion. Increasing pilot gain, K_p, drives the closed loop poles along the locus in the direction of the arrowheads; at zero gain the poles are those of the open loop (symbol X) and at infinite gain they correspond to the open loop zeros (symbol $\odot$). The closed loop poles for the pilot gain actually measured in this particular case (see Table IV) are indicated by the symbol ■.

Similar root loci, again with no pilot equalization, have been constructed for all of the Hall airframe configurations in Table III. The important features of these loci are shown in Figures 17 and 18. In these figures only the incomplete locus emanating from one short period pole is drawn, the remaining portions of the locus, and the additional poles, zeros, high gain behavior, etc., being

-----

*Note that $e^{-\tau s} = \frac{(e^{-\tau s/2})}{(e^{\tau s/2})} \doteq \frac{(1 - \frac{\tau s}{2})}{(1 + \frac{\tau s}{2})}$. For $\tau = 0.20$, this lead-lag approxima-

tion to $e^{-\tau s}$ involves phase errors of less than 3 degrees for frequencies up to 4 rad/sec.
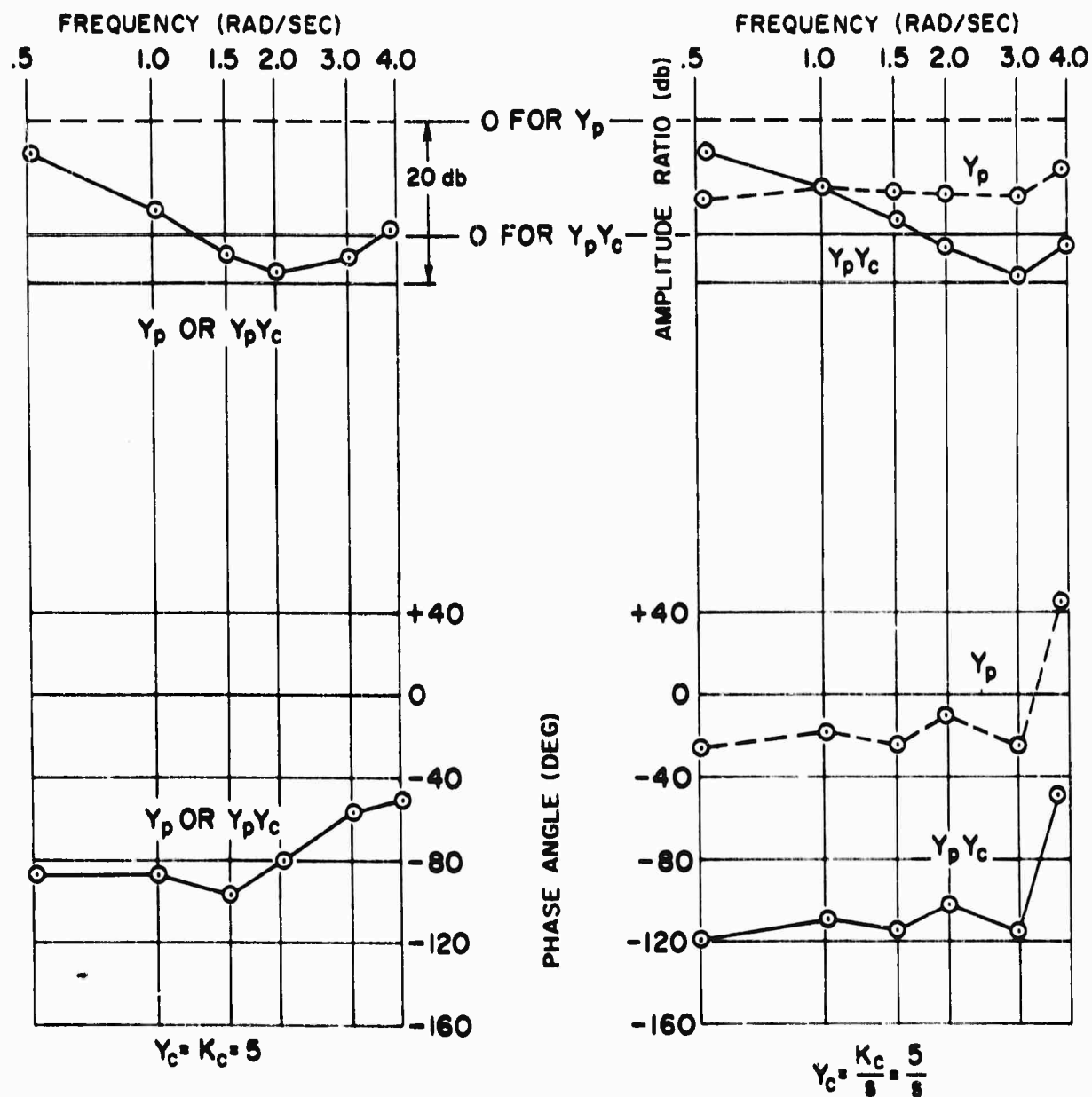
FIGURE 15

DESCRIBING FUNCTIONS FOR HALL CONFIGURATIONS
K_c & K_c/s WITH $K_c = 5$

quite similar or identical to those shown in Figure 16. The values of K_p (lb/rad) corresponding to zero damping (neutral stability) of the closed loop, short period mode are indicated near the imaginary axis. These can be compared with the values of K_p actually adopted (on the average) by the pilot, as given in Table IV. Such a comparison, given in Table V, for configuration groupings corresponding to those of Figures 9-11 shows that a gain ratio based on the simple Y_p form assumed cannot account for the large differences in observed opinion. In fact, certain of the configurations classified as "unacceptable" appear to have gain ratios comparable to those in the "acceptable" category.

TABLE V

APPARENT GAIN MARGINS FOR UNEQUALIZED PILOT MODEL, $Y_p = K_pe^{-0.2s}$

Configuration		Reference Figure	Opinion	Pilot Gain, K_p		Gain Ratio (db)
ω_n	ζ			Actual[1]	Neutral[2] Stability	
1.57	.75	9(a)	Good	254	540	6.5
2.51	1.0	9(a)	Good	269	780	9.2
3.77	.75	9(a)	Good	215	540	8.0
1.57	1.0	9(b)	Acceptable	380	900	7.5
2.51	.5	9(b)	Acceptable	135	340	8.0
6.28	.75	9(b)	Acceptable	339	430	2.0
3.77	.2	10	Poor	170	130	-2.3
6.28	.35	10	Poor	170	205	1.6
1.57	.2	11	Unacceptable	86	110	2.2
1.57	.35	11	Unacceptable	120	215	5.1
2.51	.2	11	Unacceptable	135	110	-1.8
0.63	.35	11	Unacceptable	76	90	1.5
0.63	.75	11	Unacceptable	135	230	4.6
(1) From Table IV. (2) From Figures 17 and 18.						

Consider now the apparent equalizations adopted by the pilot as revealed by the describing function data of Figures 9-11. The "good" configurations [Figure 9(a)] require little, if any, equalization. For these cases the gain ratios of Table V will approximate gain margins, and the stability margins indicated on

FIGURE 16

ROOT LOCUS PLOT FOR $Y_p Y_c$; $Y_p = -K_p \dfrac{(s-10)}{(s+10)}$, $Y_c = \dfrac{42.6(s+1.67)}{s[s^2+2(.75)3.77s+3.77^2]}$
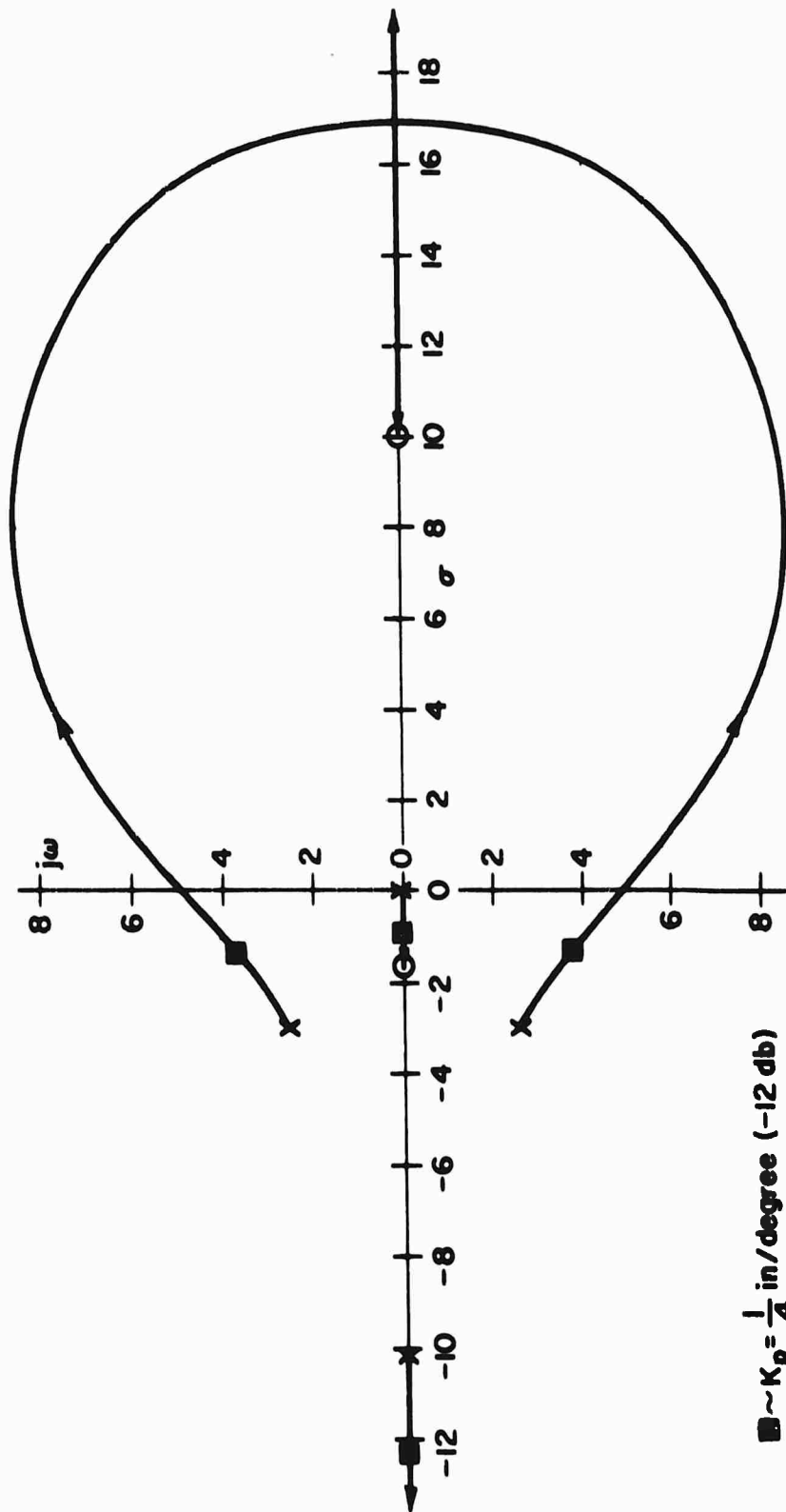
■ ~ $K_p = \dfrac{1}{4}$ in/degree (−12 db)

$= \dfrac{1}{4} \cdot .15$ lb/in $\cdot 57.3 = 2I5$ lb/rad

LEGEND REFERS TO VALUE OF
$\omega_n - \zeta$
ASSOCIATED WITH EACH LOCUS

$K_p(lbs/rad) = 430$
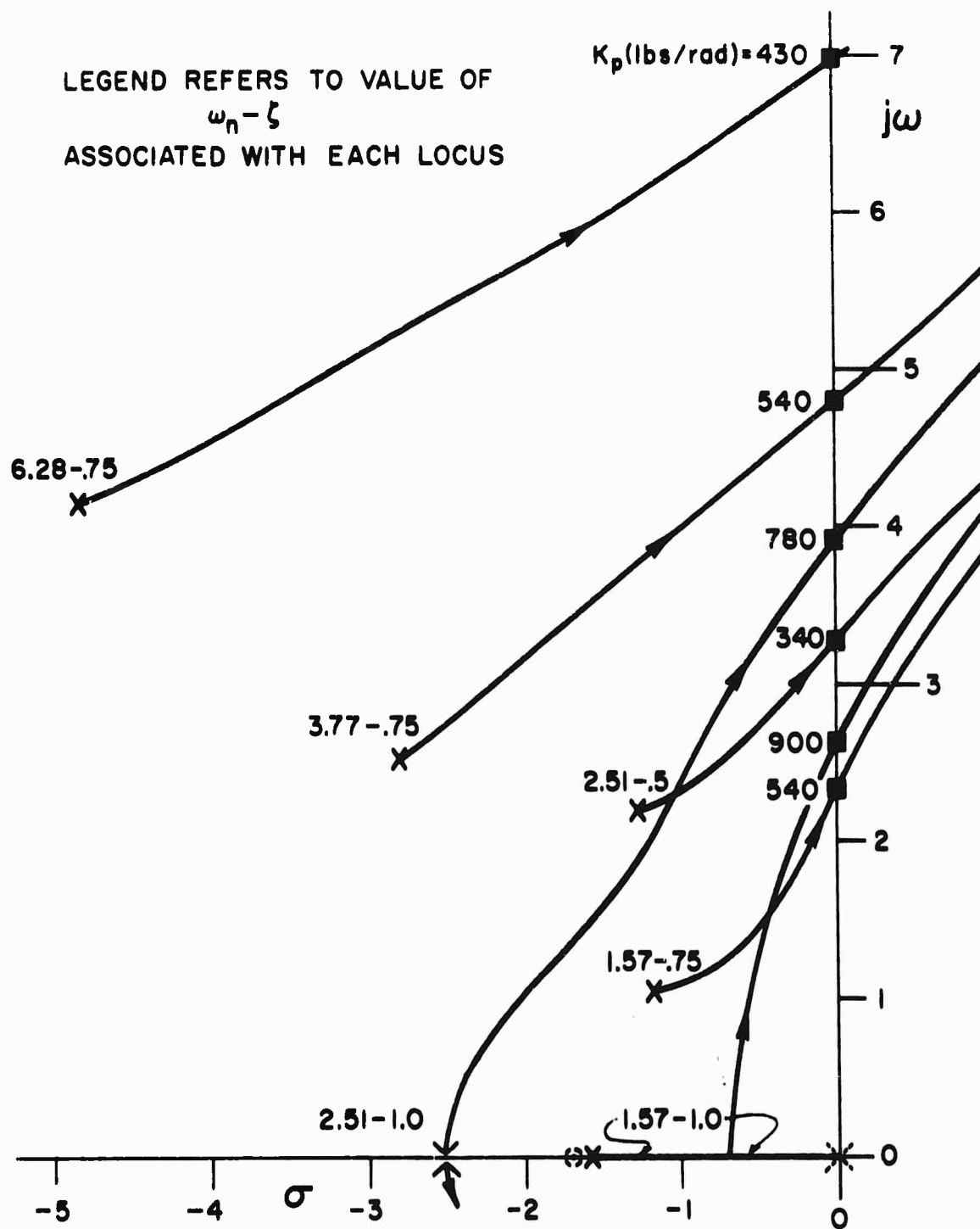
FIGURE 17
SHORT-PERIOD ROOT LOCI FOR THE HALL
"ACCEPTABLE" & "GOOD" CONFIGURATIONS
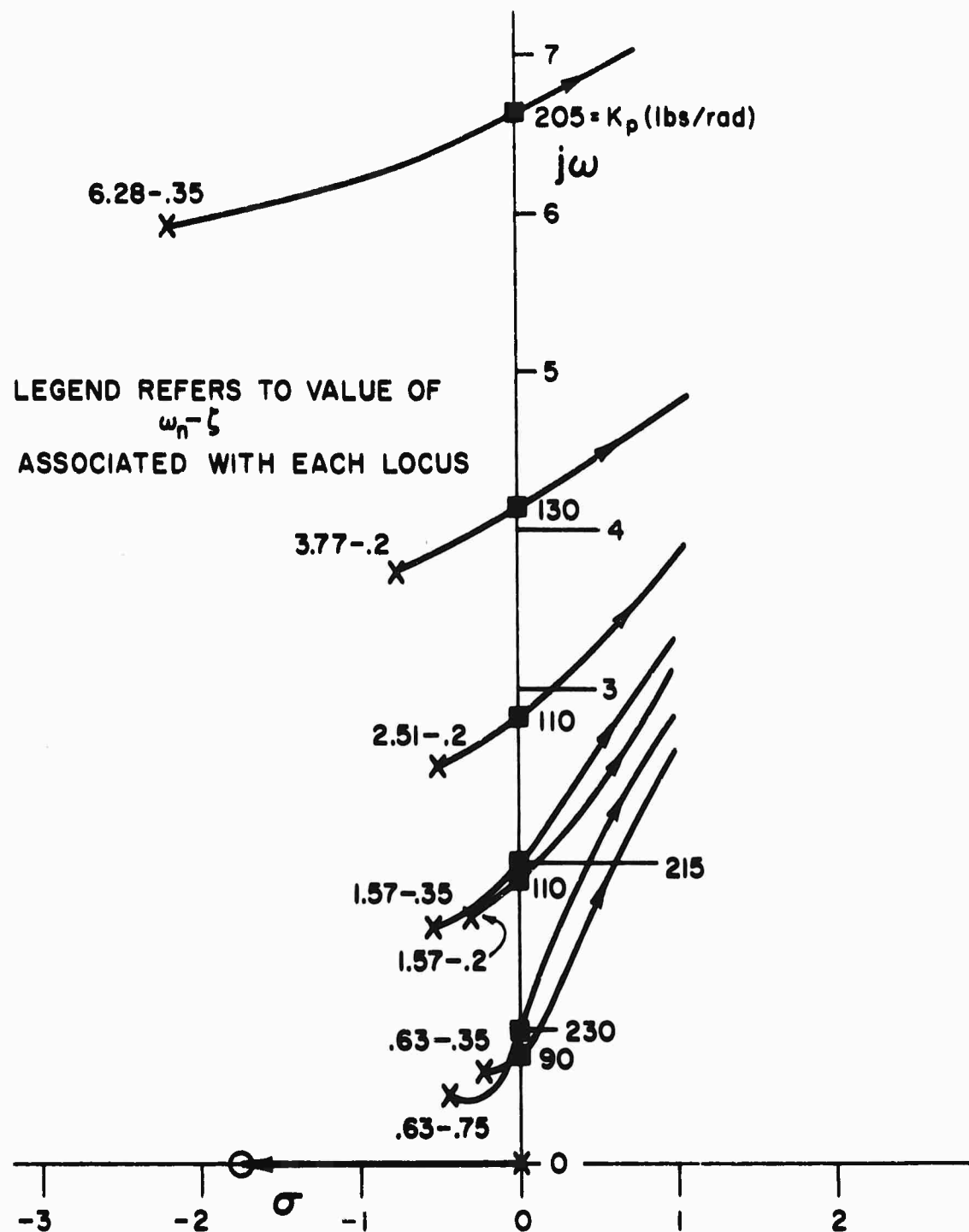
FIGURE 18
SHORT-PERIOD ROOT LOCI FOR THE
HALL "POOR" & "UNACCEPTABLE" CONFIGURATIONS

$$Y_C = \frac{5(0.6s+1)}{s\left[\left(\frac{s}{\omega_n}\right)^2 + 2\left(\frac{\zeta}{\omega_n}\right)s + 1\right]} = \frac{3\omega_n^2(s+1.67)}{s(s^2+2\zeta\omega_n s + \omega_n^2)}$$

LAG-LEAD

SYMBOL	PILOT EQUALIZATION FORM
⊙ ⟶	NO EQUALIZATION
△ ⟶	LAG-LEAD
▽ ⟶	LEAD-LAG
⊡ ⟶	LEAD
✕ ⟶	DOUBLE LEAD

DOUBLE LEAD

LEAD-LAG

FIGURE 19
PILOT EQUALIZATION CHARACTERISTICS AS A FUNCTION OF SHORT-PERIOD COMPLEX ROOTS

this basis are fairly large. Also, the closed loop damping ratios, as inferred by interpolation on the loci of Figure 17, are relatively high. The "acceptable" configurations of Figure 9(b) definitely require some pilot equalization to avoid a marginally stable condition (gain margin < 6 db) and/or improve closed loop damping. The remaining "poor" and "unacceptable" configurations of Figures 10 and 11 are all marginally stable without lead equalization and apparently require progressively increasing equalizing efforts by the pilot. The foregoing observations are summarized in Figure 19, an s-plane representation which indicates the equalization form adopted by the pilot in various regions occupied by the complex short period roots. The short period root points in this figure are coded to correspond to the pilot describing function equalization characteristics of Figures 9-11, and the shaded boundaries define rough areas of approximately similar equalization form as indicated. Figure 20 presents two typical examples of how member sets on this plot fit the actual data. Figure 20(a) is a no-equalization pilot fitted to configuration 2.51-1.0, the highest rated airframe, and Figure 20(b) is a lead-lag fit to configuration .63-.35, the lowest rated of the Hall short period airframes. These curve fits, of course, are only intended to lend some credence to the rough curve fits used to construct the regions shown in Figure 19. The detailed reasons for such adaptation, however, remain to be clarified.

It may be seen from Figure 19 that the boundary between the lag-lead and the lead-lag regions is actually a region where no equalization is adopted. Since such a form represents minimal activity on his part, it can be argued that along this boundary the pilot must be reasonably happy with the closed loop system characteristics; were he not, he would c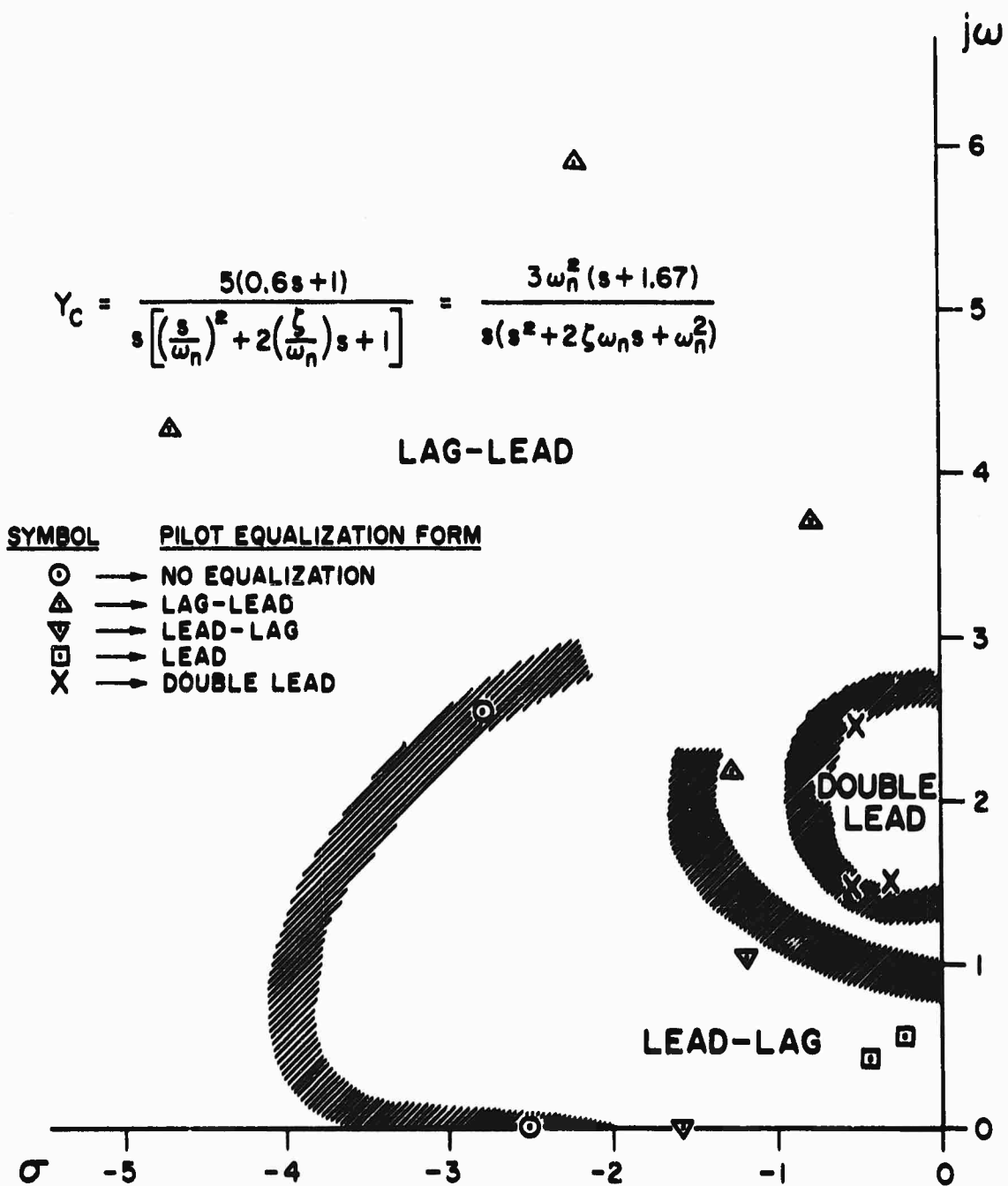ertainly have adopted some equalization in an attempt to improve them. Furthermore, the two data points that fall on this boundary (2.51-1.0 and 3.77-.75) both represent good-opinion configurations (see Table III) which can be associated directly with pilot gain values. These factors reinforce the notion that the pilot is satisfied with the closed loop characteristics. Examining, now, these characteristics for the actual pilot gains observed, Figure 21 shows the low frequency, closed loop pole-zero locations in the upper s-plane (see Figure 16 for the complete set for configuration 3.77-.75). It can be seen that the closed loop denominator time constant in both cases is very nearly the same as the numerator time constant. Under these circumstances these terms tend to cancel each other, and the dominant closed loop mode is the second order with undamped natural frequency and damping ratio ranging from about 2 to 4 and about 0.35 to 0.50, respectively. It is of interest to note that the best possible second order system from the standpoint of minimizing the rms error to a "white noise" input is one with a damping ratio ranging from about 0.4 to 0.7 (the rms error variation is very small throughout this region). It appears that the pilot, in actively attempting to minimize the error presented to him, is adopting approximately the theoretically "correct" equalization in this particular case. On the basis of this one example, it might be hypothesized that the pilot tries to force the closed loop into a particular region which happens to be consistent with the servo criterion for minimizing the rms error.

To examine this hypothesis further, the effect of the pilot-adopted transfer form on the closed loop system was determined for all the test configurations. In each case the loop was closed with the apparent pilot gain listed in Table IV, and an analytical approximation to the equalization consistent with the describing function data. The assumed pilot equalizations used cannot be considered data fits in the sense of those of Reference 2, but are adequate representations of the adopted form. Rather than present all of these analyses, many of which
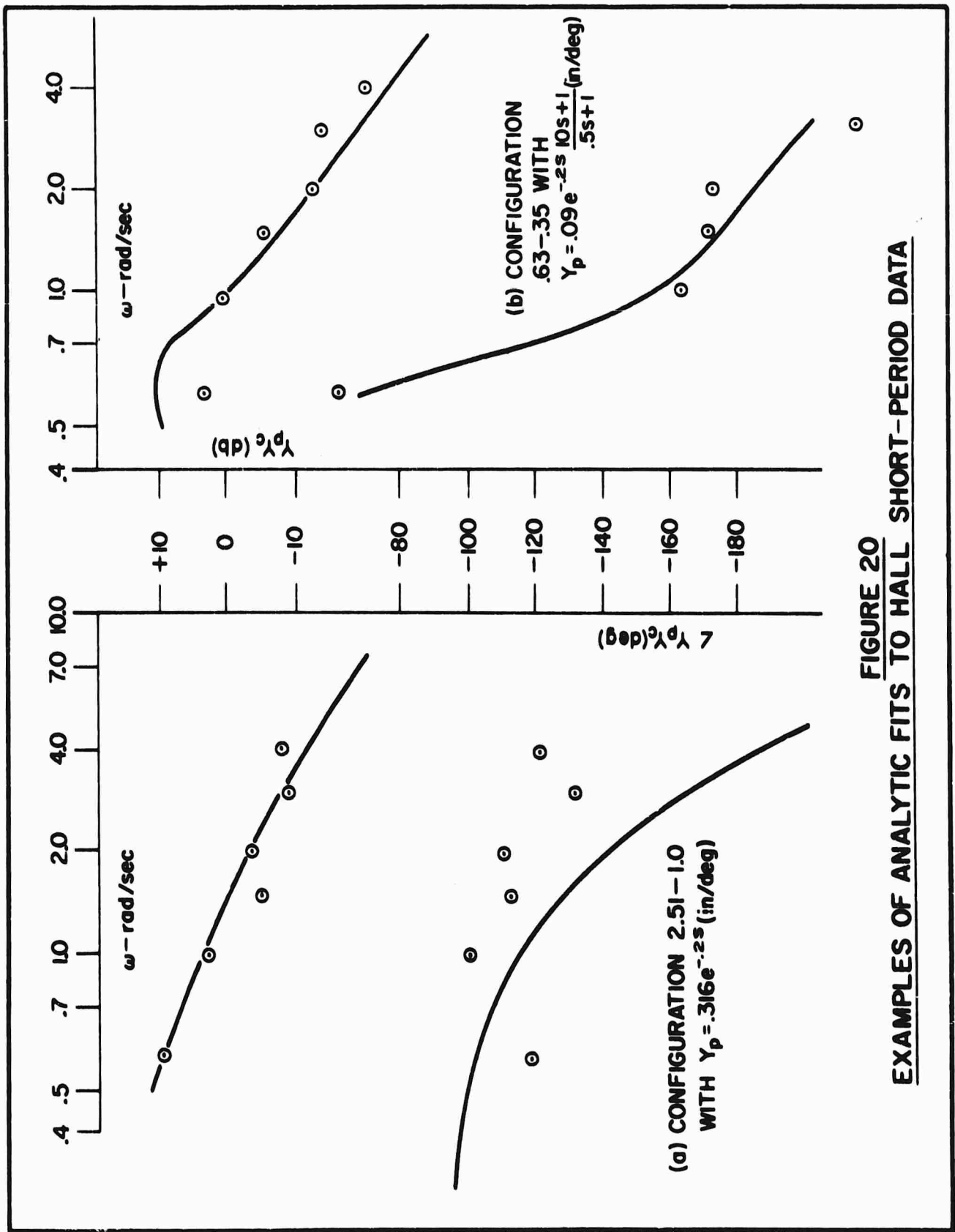
FIGURE 20

EXAMPLES OF ANALYTIC FITS TO HALL SHORT-PERIOD DATA

(a) CONFIGURATION 2.51–1.0
WITH $Y_p = .316e^{-.2s}$ (in/deg)

(b) CONFIGURATION
63–35 WITH
$Y_p = .09e^{-.2s} \dfrac{10s+1}{.5s+1}$ (in/deg)
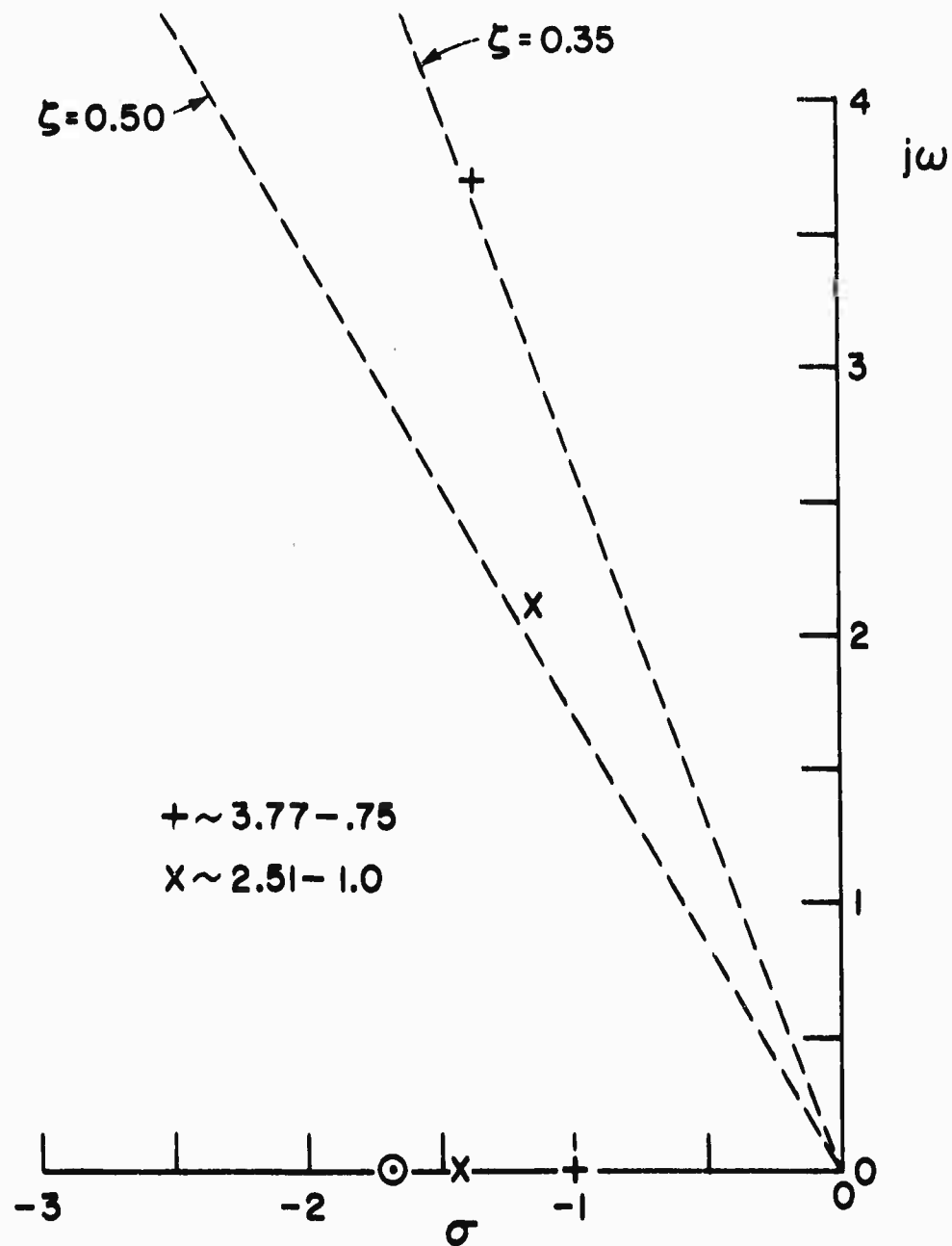
FIGURE 21
LOW FREQUENCY CLOSED-LOOP ROOTS FOR SHORT-PERIOD
CONFIGURATIONS REQUIRING NO PILOT EQUALIZATION

show similar trends, five representative configurations have been selected for the discussion which follows.

Two root loci for each of the five cases are given in Figure 22, one for the approximate equalization actually adopted by the pilot and the other for no equalization. The latter is presented to serve as a possible comparison with the former. Again, as in such preceding plots, only the upper s-plane is presented and in most cases the high frequency behavior is not shown, reference to Figure 16 for the remaining portions of the loci being inferred. In all cases the closed loop poles for the actual gains employed are denoted by the closed square (■) symbol. Also shown (Figure 23) are asymptotic amplitude Bodes for the closed loops. Pertinent comments for each configuration are presented below.

Configuration 6.28-.75. Figure 22(a) —— In both cases shown the closed loop zero (symbol ⊙, since open loop and closed loop zeros are identical) is approximately canceled by the first order closed loop pole. The closed loop system is thus predominantly second order, the effect of the lag insertion being to reduce frequency and increase damping (the heavily damped high frequency mode at $\omega \doteq 9$ is outside the frequency range of interest).

Configuration 1.57-1.0. Figure 22(b) —— Again the first orders nearly cancel in both cases and the second order damping is improved with equalization, with, however, an accompanying increase in frequency.

Configuration 3.77-.2. Figure 22(c) —— The first order cancellations noted in the preceding cases are not apparent here and the closed loop is higher than second order. However, the lag-lead equalization does improve the damping and reduce the frequency of the second order short period mode. The pass band characteristics are also improved (see Figure 23) in that the first break point is increased in frequency. A double lag would result in a better system, but there is little evidence that a human pilot would adopt this form except in most unusual circumstances.

Configuration .63-.35. Figure 22(d) —— Here again the first order terms are largely self-canceling and both systems are basically second order. The effect of lead-lag equalization is to increase both frequency and damping.

Configuration 1.57-.35. Figure 22(e) —— In this case the double lead equalization has a strongly beneficial effect on the closed loop short period damping, but it results in considerable low frequency "droop" (see Figure 23).

For all the representative cases shown, the effect of the indicated pilot equalization is to increase the closed loop short period damping (over the non-equalized case). For configurations 6.28-.75 and 1.57-1.0, rated "acceptable" or "good," the resulting damping coefficients are close to being "optimum" from the standpoint of minimum rms error. Adding the closed loop poles of these cases, including one point for the nonequalized pilot of Figure 22(b) which is assumed to represent an "undesirable" situation since the pilot actually adopted equalization, to those of Figure 21 defines the "desirable" and "optimum" region shown in Figure 24.
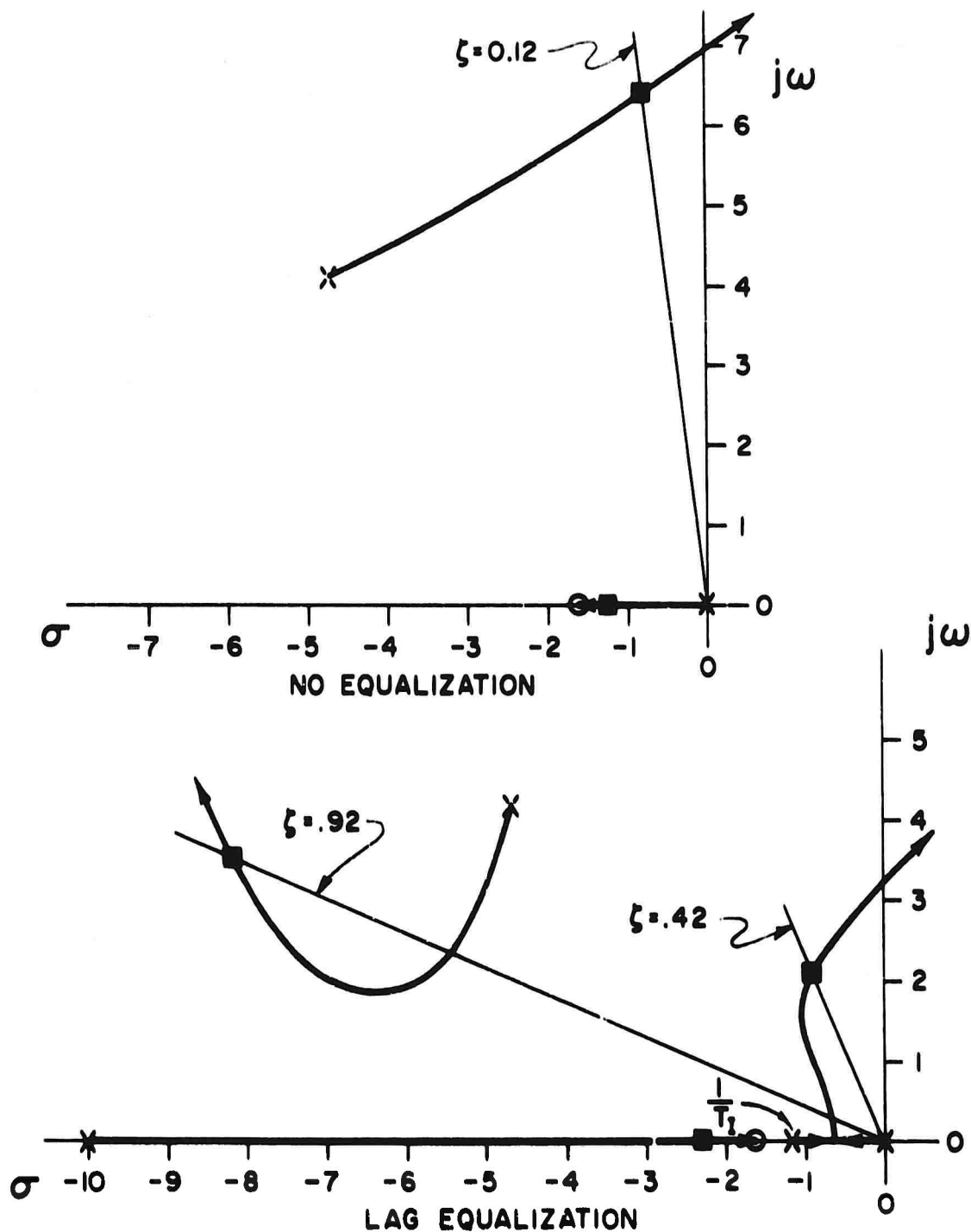
(a) CONFIGURATION 6.28-.75

FIGURE 22

ROOT LOCI FOR TWO FORMS OF PILOT EQUALIZATION & CLOSED-LOOP ROOTS FOR BOTH AT THE OBSERVED PILOT GAIN

NO EQUALIZATION

LEAD-LAG EQUALIZATION
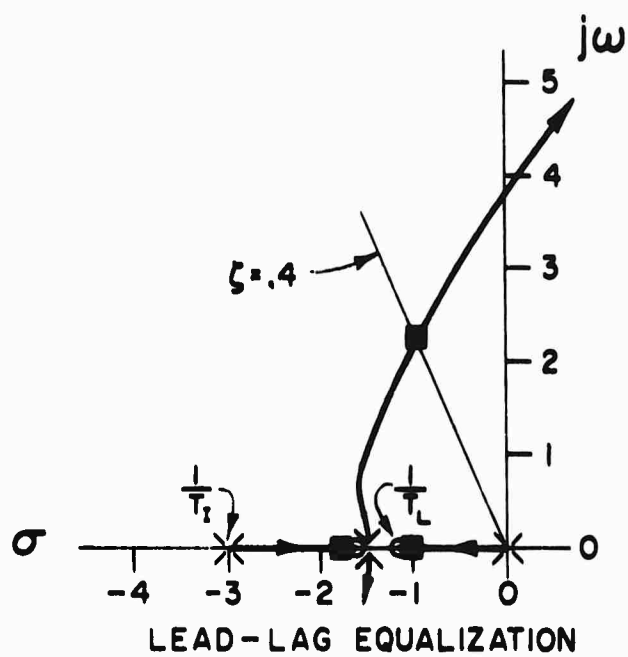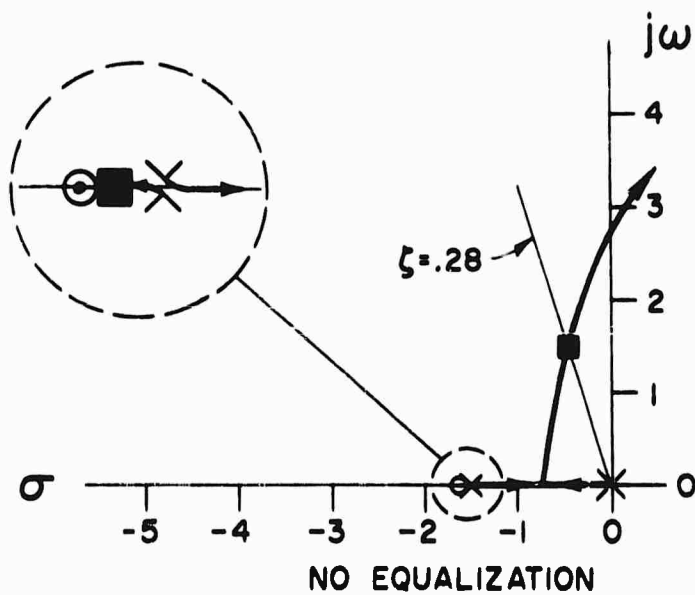
(b) CONFIGURATION 1.57-1.0

FIGURE 22 (CONTINUED)
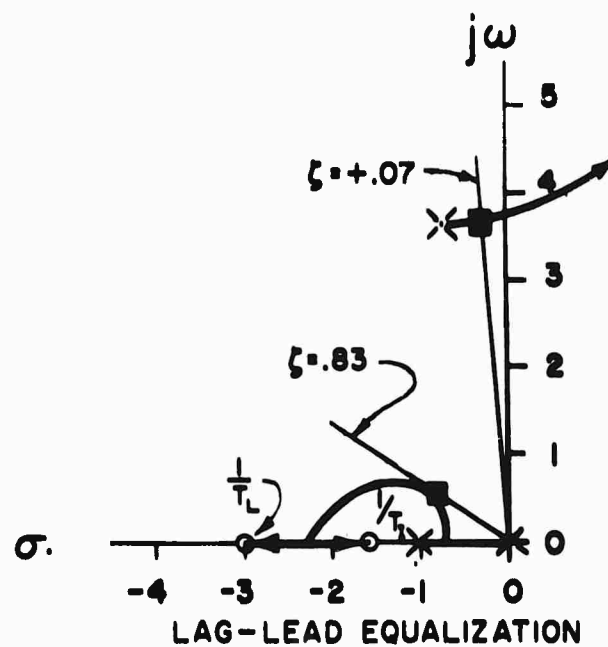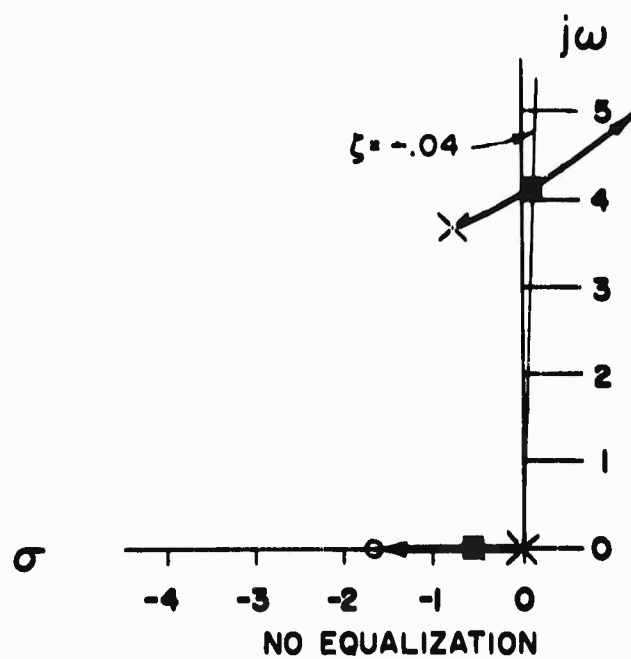
(c) CONFIGURATION 3.77-.2

FIGURE 22 (CONTINUED)
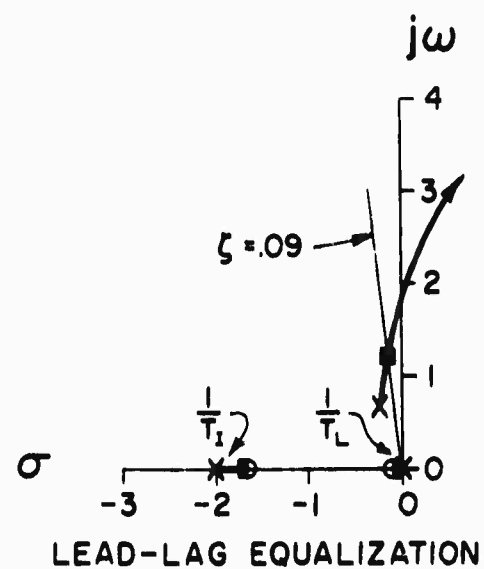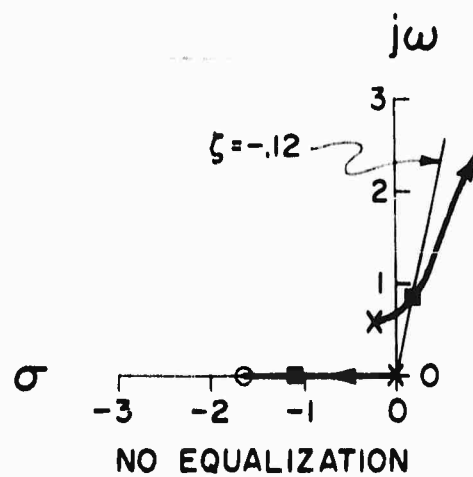
(d) CONFIGURATION .63−.35

FIGURE 22 (CONTINUED)

NO EQUALIZATION

DOUBLE LEAD EQUALIZATION
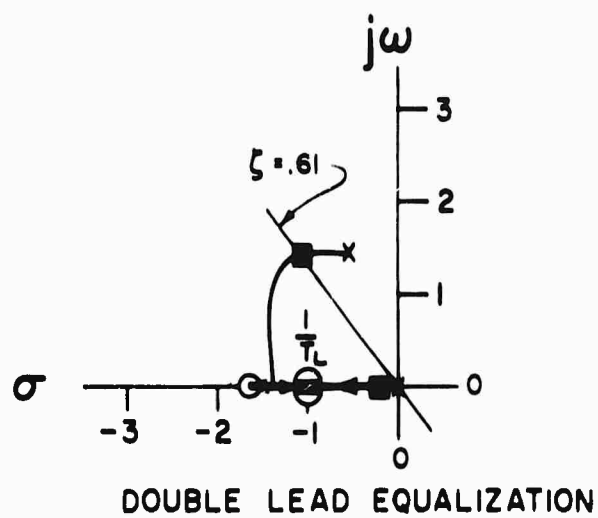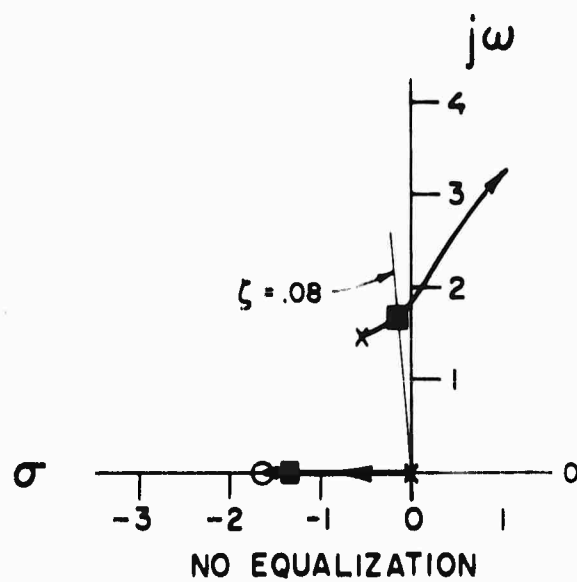
(e) CONFIGURATION 1.57−.35

FIGURE 22 (CONCLUDED)
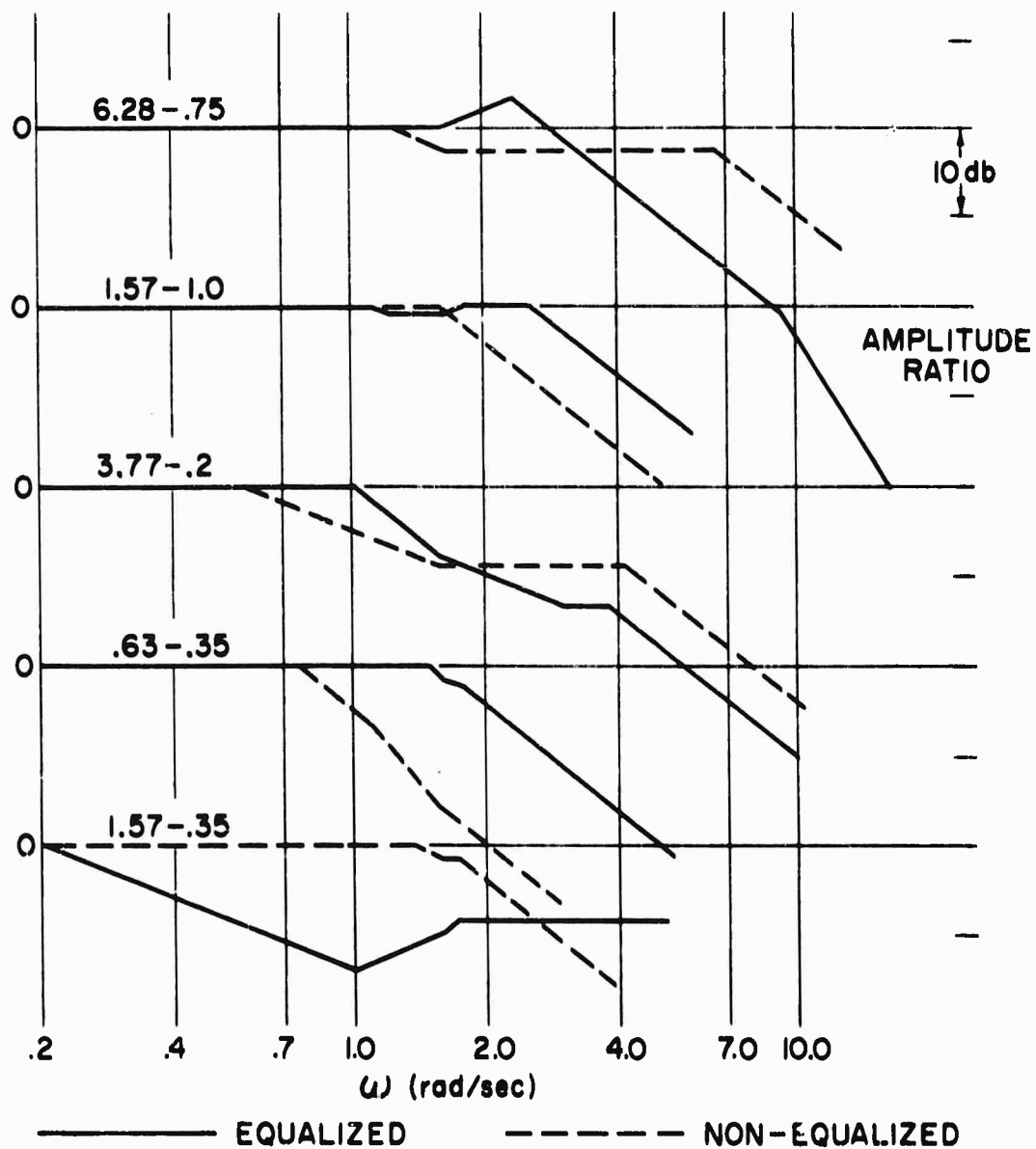
FIGURE 23

CLOSED LOOP AMPLITUDE BODE PLOTS, $\left|\dfrac{Y_p Y_c}{1 + Y_p Y_c}\right|$,

FOR THE SELECTED CONFIGURATIONS OF FIGURE 22
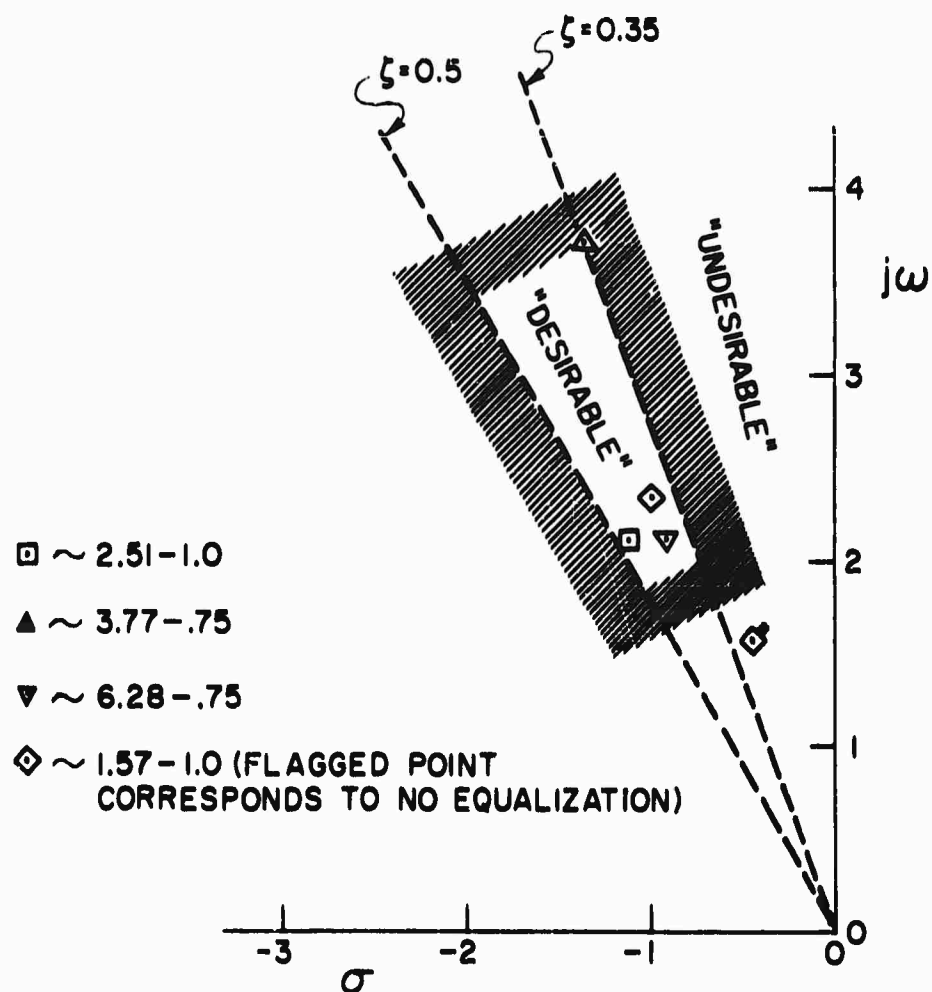
FIGURE 24
"DESIRABLE" CLOSED LOOP SECOND-ORDER CHARACTERISTICS DEDUCED USING ANALYTIC EXPRESSIONS FOR Y_p CONSISTENT WITH DESCRIBING FUNCTION DATA

A. INTRODUCTION

The preceding chapters present in considerable detail certain aspects of observed pilot behavior in closed loop control situations. In addition certain correlations between pilot opinion and closed loop and/or pilot dynamic characteristics are shown. These correlations, and the pilot behavior model, can now be applied to theoretical investigations of longitudinal handling qualities. Such investigations, while they shed some additional light on areas already covered by handling quality tests, are especially illuminating for situations which have not yet been covered experimentally. In the former instances the "findings" of the theory are not nearly as complete with regard to the delineation of the fine-grain pilot-opinion regions as are the specific tests. This is not surprising in view of the paucity of data which allow useful correlation of pilot opinion with the objective opinion factors detailed in Chapter III; nevertheless the gross implications and trends exhibited by the test data are predicted by the theory. In the latter instances, the theory serves to readily identify areas of possible difficulty which have not yet been subjected to experimental treatment.

The initial theoretical examination, detailed in the section immediately following, is directed at the conventional, damped second order, short period mode. More specifically it is directed at the short period configurations investigated by Hall. In this sense the Hall data are reused to serve as a comparison with theoretical conclusions which stem in part (as concerns criteria, etc.) from the same data. The fact that the Hall opinion data differ somewhat from similar data obtained in flight is investigated in the next section and is shown to be consistent with theoretical considerations.

On the basis of this demonstrated usefulness of the servo approach, it is then pertinent and permissible to apply it to handling qualities problems which may be quite "radical" and for which little, if any, dynamic response or handling qualities data exist. These problems include gross variations of the numerator time constant and the aperiodic divergence resulting from negative maneuver margin. Preliminary consideration of the e more unusual aspects of short period handling qualities is the subject of the later sections.

B. THEORETICAL ASPECTS OF CONVENTIONAL SHORT PERIOD OPINION BOUNDARIES

The available pilot model and associated opinion factors, together with conventional servoanalysis techniques, can be used to predict certain boundaries similar to those (found experimentally) in Figure 30. In particular, those short period characteristics which do not involve equalization efforts on the part of the pilot can be easily delineated. The general approach involves closing the loop with a nonequalized pilot describing function and then checking the closed loop performance to see if it meets the criteria established in Chapters II and III. The short period characteristics for which these criteria can just be met form a boundary beyond which the pilot will adopt equalization. If the controlled element gain has been chosen so that the resulting pilot gain

is in the "good" region (see, e.g., Figure 7), then the pilot will classify all configurations within the boundary as "good." For points outside the boundary the form and magnitude of pilot equalization required to meet the criteria give a relative opinion gradation (i.e., the pilot will prefer a small amount of lag to a large double lead, etc.).

The short period dynamics selected for this example are those used by Hall so that the resulting system-derived boundaries can then be checked by Hall's experimental points. Therefore the aircraft short period lead time-constant, T_{θ_2}, is fixed at a value of 0.60 seconds (representative of normal lift curve slopes similar to that of the Navion airplane used by Hall), and the short period frequency and damping are varied over a range covering most aircraft with positive static margins. The pilot model is a pure gain plus an "effective" reaction time delay (which includes neuromuscular lag), and the open loop transfer function is then

$$Y_p Y_c \;=\; \frac{K_p K_c e^{-\tau s}(0.6s + 1)}{s\left[\left(\frac{s}{\omega_{sp}}\right)^2 + \frac{2\zeta_{sp}}{\omega_{sp}}\,s + 1\right]}$$

or, alternatively, $\qquad\qquad\qquad\qquad\qquad\qquad\qquad\qquad\qquad\qquad$ (9)

$$Y_p Y_c \;\doteq\; \frac{K_p K_c(0.6s + 1)(-\frac{\tau}{2}\,s + 1)}{s(\frac{\tau}{2}\,s + 1)\left[\left(\frac{s}{\omega_{sp}}\right)^2 + \frac{2\zeta_{sp}}{\omega_{sp}}\,s + 1\right]}$$

The gain crossover criterion is a constant phase margin, φ_m, and the effect of varying its magnitude is considered.

The general procedure of these system surveys is to vary the short period frequency and damping and see how the closed loop roots are affected. Generic families of Bode plots and root loci are used, following the methods detailed in Reference 5. For the cases investigated here, the $Y(j\omega)$ and $Y(-\sigma)$ Bode diagrams give sufficient information so no root locus plots are necessary. The specific steps followed are outlined below and include references to a detailed example for $\omega_{sp} = 3.33$ radians/second, $\zeta_{sp} = 0.7$, $\tau = 0.2$ seconds, and $\varphi_m = 60°$. These steps are as follows:

1. Construct the asymptotic Bode plot for the transfer function(s) under consideration. (See Figure 25 for the example.)

2. Locate the 60-degree phase margin open loop crossover frequency (Point ① on the diagram). This locates the zero-db gain crossover on the $Y(j\omega)$ plot (Point ②). Note that the actual departure of $Y(j\omega)$ from the asymptote must be used.

3. Construct the $Y(-\sigma)$ plot in the region near the crossover gain. The intersections of the zero-db gain line with this "sigma" Bode locate the closed loop real roots; $1/T_{CL_1}$ (Point ③) and $1/T_{CL_2}$ (Point ④).
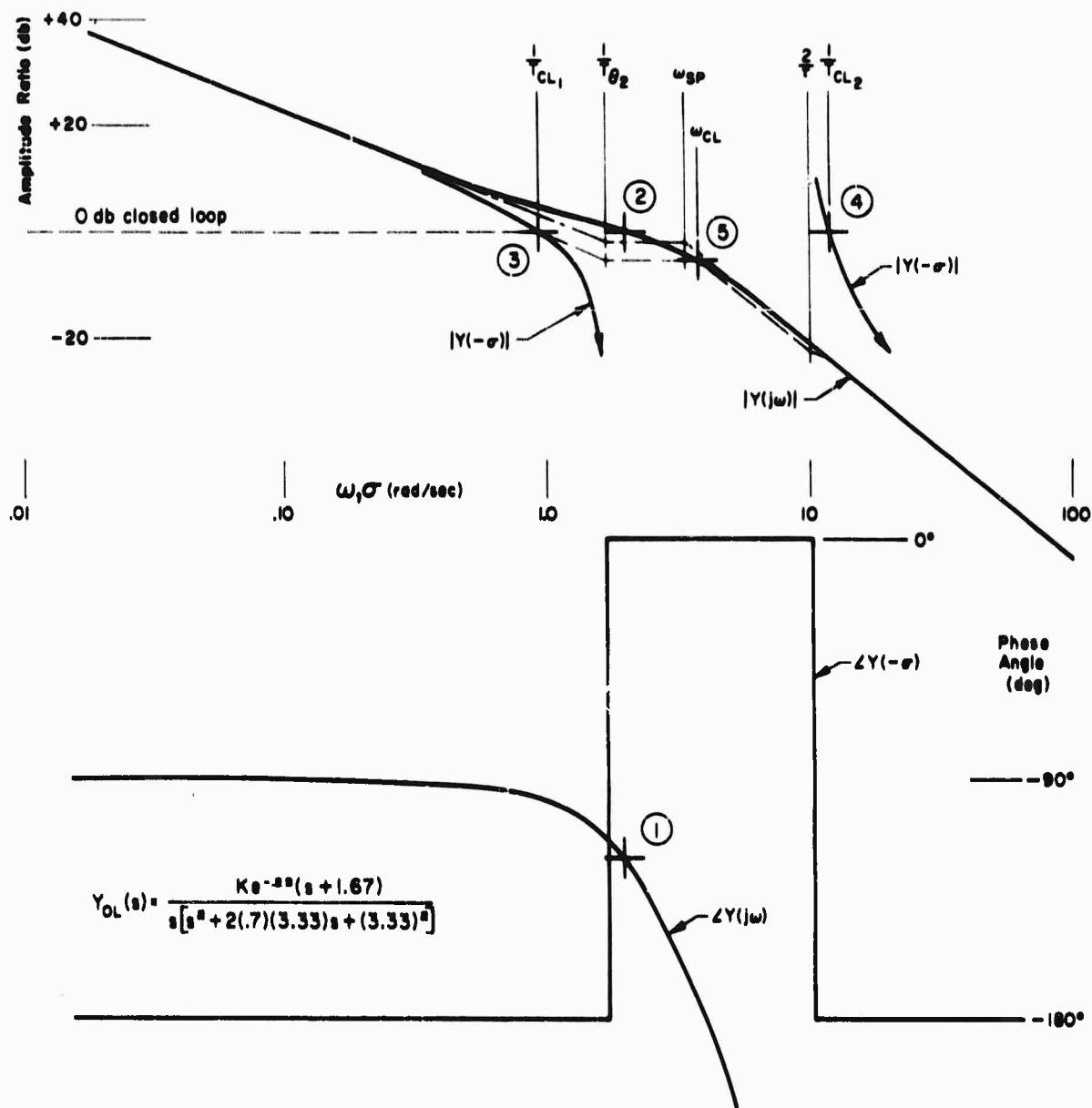
FIGURE 25
SYSTEM SURVEY FOR $\omega_{sp} = 3.33$, $\zeta_{sp} = .7$
NON-EQUALIZED PILOT, $\phi_m = 60°$

$$Y_{OL}(s) = \frac{Ke^{-s}(s+1.67)}{s\left[s^2 + 2(.7)(3.33)s + (3.33)^2\right]}$$

4. Locate the oscillatory closed loop roots, ω_{CL} (Point ⑤).
    In this case the property that the open and closed loop high
    frequency asymptotes are identical is used to locate the ω_{CL}
    asymptotic break point. Since both closed loop real roots
    are known, and since the closed loop low frequency and high
    frequency asymptotes are known, it is possible to construct
    the complete closed loop asymptotic plot by working from both
    ends to locate the unknown break point frequency somewhere in
    the middle.

5. Calculate ζ_{CL}. For this case, the property that the sum of
    the denominator real parts of the closed loop roots is equal
    to the sum of the real parts of the open loop denominator
    roots (always true when the denominator is two or more orders
    higher than the numerator) is used to calculate ζ_{CL}.

$$\zeta_{CL} = \frac{2\zeta_{sp}\omega_{sp} + \frac{2}{\tau} - \frac{1}{T_{CL_1}} - \frac{1}{T_{CL_2}}}{2\omega_{CL}}$$

This completes the system analysis for this particular frequency and damping
ratio. Similar analyses must be performed for other frequencies and other damp-
ing ratios (note that the same plot may be used to vary the damping since the
asymptotes are not a function of the damping ratio). The object of these
analyses is to obtain sufficient information about the closed loop performance
as a function of airframe short period characteristics to be able to determine
where low frequency response and oscillatory damping begin to deteriorate.

As regards the adequacy of the low frequency response, there are three
possible dynamic parameters which must be checked. The first is the crossover
frequency, ω_c, which, as noted in Chapter II, must be greater than the forcing
function cutoff frequency, ω_{co}. The second is the value of the closed loop
time constant, T_{CL_1}, which must be sufficiently small so that objectionable low
frequency "droop" effects are not encountered. The third is the value of ω_{CL}
which, for those cases where it is lower than $1/T_{CL_1}$, becomes the "droop-
producing" parameter. Thus, low frequency response is considered marginal when

$$\omega_c \doteq 1.0 \text{ radians/second}$$

$$\frac{1}{T_{CL_1}} \doteq 0.8 \text{ radians/second}$$

$$\omega_{CL} \doteq 0.8 \text{ radians/second}$$

The criterion for marginal damping of the closed loop second order is
$\zeta_{CL} = 0.35$ in accordance with the findings of Chapter III. These criteria lead
to the various boundaries shown in Figure 26. Since airframe roots falling out-
side of any of these boundaries will require pilot equalization, they can be
consolidated, as in Figure 27, into a single boundary. The data points shown
in this figure are the Hall simulator results and indicate both pilot opinion
of the configuration and his adopted equalization. These points tend to verify
the predicted nonequalized boundary. This boundary, as drawn, might be con-
sidered a sharp dividing line between good and not so good airframes, but two
possible influences tend to blur this line. The first is the fact that the
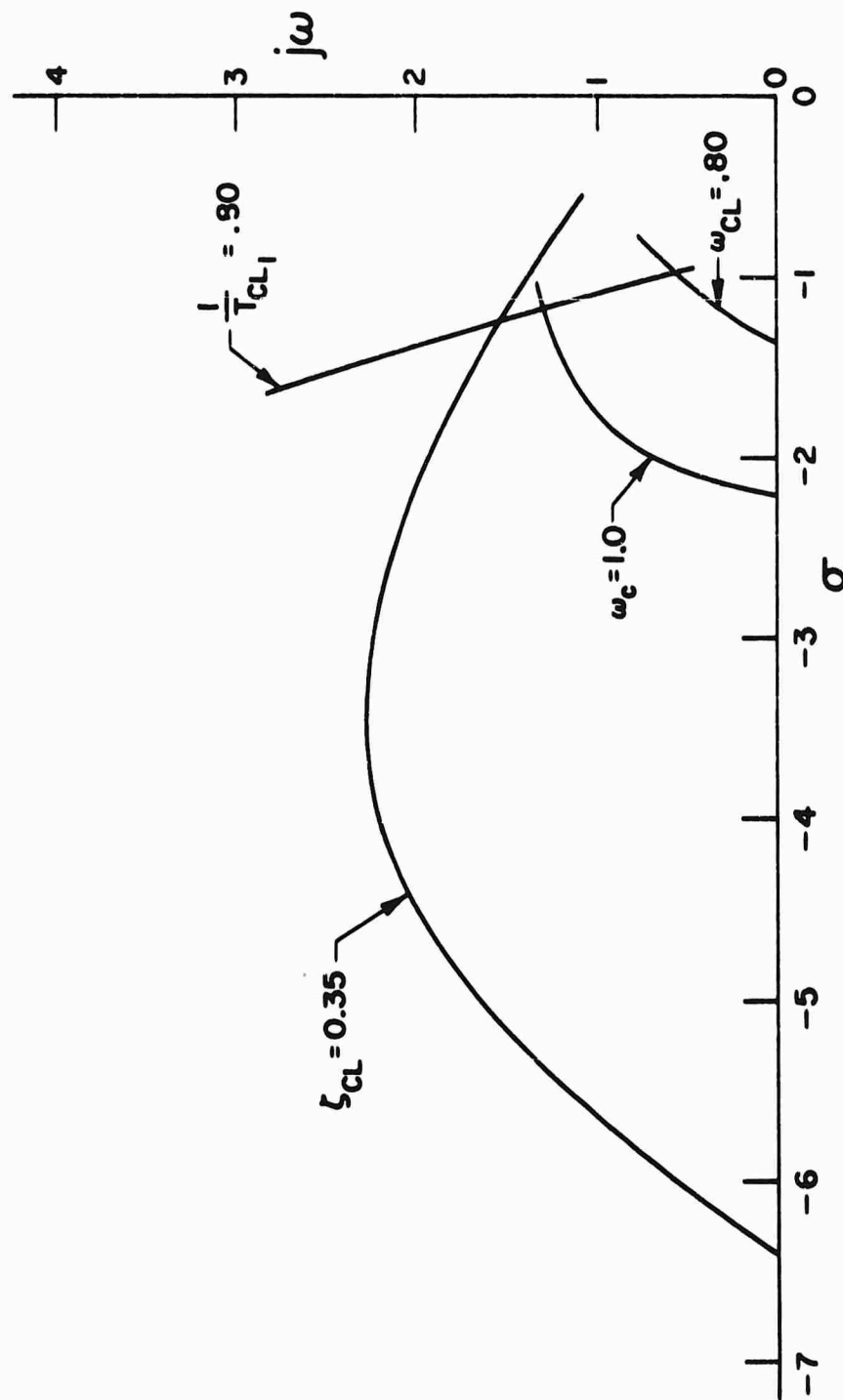line does depend to some extent on the criteria and reaction times used to

FIGURE 26

BOUNDARIES SHOWING CLOSED LOOP CRITERIA

FOR NON-EQUALIZED PILOT; $\tau = .2$ sec, $\phi_m = 60°$, $^1/\tau_{\theta_2} = 1.67$

FIGURE 27

COMPARISON OF THEORETICAL NON−EQUALIZED BOUNDARY WITH HALL MEASURED DATA; $\tau = .2\,\text{sec}, \phi_m = 60°, 1/T_{\theta_2} = 1.67$

construct it. The second is the fact that small amounts of equalization will not be of particular consequence as concerns the pilot's opinion of the "goodness" of a particular configuration. Both these influences are discussed below.

The effect of increasing the phase margin criterion from 60 to 80 degrees, for a $\tau = 0.2$ seconds, is shown in Figure 28. While the high frequency portions of the composite boundaries are not much different (within 15-20 percent), there is a major shift in the low frequency boundary which amounts to about a 100-percent change. With reference to this major effect it should be noted that the data of Figure 5 show a stratification of phase margin with frequency. Thus, phase margins lower than the mean value of 80 degrees are largely associated with frequencies less than about 2.0 radians/second and vice versa. This implies that the low frequency shift of the $\varphi_m = 80$ degrees boundary in Figure 28 is unrealistically drastic, because, at least in this region, the pilot seems disposed to accept phase margins of about 60 degrees. Since, further, the effects of phase margin on the high frequency portions of the boundary are relatively small, the boundaries corresponding to $\varphi_m = 60$ degrees seem to be a reasonable compromise.

The effect of a spread in τ from 0.2 to 0.4, values covering the experimental extremes, is shown in Figure 29 for a phase margin of 60 degrees. Although the effective value of τ deduced from the Hall simulator experiments is close to 0.2, flight test values (Reference 4) are closer to 0.4. Thus the general (for $T_{\theta_2} = 0.6$) nonequalized boundary is blurred to this extent and the outer and inner edges of the blurred region represent expected differences between simulator and flight test results.

In practice the nonequalized boundaries should be considered as guidelines to the shape of the "best airframe" region rather than as specific dividing lines between regions of "good" and "acceptable" configurations. Although the actual boundary is thus a broad brush one, the area enclosed will definitely be the region of optimum flying qualities. Moving out of this region involves varying forms and degrees of pilot equalization with corresponding degradations in opinion. Servo theory, in conjunction with the pilot model and adjustment rules, can be used to predict the approximate required changes in equalization.

It appears, therefore, that closed loop analysis, assuming the simple pilot model and criteria proposed in Chapters II and III, can serve to identify the main aspects of attitude-control handling qualities. This statement certainly holds for airframes with conventional short period dynamics and nominal numerator time constants as "flown" in a fixed-base simulator. Whether or not it also applies to flight-test-determined handling qualities is the question considered in the next section.
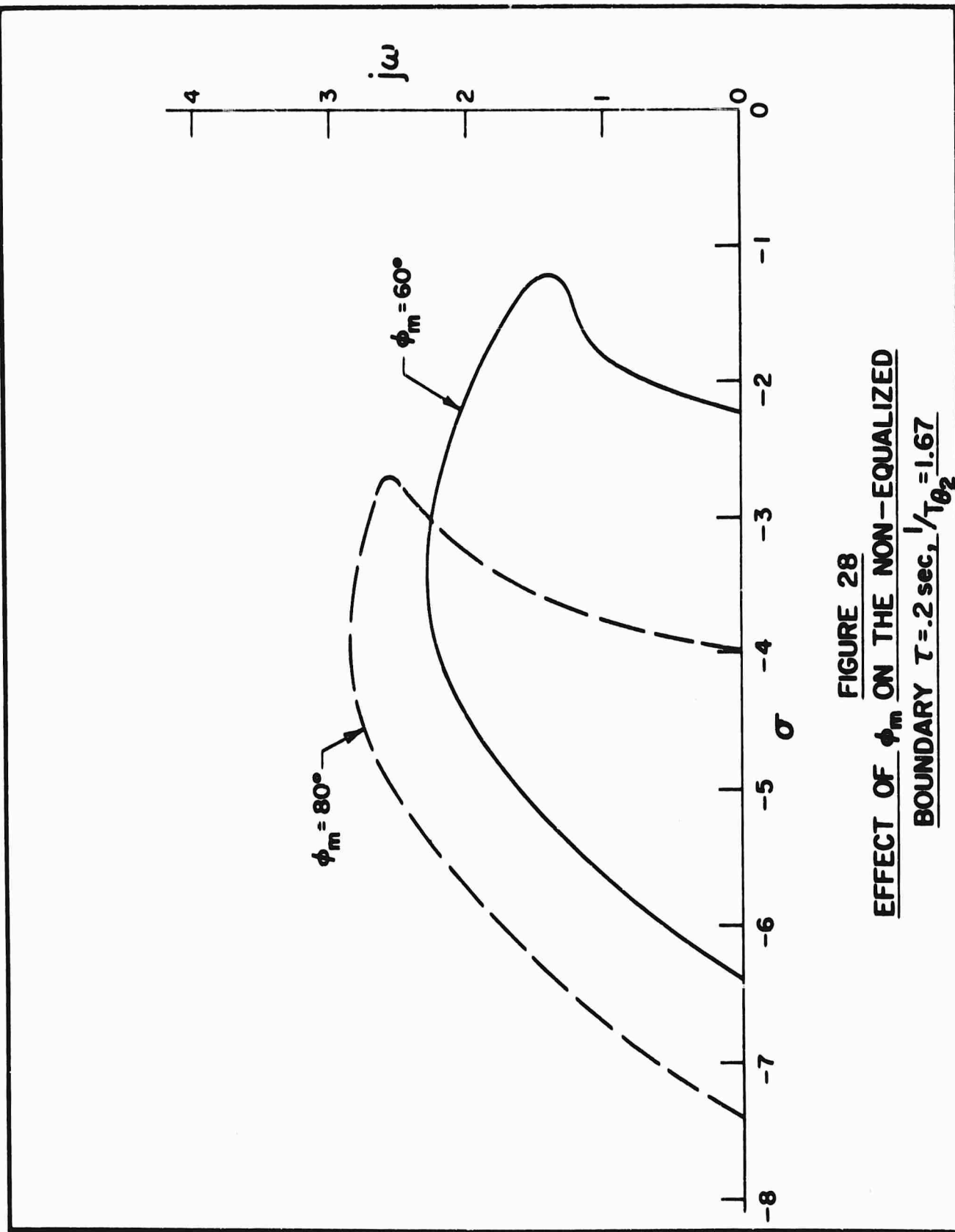
FIGURE 28

EFFECT OF ϕ_m ON THE NON-EQUALIZED

BOUNDARY $T = .2$ sec, $\frac{1}{T\theta_2} = 1.67$
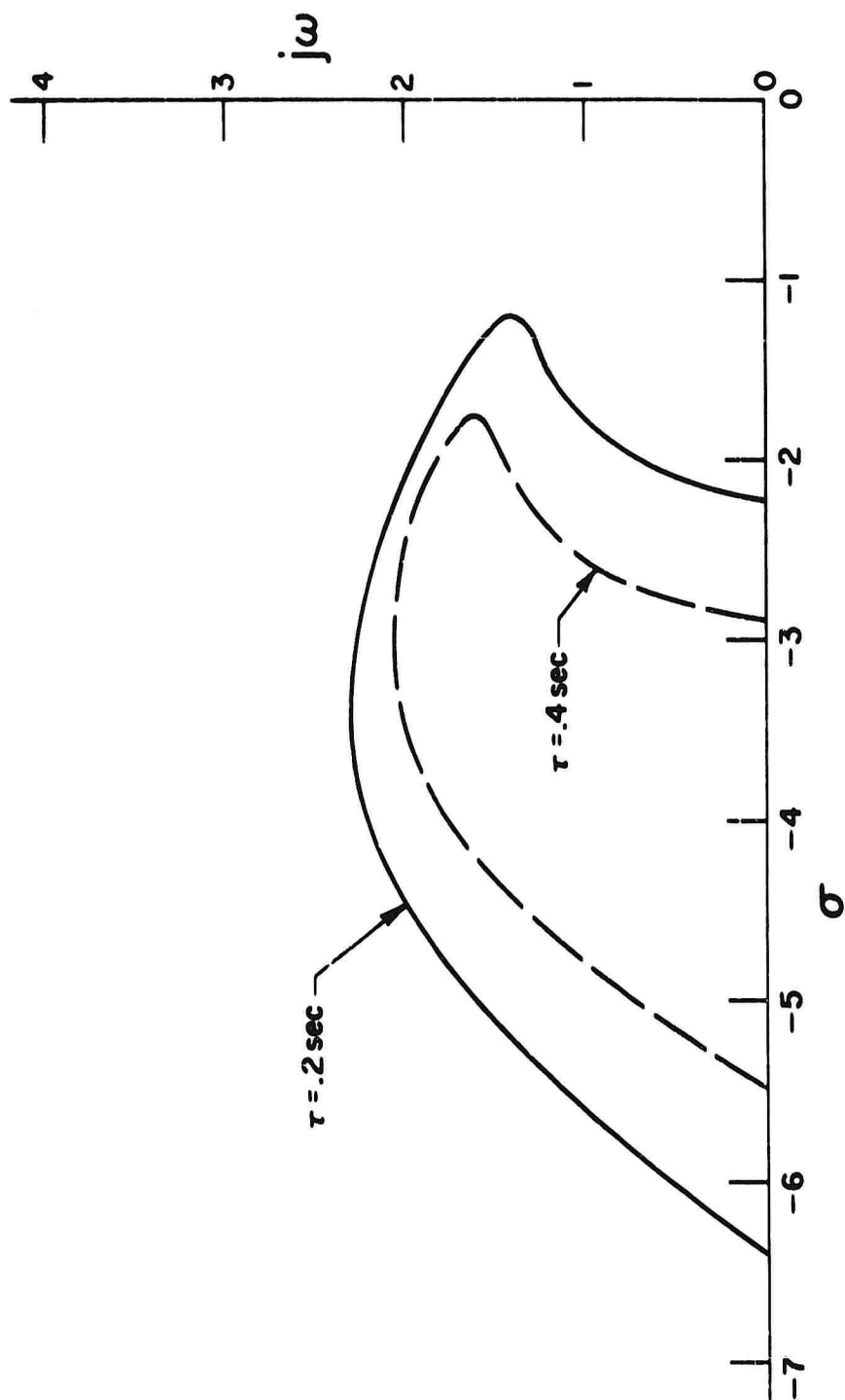
FIGURE 29

EFFECT OF τ ON THE NON–EQUALIZED BOUNDARY $\phi_m = 60°$, $\frac{1}{\tau}_{\theta_2} = 1.67$

$\tau = .4\,sec$

$\tau = .2\,sec$
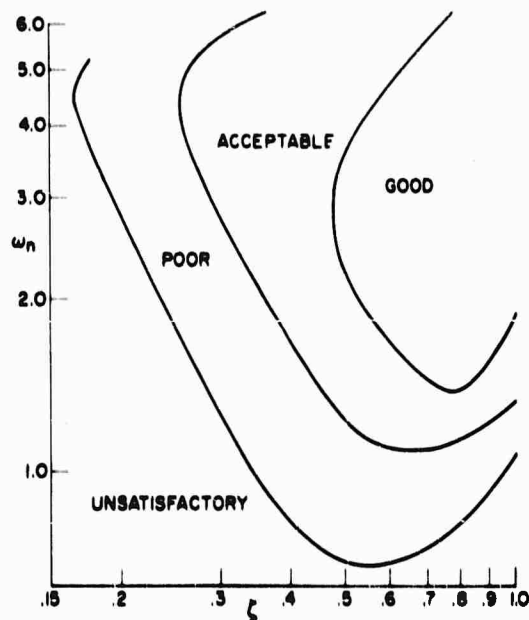
(a) FIXED-BASE SIMULATOR:
AVERAGED HALL DATA (REF. 3)
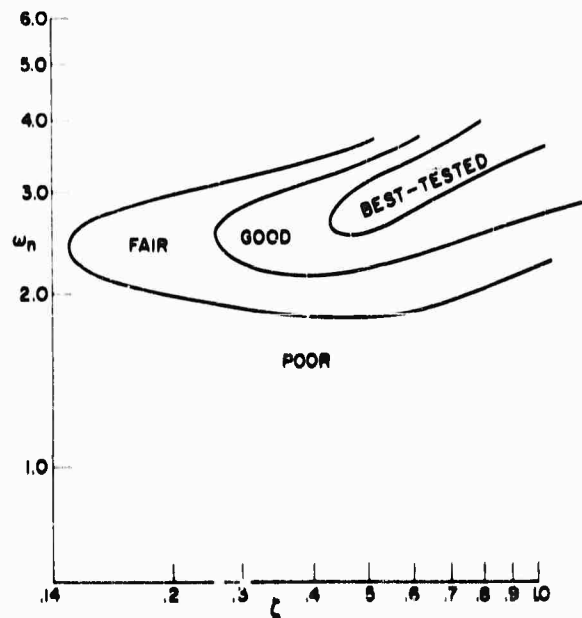
(b) VARIABLE-STABILITY LIGHT
BOMBER AIRCRAFT (REF 8)
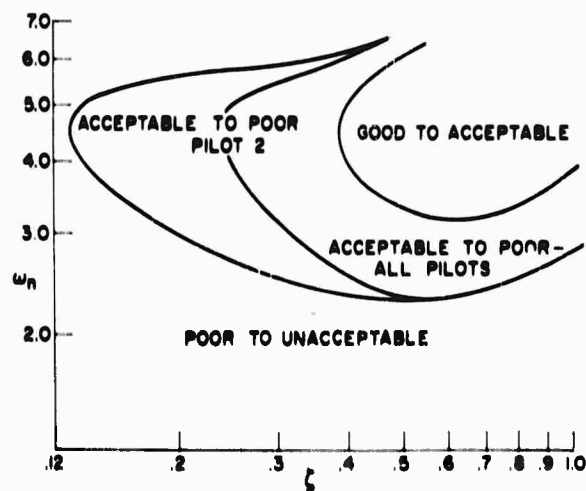
(c) VARIABLE-STABILITY FIGHTER
AIRCRAFT (REF 20)
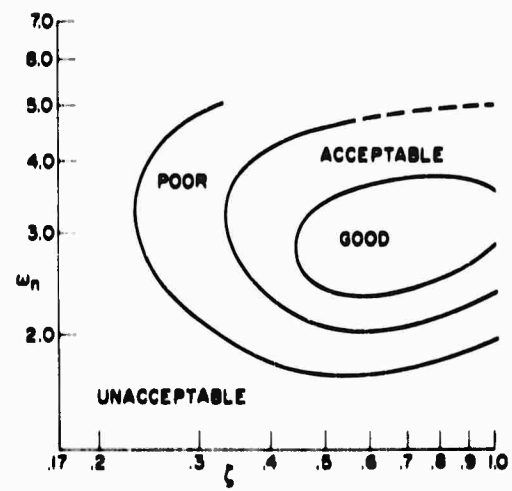
(d) VARIABLE-STABILITY FIGHTER
AIRCRAFT (REF 19)

FIGURE 30

ISO-OPINION PLOTS FOR SHORT-PERIOD MODE

C. COMPARISON OF SHORT PERIOD PILOT OPINION DATA FROM FLIGHT AND SIMULATOR

Before proceeding to evaluate the differences and similarities between flight and simulator results, it is important to note that for both kinds of tests considered here a gain parameter was held constant at a "desired" value as selected by the test pilots. Thus gain, as an opinion factor, was eliminated, leaving only the variable short period dynamics to cause changes in the pilots' ratings. Although the gain selected in the fixed-base simulator was in terms of attitude control while that in flight was in terms of stick force per g, it is shown in the Appendix that these parameters differ only by a constant multiplier independent of flight condition. Thus both flight and simulator tests can be considered to be attitude control problems involving varied short period dynamics and constant values of T_{θ_2} and $K_{\theta_{sp}}$, with $K_{\theta_{sp}}$ selected for "best" opinion results.

As regards opinion gradations observed in the various investigations, these were in all cases presented in the form of "iso-opinion" plots which are reproduced in Figure 30. The Hall data, Figure 30(a), represent an average of the two iso-opinion plots, one for each pilot, presented in Reference 3. For this study, the controlled element was, as previously mentioned, an analog computer simulation of a variable stability Navion aircraft with two-degree-of-freedom longitudinal characteristics and a fixed set of nominal three-degree-of-freedom lateral characteristics. The validity of the simulation in both axes has been verified by an in-flight study conducted with the actual aircraft (Reference 4). Figure 30(b), from Reference 18, is for a B-26 light bomber with stability variations resulting from angle of attack rate and displacement feedback to the elevator (equivalent to modifications of M_α and $M_{\dot{\alpha}}$). Opinion was based on trim characteristics, airframe response to step inputs, turn entry, horizon tracking, ground target gunnery runs, and constant-g pullouts. Figure 30(d), from Reference 19, is for an F-94A fighter aircraft with short period variations accomplished by M_α and $M_{\dot{\alpha}}$ variations, as above. Evaluation maneuvers were similar to those for the B-26 study. Figure 30(c), from Reference 20, is for the same F-94A aircraft with some modifications to permit investigation of higher frequencies.

The iso-opinion plots in Figure 30, although basically similar in shape, do not have point-to-point correspondence even though the airframe gain is optimum. There are several reasons, from the theoretical standpoint, why such variations should exist. First differences in pilots, pilot indoctrination, opinion scales, and assigned tasks can lead to variability in ratings, even of identical configurations (Reference 21). Also, differences in the transfer functions for aircraft with the _same_ short period dynamics will lead directly to differences in pilot adaptation and opinion. The most obvious of these is the numerator time constant, T_{θ_2}, but other less obvious differences may exist in the control system dynamics (see Figure 1) including nonlinearities due to friction, etc. Finally, there will be, as noted in the preceding section, a difference in the pilot's effective reaction-time delay when comparing simulator with flight test results. Differences in motion stimuli (References 4 and 6) will also cause differences of opinion between aircraft and simulator, although these differences will depend on the type of evaluation task, the acceleration loads involved, etc. As regards the present comparisons, this effect is considered insignificant.

A good example of differences occurring with essentially identical configurations is the comparison between Figures 30(c) and 30(d). Here, although the airplane was essentially identical, as were the _intended_ tasks, opinion scales,

etc., it was flown for each investigation at a different flight condition. While this changed the value of $T\theta_2$ for the two test conditions (from about 0.6 to about 0.5), the small change involved is theoretically insignificant as shown in the next section. Thus, both configurations were essentially identical and the differences in the iso-opinion plots must be due to those (or other) sources of variability noted above.

Even more drastic changes appear in the plots of Figure 30(b). Again the possible difference due to $T\theta_2$, which was about 1.0 in this case, is not considered significant. However, it does appear reasonable to suspect the possible influence of control system dynamics because there are obvious differences in such systems between bomber and fighter aircraft. Unfortunately these suspected differences are not evaluated in either of the referenced investigations nor in the available literature on the two aircraft involved. Thus, while some important portion of the differences between Figure 30(b) and either of Figures 30(c) or 30(d) may be ascribed to the aforementioned source of variability, a significant difference in the transfer function due to control system dynamics must also be considered an important possibility.

As concerns the ultimate comparison desired here — that between the simulator data of Figure 30(a) and the flight data of Figures 30(b), 30(c), and 30(d) — it is pertinent, first of all, to rule out variations in $T\theta_2$. The complete spread of $T\theta_2$ for all four examples, from about 0.5 to about 1.0, is, as noted above, considered practically insignificant. Aside from inherent variabilities and some unknown variations in controlled element transfer function due to the control system, the basic difference between simulator and flight results will be due, then, to differences in the pilot reaction time, τ. As noted in the preceding section, this difference (higher τ for flight) exercises a direct effect on the size of the various opinion regions. Thus, from a theoretical standpoint similar iso-opinion regions are expected to have a smaller frequency range when measured in flight than when they are measured in a fixed-base simulator. This very basic difference, which in fact seems to be the only significant difference shown, is amply demonstrated by the plots of Figure 30.

Having thus shown the general applicability of the theoretical approach, it is now pertinent to investigate its implications as regards short period handling quality areas so far not explored.

D. EFFECTS OF NUMERATOR TIME CONSTANT

The short period numerator (or lead) time constant, $T\theta_2$, is primarily determined by the airframe stability derivative Z_W, as is shown in the Appendix. The approximate relationship given by the expression

$$\frac{1}{T\theta_2} \doteq -Z_W \doteq \frac{\rho S U_o}{2m} (C_{L_\alpha} + C_D) \doteq \frac{\rho g U_o}{2} \frac{1}{\left(\frac{W}{S}\right)} C_{L_\alpha} \tag{10}$$

shows that large changes in $T\theta_2$ can be expected as altitude and speed increase, and as wing loadings and lift curve slopes change with vehicle design advances.

Changes in T_{θ_2} will also affect the airframe gain, as indicated by the approximate short period transfer function (see Appendix).

$$\left(\frac{\theta}{\delta_e}\right)_{sp} = \frac{K_\theta(T_{\theta_2}s + 1)}{s\left[\left(\frac{s}{\omega_{sp}}\right)^2 + \frac{2\zeta_{sp}}{\omega_{sp}}s + 1\right]}$$

$$K_\theta = \frac{M_\delta}{\omega_{sp}^2 T_{\theta_2}}$$

The gain, K_θ, is not, however, that which is of chief concern to the pilot as an opinion-generating factor. He is, as indicated previously, primarily influenced by the value of gain, K_p, which he must adopt. As will be shown in the system survey plots of Figures 31, 33, and 34, the value of K_p is directly associated with the controlled element gain at ω_{sp}, rather than the value of K_θ. Therefore the value of the controlled element gain which sets the pilot gain and influences his opinion is

$$K_{\theta_{sp}} = K_\theta T_{\theta_2} = \frac{M_\delta}{\omega_{sp}^2} \tag{11}$$

On the basis of this argument it appears that variations in T_{θ_2} will only influence pilot opinion by the manner in which they alter the system dynamics. Such influences can best be demonstrated by a series of system surveys, similar to those in Reference 5, in which the magnitude of the inverse lead time constant (relative to the short period frequency) is varied. The most direct approach to such a demonstration is to take a "good" airframe and vary the lead time constant between maximum and minimum feasible values while maintaining constant "good" short period frequency and damping. Proper loop closure and application of the opinion rules of the previous sections can then be used to determine the probable effects of the various lead values. Besides serving this direct purpose, such surveys have additional significance in that equivalent airframes with constant "good" short period frequency and damping values, but variable lead, are becoming more common. This stems from the fact that short period damping and frequency characteristics are ordinarily maintained constant by stability augmenters which involve the generation of control moments, while augmentation of T_{θ_2} requires the generation of lift forces.

The airframe characteristics chosen as the basis for the surveys correspond to the best rated configuration (2.51 - 1.0) of the Hall study. The use of this configuration is advantageous since the required (and observed) pilot equalization is nearly zero. A generic plot of this system, using a pure gain with a 0.2-second time delay for the pilot model and a 60-degree phase margin as the loop closure criterion, is shown in Figure 31. The required pilot gain, K_p, is 0.266 inches per degree of stick motion (-11.5 db) which corresponds quite closely to the experimentally observed value of 0.316 (-10 db). Neglecting the high frequency pole-zero pair corresponding to the reaction-time delay, the closed loop transfer function is
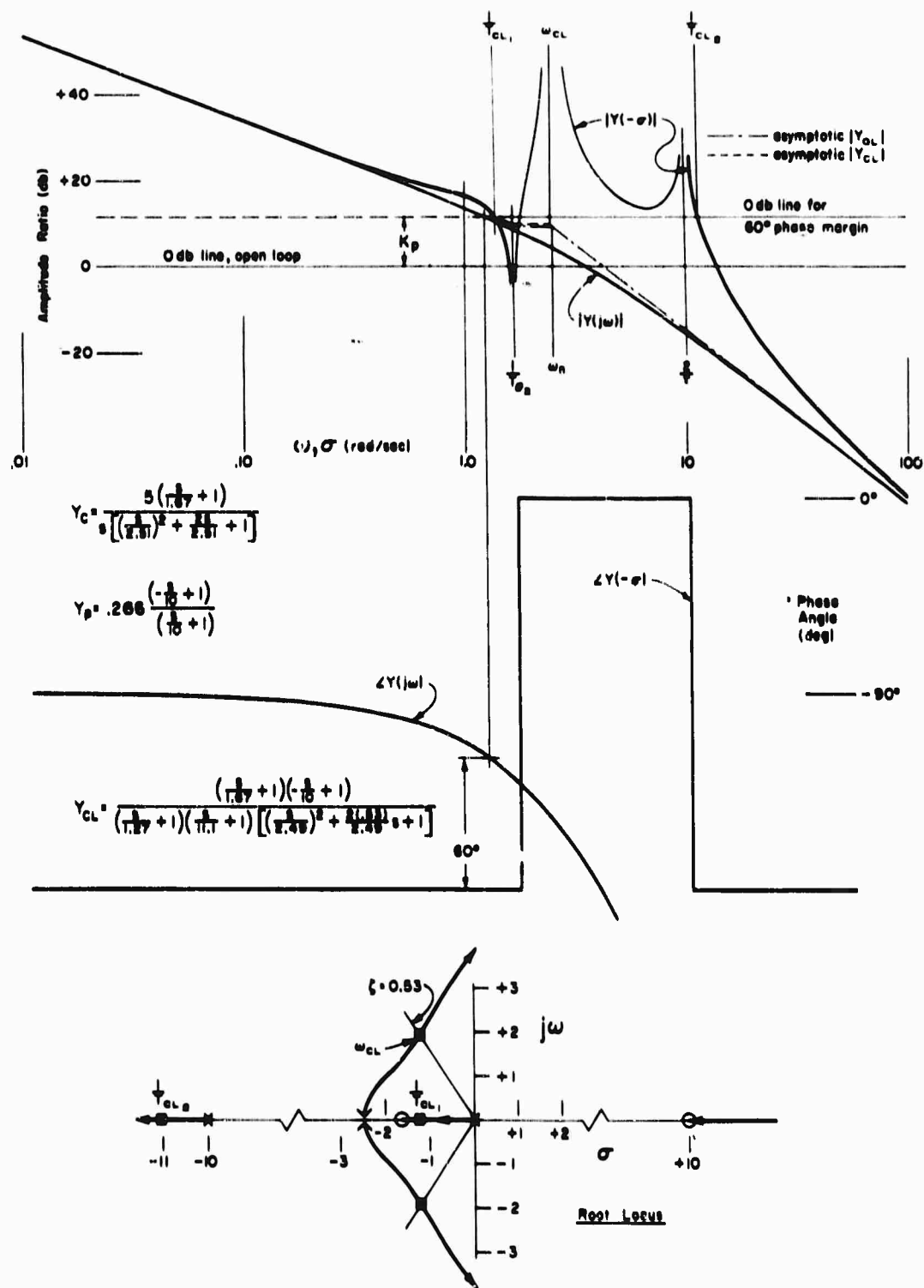
FIGURE 31
SYSTEM SURVEY FOR HALL CONFIGURATION 2.51–1.0

$$Y_C = \frac{5(T_{\theta_2} s + 1)}{s\left[\left(\frac{s}{2.51}\right)^2 + 2\left(\frac{1}{2.51}\right)s + 1\right]}$$

$$Y_p = K_p \frac{\left(-\frac{s}{10} + 1\right)}{\left(\frac{s}{10} + 1\right)}$$

REAL AXIS LOCI

$T_{\theta_2} = 6 = 1/.1667$
$= 2.22 = 1/.45$
$= .6 = 1/1.667$
$= .398 = 1/2.51$
$= .222 = 1/4.5$

$T_{\theta_2} = .222$
$T_{\theta_2} = 2.22, 6$
$T_{\theta_2} = .6$
$T_{\theta_2} = .398$
$T_{\theta_2} = .222$
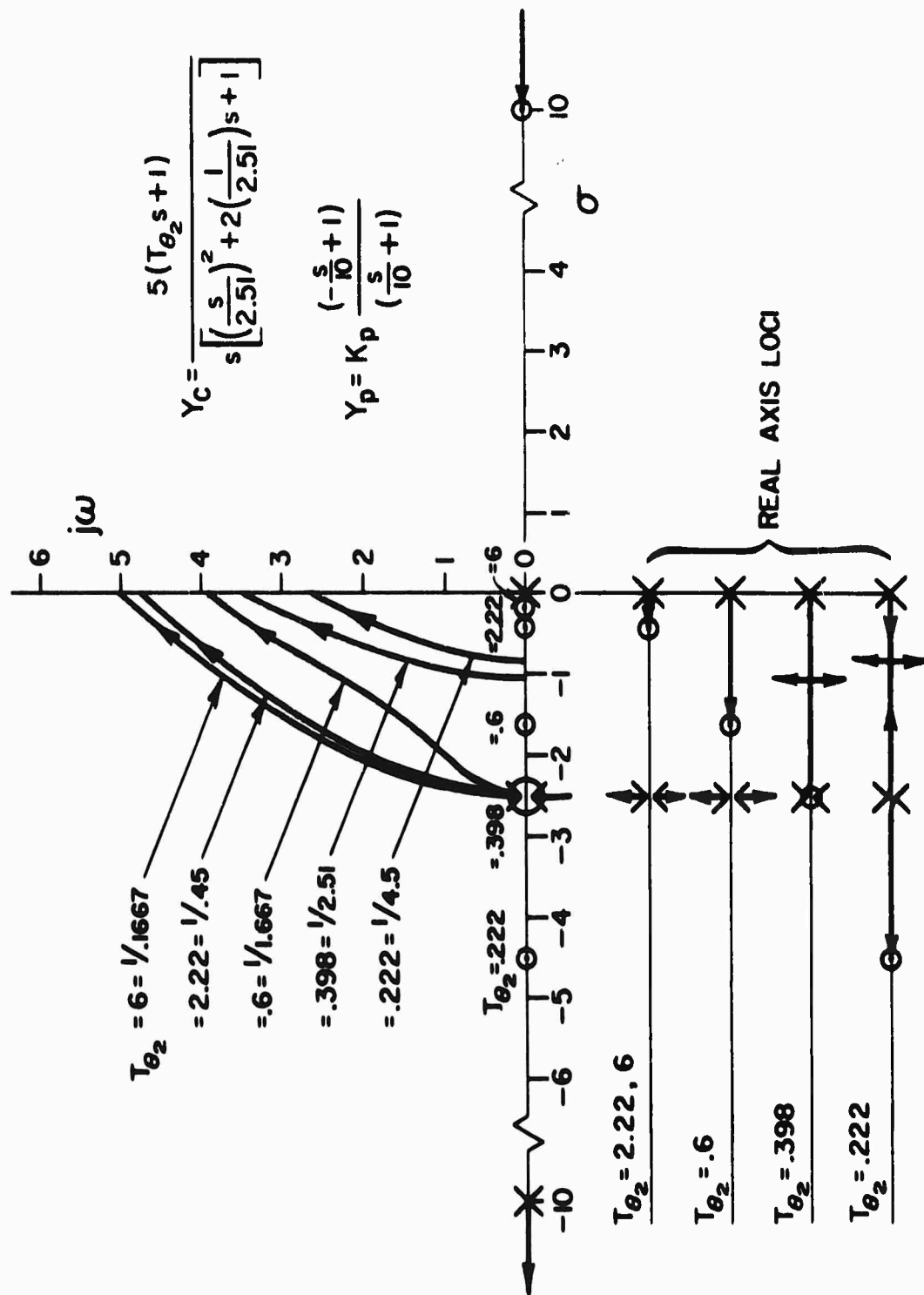
FIGURE 32

LOCUS SHAPES FOR VARYING T_{θ_2}, HALL CONFIGURATION 2.51—1.0
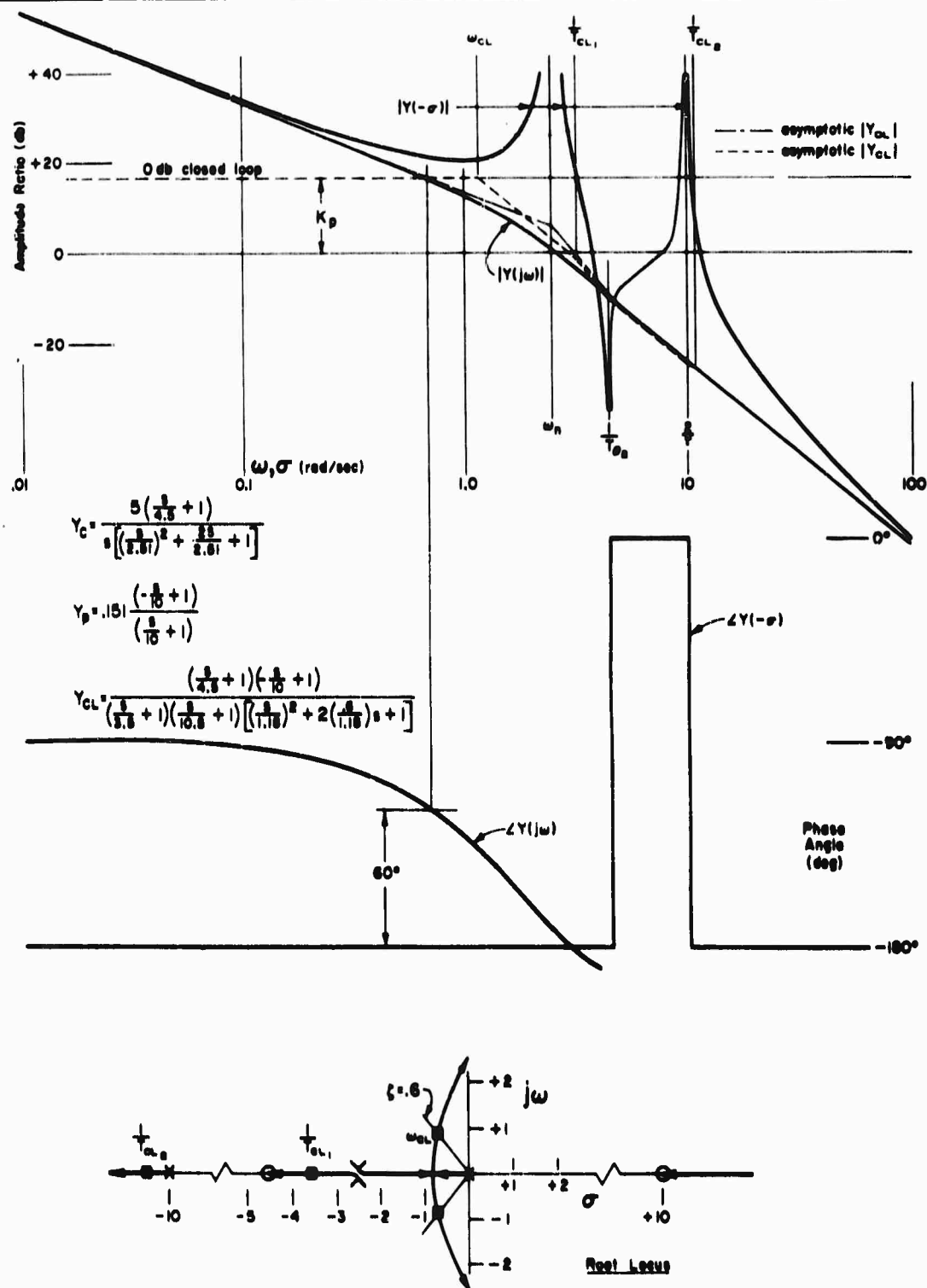
FIGURE 33
SYSTEM SURVEY FOR MINIMUM AIRFRAME LEAD TIME-CONSTANT

$$Y_{CL} \approx \frac{(\frac{s}{1.67} + 1)}{(\frac{s}{1.27} + 1)\left[(\frac{s}{2.49})^2 + 2(\frac{.53}{2.49})s + 1\right]} \qquad (12)$$

As indicated in Chapter III, this is close to an optimum closed loop system.

Effects of lead time-constant variation on this system may be seen in Figure 32 which shows the modification of the s-plane root locus shape as T_{θ_2} is varied. It will be noted that, as T_{θ_2} decreases, both the closed loop lag time constant and the short period undamped natural frequency decrease, and the converse is true as T_{θ_2} is increased. These are directions of opposing desirability for this case, as will be shown by detailed examination of both the maximum and minimum values of T_{θ_2}.

A generic system survey plot for the minimum lead time constant case of Figure 32, for a 60-degree phase margin loop-closure criterion, is shown in Figure 33. The low frequency approximation to the closed loop transfer function is

$$Y_{CL} = \frac{(\frac{s}{4.5} + 1)}{(\frac{s}{3.5} + 1)\left[(\frac{s}{1.18})^2 + 2(\frac{.6}{1.18})s + 1\right]} \qquad (13)$$

Thus, the closed loop damping is near optimum as it was for the nominal case and offers no basis for a revised opinion. However, the low frequency characteristics are dominated not by the first order time constant which is quite small (0.286 seconds), but by the second order frequency which is too low for good response. As a matter of fact, the dominant low frequency characteristic is now the crossover frequency which, as may be seen from Figure 33, is considerably less than the cutoff frequency, $\omega_{co} = 1.0$ radians/second. Therefore, on the basis of the adjustment rules and the foregoing observations, pilot adaptation will involve more than the postulated simple gain. To obtain the desired closed loop dynamics the pilot will utilize a lead-lag equalization, and his opinion (relative to the nominal T_{θ_2} case) will be degraded accordingly. For example, to make the closed loop configuration exactly the same as in the nominal case, the adapted lead-lag would be

$$\frac{T_L s + 1}{T_I s + 1} = \frac{\frac{s}{1.67} + 1}{\frac{s}{4.5} + 1} \qquad (14)$$

The above degree of lead equalization results, per Figure 13, in a small opinion degradation.

While the foregoing example indicates that a reduction in T_{θ_2} to a near-minimum value is detrimental to pilot opinion, this trend can be reversed as

the following simple demonstration will show. Consider the Hall configurations which resulted in pilot adaptation of lag or lag-lead equalizing characteristics (refer to Figure 19). Reducing the controlled element lead (in effect, increasing the controlled element lag) will serve to reduce the required pilot generated lag. The small lead time constant is, for this case, beneficial and would result in a higher pilot opinion. On the other hand, for those nominal configurations requiring the adaptation of lead or lead-lag equalization, large reductions in T_{θ_2} will, by the converse argument, demand increased pilot lead, again resulting in a degraded pilot opinion. It appears then that small lead time constants can have varying effects, depending on the airframe short period characteristics involved.

While the minimum T_{θ_2} considered above is hypothetically achievable at very low altitudes, with high lift curve slopes, etc., it is an extreme not likely to be often encountered in routine operations. On the other hand, with modern high altitude aircraft it is very likely that the magnitude of the lead time constant will be considerably larger than the nominal Hall value.

Generic plots of a system with a near-maximum value of T_{θ_2} are shown in Figure 34. Using the 60-degree phase margin closure criterion and a nonequalized pilot as before, Figure 34 shows the low frequency approximation to the closed loop transfer function to be

$$Y_{CL} \doteq \frac{(\frac{s}{.167} + 1)}{(\frac{s}{.109} + 1)\left[(\frac{s}{3.7})^2 + 2(\frac{.3}{3.7})s + 1\right]} \tag{15}$$

The closed loop lag time constant for this case is large (9.18 seconds) and the resultant droop effect will seriously influence performance as well as opinion; furthermore, the closed loop second order damping is marginal. Probable pilot corrective equalization will be a lag or a lag-lead. A generic plot of the system with the latter equalization form is shown in Figure 34(b). The equalization values are arbitrary and were chosen to demonstrate a general effect; they result in a closed loop transfer function given by

$$Y_{CL} \doteq \frac{(\frac{s}{.167} + 1)(\frac{s}{2} + 1)}{(\frac{s}{.15} + 1)(\frac{s}{1.7} + 1)\left[(\frac{s}{2.1})^2 + 2(\frac{.57}{2.1})s + 1\right]} \tag{16}$$

It is seen, by comparing Eqs. (15) and (16) and the asymptotic $|Y_{CL}|$'s of Figures 34(a) and 34(b), that performance has been considerably improved by the assumed equalization. In particular, the droop has been greatly reduced, and the damping of the second order mode has been increased to a more desirable value. In fact, the closed loop characteristics are now very similar to those for the nonequalized pilot and the nominal T_{θ_2} of Figure 31. This similarity has been achieved, however, only by fairly strenuous lag-lead efforts on the
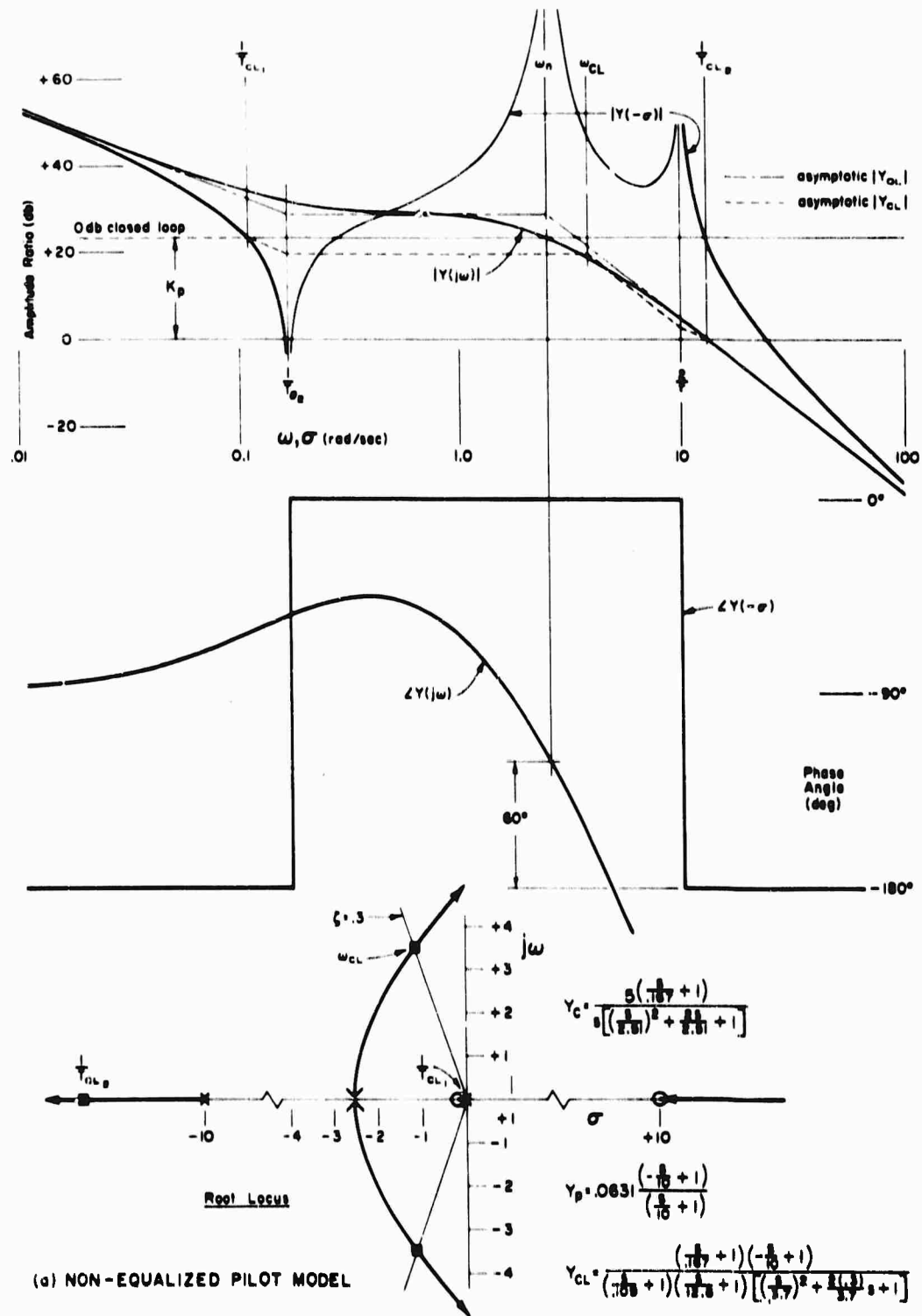
FIGURE 34
SYSTEM SURVEY FOR LARGE AIRFRAME LEAD TIME CONSTANT

(b) LAG-LEAD PILOT EQUALIZATION

$$Y_C = \frac{5\left(\frac{1}{.167}+1\right)}{s\left[\left(\frac{s}{2.51}\right)^2+\frac{2.8}{2.51}+1\right]}$$

$$Y_p = \frac{.14\left(\frac{s}{.2}+1\right)\left(-\frac{s}{10}+1\right)}{\left(\frac{s}{.3}+1\right)\left(\frac{s}{10}+1\right)}$$

$$Y_{CL} = \frac{\left(\frac{1}{.167}+1\right)\left(\frac{s}{.2}+1\right)\left(-\frac{s}{10}+1\right)}{\left(\frac{s}{.18}+1\right)\left(\frac{s}{1.7}+1\right)\left(\frac{s}{11.1}+1\right)\left[\left(\frac{s}{2.1}\right)^2+2\frac{(.57)}{2.1}s+1\right]}$$

FIGURE 34 (CONCLUDED)

part of the pilot, so his opinion will be correspondingly degraded from that for the nominal T_{θ_2} case. As opposed to the small lead time constant which can have varying effects, the large lead time constant will always require lag or lag-lead equalization as demonstrated above.

These surveys have shown that the effects of airframe lead time constant can be important in closed loop attitude control situations. In particular, large values will generally lead to degradation of pilot opinion, whereas small values can be either beneficial or detrimental. In any event it is advisable to assess such effects for particular airframes by analyses similar to those demonstrated above.

As a final note it should be observed that the dynamic relationship between pitching velocity and normal acceleration, approximately equal to $T_{\theta_2}s + 1$ [see Eq. (A-8) in the Appendix], will change very greatly with T_{θ_2}. For small lead time constants, pitching velocity and normal acceleration will be essentially interchangeable pilot cues as they are in "conventional" airframes. However, for increasing time constants there will be an increasing discrepancy between these normally equivalent quantities. The effect of such a departure from nominal behavior on pilot opinion is difficult to assess although opinion will almost certainly be degraded because of the pilot behavioral changes required.

E. CONTROL OF THE SHORT TIME-CONSTANT DIVERGENCE

As noted in the Appendix, the airframe short period transfer function can assume the form

$$Y_c = \frac{-K_c(T_{\theta_2}s + 1)}{s(-T_{s_1}s + 1)(T_{s_2}s + 1)} \tag{17}$$

where the various inverse time constants are given by

$$-\frac{1}{T_{s_1}T_{s_2}} \doteq Z_w M_q - M_\alpha$$

$$\frac{1}{T_{s_2}} - \frac{1}{T_{s_1}} \doteq -Z_w - M_q - M_{\dot\alpha} \tag{18}$$

$$\frac{1}{T_{\theta_2}} \doteq -Z_w$$

The first of Eqs. (18) associates the appearance of the first order (aperiodic) divergence with the condition of negative maneuver margin. This in turn usually arises from positive (unstable) values of M_α, since $Z_w M_q$ is ordinarily positive. Additionally, Eqs. (18) show, within the limits of their validity, that

$$\frac{1}{T_{s_2}} \doteq \frac{1}{T_{s_1}} + \frac{1}{T_{\theta_2}} - M_q - M_{\dot\alpha} \tag{19}$$
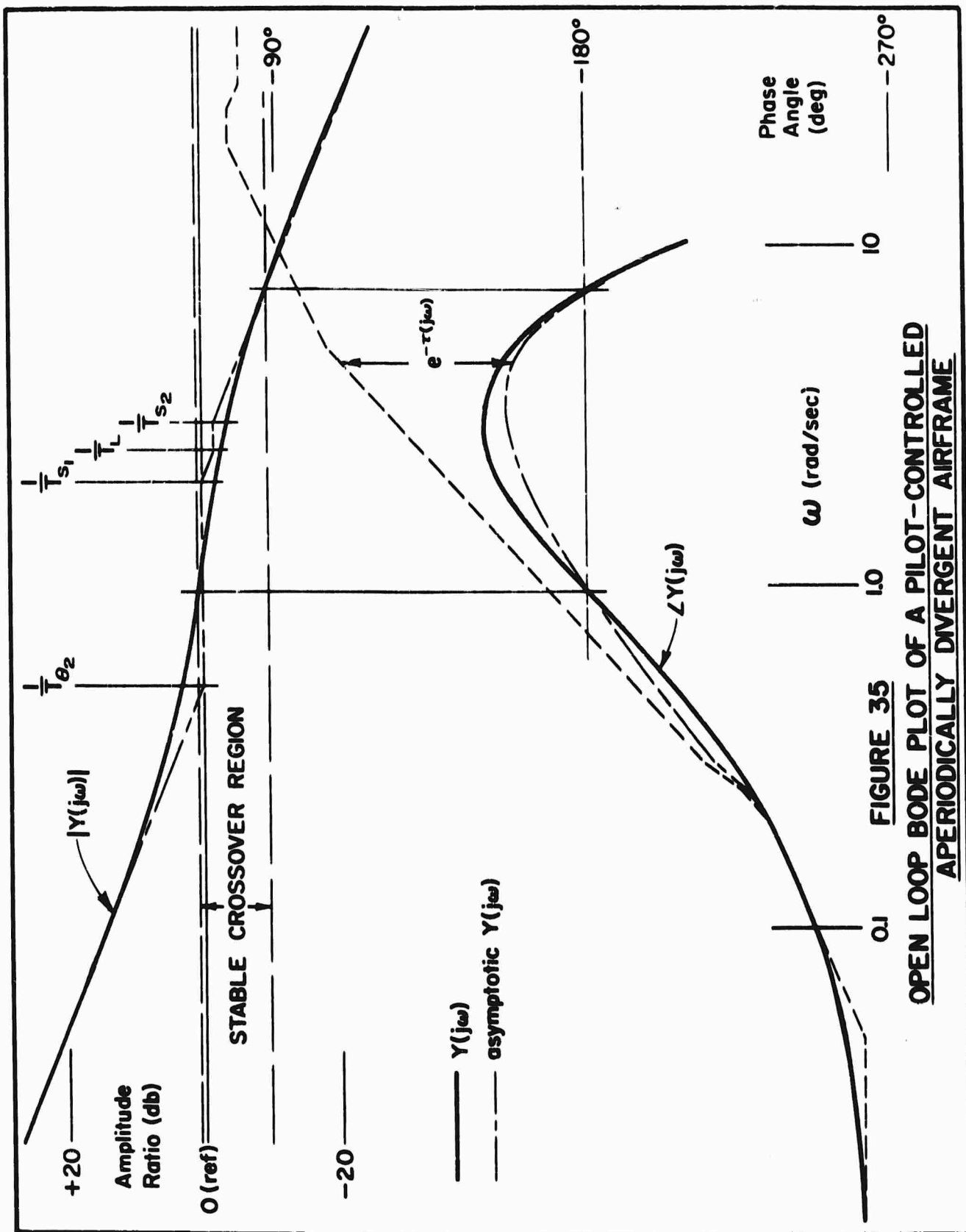
FIGURE 35

OPEN LOOP BODE PLOT OF A PILOT-CONTROLLED
APERIODICALLY DIVERGENT AIRFRAME

Since the sum of M_q and $M_{\dot{d}}$ is usually negative in practical cases (it can be positive for very unconventional configurations), the above expression indicates that $1/T_{s_2}$ will almost always be greater than the sum of $1/T_{\theta_2}$ and $1/T_{s_1}$. The relative values of $1/T_{s_1}$ and $1/T_{\theta_2}$ cannot in general be inferred, but since interest here is centered on exploring the maximum value of $1/T_{s_1}$ which can be controlled by a pilot, it will be assumed that $1/T_{s_1} > 1/T_{\theta_2}$.

Figure 35 shows a typical $Y(j\omega)$ Bode plot for the pilot-airframe open loop in which the pilot transfer function is taken as

$$Y_p = K_p e^{-\tau s}(T_L s + 1)$$

This is the simplest form of adaptation the pilot can make and still hope to control the system. The value of $1/T_L$ is set somewhere between $1/T_{s_1}$ and $1/T_{s_2}$ which, as will be apparent later, is its most effective location. Also, the relative values of the remaining time constants correspond to Eq. (19), assuming the sum of M_q and $M_{\dot{d}}$ to be about equal to Z_w. The complete Bode plot (solid) as well as the asymptotic approximations (broken) to the amplitude and phase are shown. The asymptotic approximation to the phase is obtained by adding the exact contribution due to reaction-time delay ($\tau = 0.2$) to the asymptotic contributions of the first order terms (dashed) as indicated.

For the nonminimum phase system under consideration here, the generalized Nyquist criterion for stability requires that the loop be closed with gain greater than one (zero db) at the low frequency -180-degree phase point and less than one at the high frequency -180-degree phase point. The region of stable closure is indicated in Figure 35. A necessary condition for stability, therefore, is that the maximum sum of the phase contributions of the various first order terms and the time delay be greater than 90 degrees. That is,

$$\tan^{-1} T_{\theta_2}\omega + \tan^{-1} T_{s_1}\omega + \tan^{-1} T_L\omega - \tan^{-1} T_{s_2}\omega - \tau\omega > 90^\circ \qquad (20)$$

where the ω is chosen to give the maximum phase peak. Even though this requirement be met, practical closures may be impossible unless the stable gain region is sufficiently wide.

These two requirements — phase contribution greater than 90 degrees and a minimum "crossover" gain margin — account for the "best" location of $1/T_L$, as shown, between $1/T_{s_1}$ and $1/T_{s_2}$. Selecting $1/T_L$ smaller than $1/T_{s_1}$, while tending to broaden the frequency region where the phase angle is greater than -180 degrees, actually severely restricts the region of stable closure because of its adverse effect on the amplitude ratio. This is illustrated in Figure 36(a) which utilizes asymptotic constructions only and may be compared, on this basis, with Figure 35. On the other hand, selecting $1/T_L$ larger than $1/T_{s_2}$ reduces the phase angle to the extent that stable loop closure can become impossible or, at best, very marginal. Figure 36(b), which shows a neutrally stable situation for a single value of the open loop gain, illustrates this effect. Therefore, since the adaptation "rules" imply a behavior akin to that of a good servo system, the pilot will adjust his lead term to lie between $1/T_{s_1}$ and $1/T_{s_2}$. Unfortunately, direct evidence of such lead adaptation (from measured human dynamic response data) has not been obtained to verify this prediction.

In accordance with the probable adjustment noted above, the pilot lead term will approximately cancel the lag due to T_{s_2}. Then the phase margin criterion, Eq. (20), can be written

$$\varphi \doteq \tan^{-1} T_{\theta_2}\omega + \tan^{-1} T_{s_1}\omega - \tau\omega$$

$$\varphi_{max} > 90^\circ \tag{21}$$

and the "phase crossover" frequencies can be determined by setting $\varphi = 90^\circ = 1.57$ radians. Doing this, denoting "phase crossover frequency" by ω_0, and expressing it in terms of $1/T_{s_1}$,

$$\tan^{-1} \frac{T_{\theta_2}}{T_{s_1}}\left(\frac{\omega_0}{1/T_{s_1}}\right) + \tan^{-1}\left(\frac{\omega_0}{1/T_{s_1}}\right) - \frac{\tau}{T_{s_1}}\left(\frac{\omega_0}{1/T_{s_1}}\right) = 1.57 \tag{22}$$

Solving for T_{s_1}/τ in terms of $\omega_0/(1/T_{s_1})$ for various fixed values of T_{s_1}/T_{θ_2} gives the results shown in Figure 37. Both "phase crossover" frequencies are implicit in the double valued curves drawn, as is the value of T_{s_1}/τ for zero degrees phase margin (minimum T_{s_1}/τ). Also shown is a line connecting the high frequency crossovers which result in a stable crossover region 6 db wide. The point on this line corresponding to $T_{s_1}/T_{\theta_2} = 1.0$ is simply obtained by picking a value of T_{s_1}/τ for which the high value of ω_0 is twice the low value. This follows because for the particular case, $T_{s_1}/T_{\theta_2} = 1.0$, the open loop amplitude Bode plot is a straight line of -6 db/octave slope, so a 2:1 ratio of crossover frequencies provides 6 db of stable crossover region. For values of T_{s_1}/T_{θ_2} approaching zero, however, the amplitude Bode includes a wide region between the lead and lag break frequencies, $1/T_{\theta_2}$ and $1/T_{s_1}$, of zero slope. Because the low amplitude crossover occurs in this region, the desired 6-db margin requires that the high amplitude crossover occur at a frequency such that the attenuation due to the lag is 1/2; i.e., $\sqrt{(T_{s_1}\omega_0)^2 + 1} = 2$ or $\frac{\omega_0}{1/T_{s_1}} = \sqrt{3} = 1.732$. Both these points serve to orient the line shown which, in turn, determines the minimum values of T_{s_1}/τ at which the 6-db gain margin can be obtained. Before these values can be accepted as being truly critical, however, it is advisable to check the available phase margins.

The available phase margin is a maximum at a crossover frequency approximately midway between the high and low phase crossover frequencies of Figure 37. More precisely from Eqs. (21) and (22),

$$(\varphi_m)_{max} = \varphi_{max} - 90^\circ$$

$$= \tan^{-1} \frac{T_{\theta_2}}{T_{s_1}}\left(\frac{\omega_m}{1/T_{s_1}}\right) + \tan^{-1}\left(\frac{\omega_m}{1/T_{s_1}}\right) - 57.3 \frac{\tau}{T_{s_1}}\left(\frac{\omega_m}{1/T_{s_1}}\right) - 90^\circ \tag{23}$$
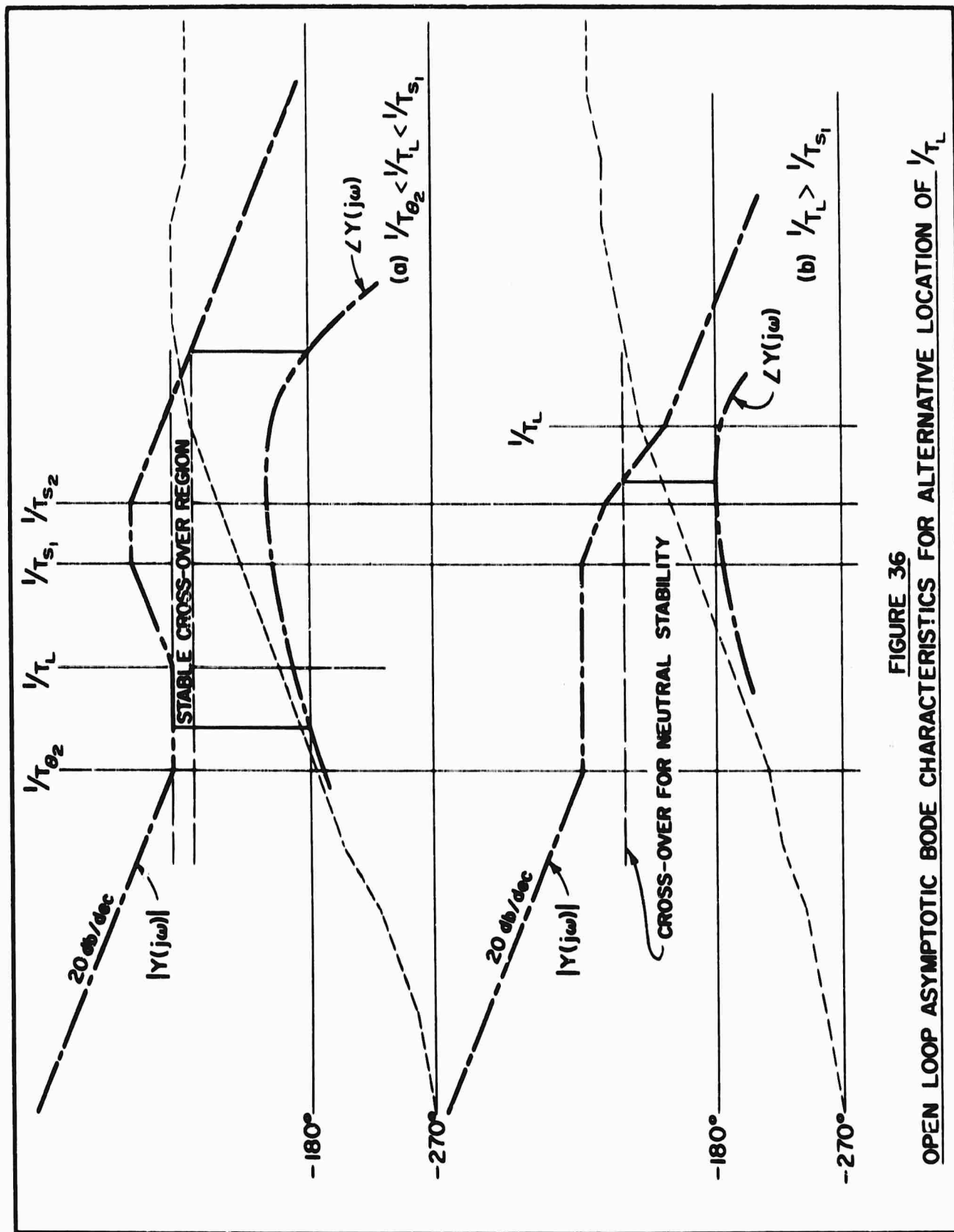
FIGURE 36

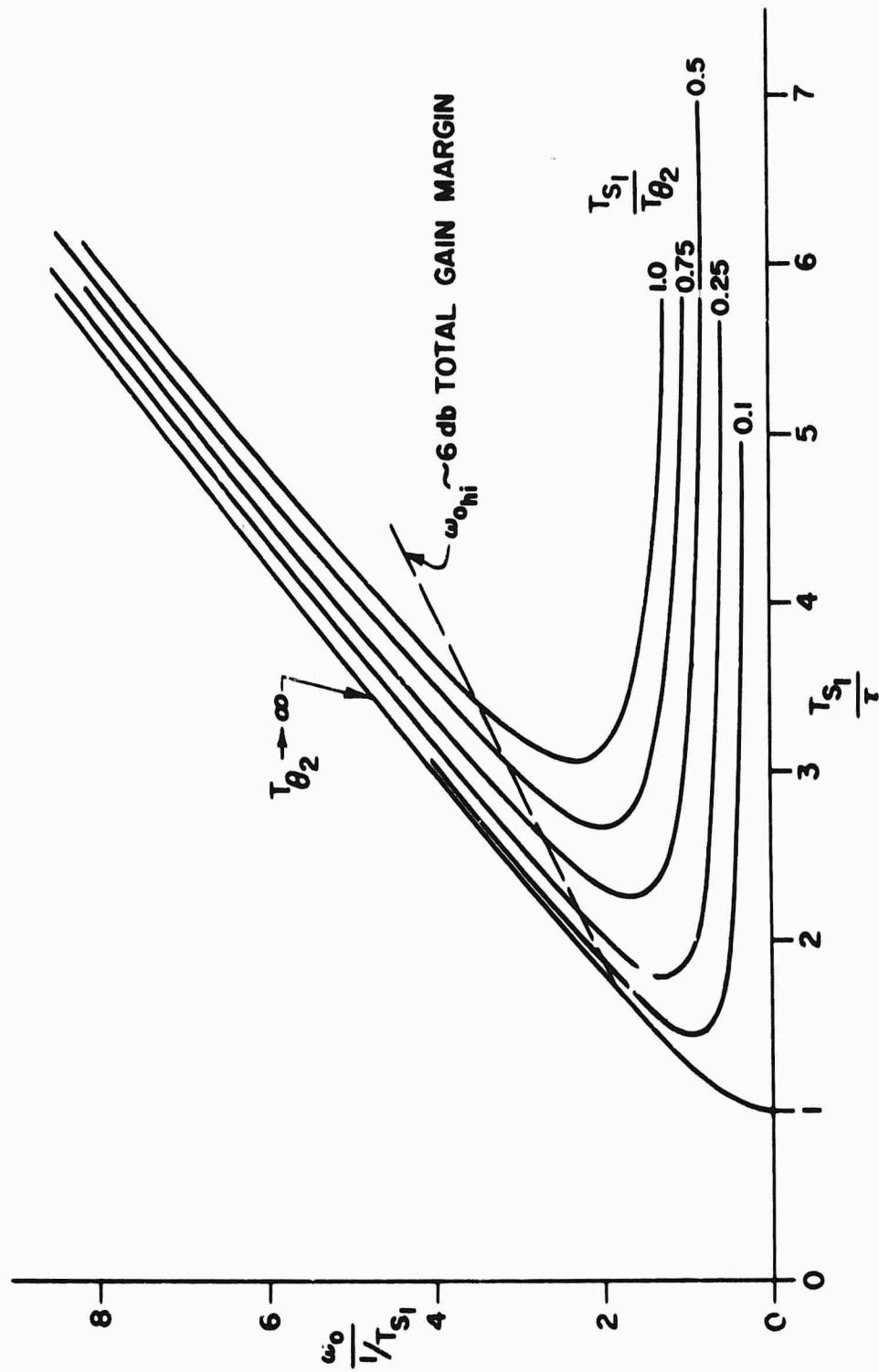OPEN LOOP ASYMPTOTIC BODE CHARACTERISTICS FOR ALTERNATIVE LOCATION OF $1/T_L$

FIGURE 37

CROSSOVER FREQUENCIES (ω_0) RELATIVE TO $\frac{1}{T_{S_1}}$ FOR $\frac{1}{T_L} = \frac{1}{T_{S_2}}$

where ω_m is the frequency corresponding to the maximum value of φ, given by the relationship

$$\frac{d\varphi}{d\left(\frac{\omega}{1/T_{s_1}}\right)} = 0 = \frac{\frac{T_{\theta_2}}{T_{s_1}}}{1 + \left(\frac{T_{\theta_2}}{T_{s_1}}\right)^2\left(\frac{\omega_m}{1/T_{s_1}}\right)^2} + \frac{1}{1 + \left(\frac{\omega_m}{1/T_{s_1}}\right)^2} - \frac{\tau}{T_{s_1}} \qquad (24)$$

Numerical solutions to these two simultaneous equations are easily obtained by assuming values of $\omega_m/(1/T_{s_1})$ for a given value of T_{θ_2}/T_{s_1}, calculating the value of τ/T_{s_1} from Eq. (24), and then substituting all three parameters into Eq. (23). The resulting maximum phase margins are shown in Figure 38. From this figure it may be seen that the phase margins associated with the 6-db gain margins of Figure 37 vary between 11 and 4 degrees for the range of T_{s_1}/T_{θ_2} covered. The latter value is probably too small, so a 10-degree phase margin is used as another indicator of the controllability limits in the summarizing plot of Figure 39.

On the basis of this plot, the maximum value of $1/T_{s_1}$ which a pilot might be expected to control as $1/T_{\theta_2}$ approaches zero corresponds to a value of $T_{s_1}/\tau \doteq 1.7$. For the minimum value of τ observed in closed loop single-dimensional tracking tasks ($\tau = 0.15$) this corresponds to $1/T_{s_1} = 3.9$. Increasing values of $1/T_{\theta_2}$ and τ will degrade this maximum capability which, incidentally, corresponds to a time-to-double-amplitude of about 0.18 seconds. It is of interest therefore to consider a more typical example.

Relating T_{θ_2} to airplane geometric and aerodynamic parameters and expressing Z_W in basic terms,

$$\frac{1}{T_{\theta_2}} \doteq -Z_W \doteq \rho \frac{g}{2} \frac{U_0}{W/S} C_{L\alpha} \qquad (25)$$

For a typical case,

$$\left.\begin{array}{rcl} h &=& 35,000 \\ M &=& 2.0 \\ C_{L\alpha} &=& 4.0 \\ W/S &=& 100 \end{array}\right\} \quad \frac{1}{T_{\theta_2}} = 0.925$$

$$\tau = 0.20 \text{ (more typical value)}$$

Because the unknown, T_{s_1}, appears in both coordinates, Figure 39 cannot be used directly to yield a solution for cases involving finite values of the parameter $1/T_{\theta_2}$. To overcome this difficulty the lower and upper limits of Figure 39 can be approximated by the inequalities,
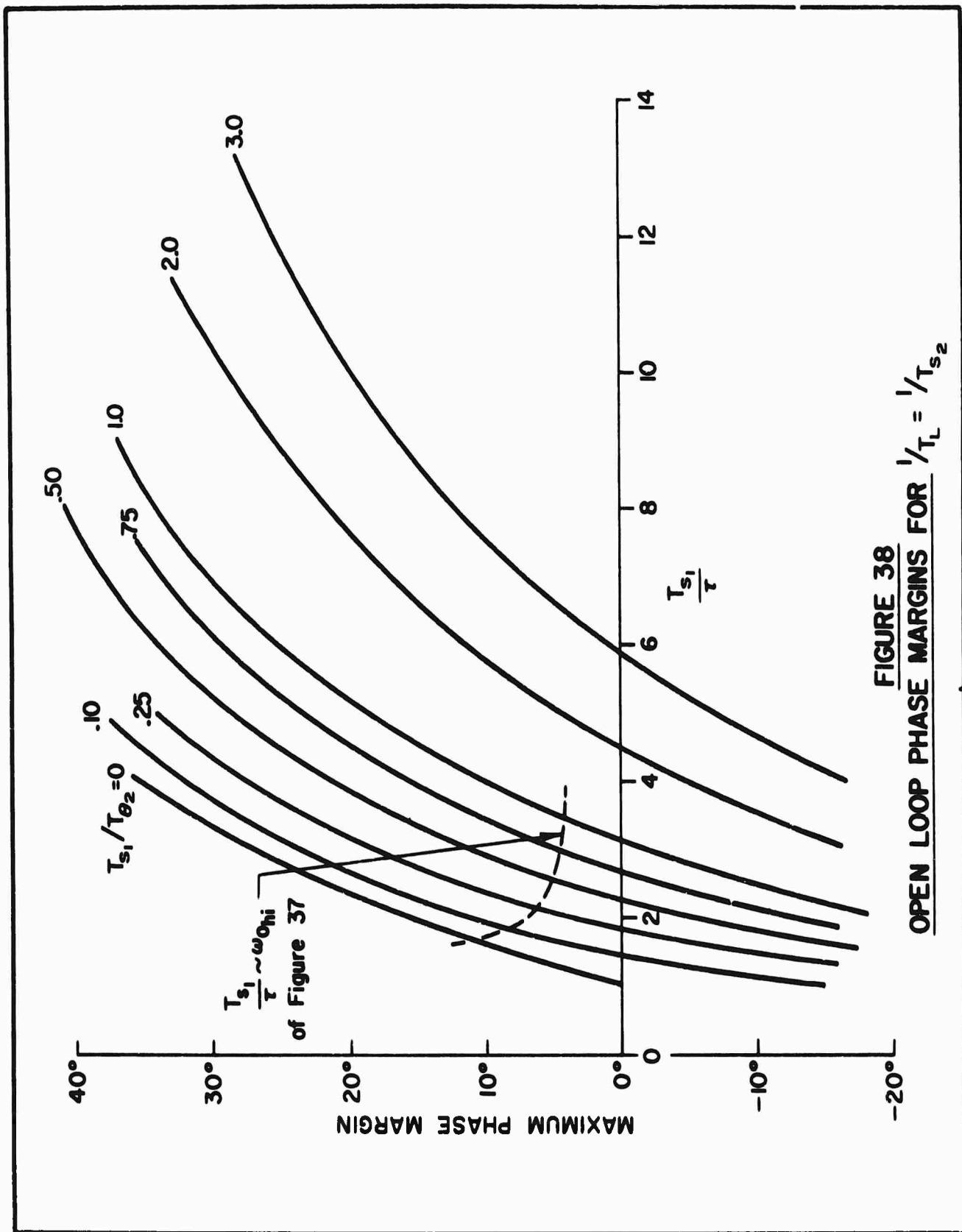
FIGURE 38
OPEN LOOP PHASE MARGINS FOR $1/T_L = 1/T_{s_2}$
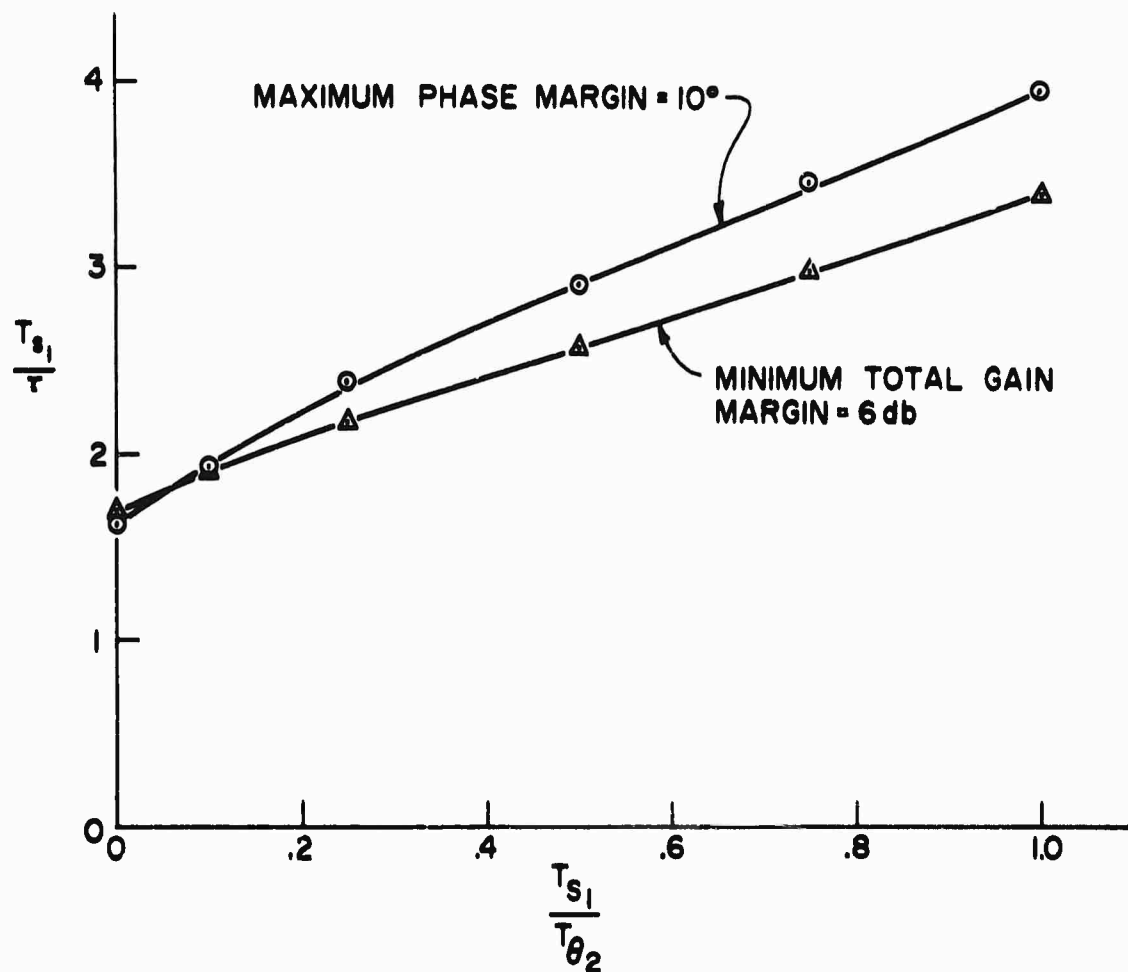
FIGURE 39

MINIMUM CONTROLLABLE VALUES OF $\frac{T_{S_1}}{T}$

$$1.75 + 1.65 \frac{T_{s_1}}{T_{\theta_2}} < \frac{T_{s_1}}{\tau} < 1.85 + 2.10 \frac{T_{s_1}}{T_{\theta_2}} \tag{26}$$

which are quite accurate for $0.25 < T_{s_1}/T_{\theta_2} < 1.0$. Collecting the T_{s_1} terms and inverting,

$$\frac{1}{1.85\tau} - \frac{2.10}{1.85T_{\theta_2}} < \frac{1}{T_{s_1}} < \frac{1}{1.75\tau} - \frac{1.65}{1.75T_{\theta_2}} \tag{27}$$

For the case at hand, this yields

$$1.65 < \frac{1}{T_{s_1}} < 1.99 \tag{28}$$

These values more nearly represent practical expectations as regards the control of longitudinal short time-constant divergences. They correspond to times-to-double amplitude between 0.35 and 0.42 seconds.

As a final observation, it must be noted that although such divergent situations can be controlled, they require a very high level of skill, adaptation, and concentration on the part of the pilot. Such extreme performance and attention cannot be maintained for long and, in spite of the fact that the pilot lead requirements may be quite modest (depending on $1/T_{s_2}$), he may rate the system as unacceptable for these reasons.

LONG PERIOD HANDLING QUALITY CONSIDERATIONS

A. CONVENTIONAL OSCILLATORY PHUGOID MODE

Some experiments have been conducted to determine the effects of the conventional airframe phugoid mode on handling qualities (e.g., References 18 and 22), but these are difficult to assess because of the pilot's basic ability to cope with all such low frequency oscillatory motions. Accordingly, pilot opinion (see Figure 40 taken from Reference 22) in such studies appears to be based not on closed loop considerations but on the degree of pilot monitoring required to maintain a desired trim. This conclusion is supported by the system surveys presented below.

The general form of the phugoid mode transfer function is (see the Appendix)

$$Y_c = \frac{K_c(T_{\theta_1} s + 1)}{\left(\frac{s}{\omega_p}\right)^2 + \frac{2\zeta_p s}{\omega_p} + 1} \tag{29}$$

where $1/T_{\theta_1}$ is always considerably smaller than ω_p. A generic system survey plot of a well damped highly rated airframe and a pure gain pilot (note that reaction time delays are negligible for the frequencies of interest) is given in Figure 41(a). The probable gain region is not shown because it is not critical for the phugoid and will be set by short period considerations. The closed loop system is always stable and more heavily damped than the open loop (basic airframe) which is, itself, quite well damped. This situation then requires only very occasional monitoring by the pilot for satisfactory control, thus enabling him to devote the major portion of his time to other tasks. Figure 41(b) presents a similar survey for a situation in which the basic airframe is only very lightly damped. Loop closure with a pure gain pilot results in increased damping with increasing gain as before (see root locus); now, however, because the open loop is very poorly damped, the uncontrolled airframe response to gust disturbances will be fairly conspicuous, requiring a relatively high pilot sampling rate for satisfactory control.

Figure 42 shows a system incorporating a negatively damped airframe. In this case the stability criterion requires that the total open loop amplitude ratio (gain) be greater than one (zero db) at 180 degrees of phase. Therefore to stabilize the closed loop requires a minimum value of (pure) pilot gain, which is, however, quite low compared to the probable gains used for short period control. Thus the system is again easily stabilized by the pilot, although he must now devote a very large portion of his time to such efforts.

These surveys clearly show that any degree of oscillatory phugoid instability can be easily controlled by a pilot. His objection to instability seems to be centered in the monitoring (sampling) effort required because this detracts from other more critical flight tasks.
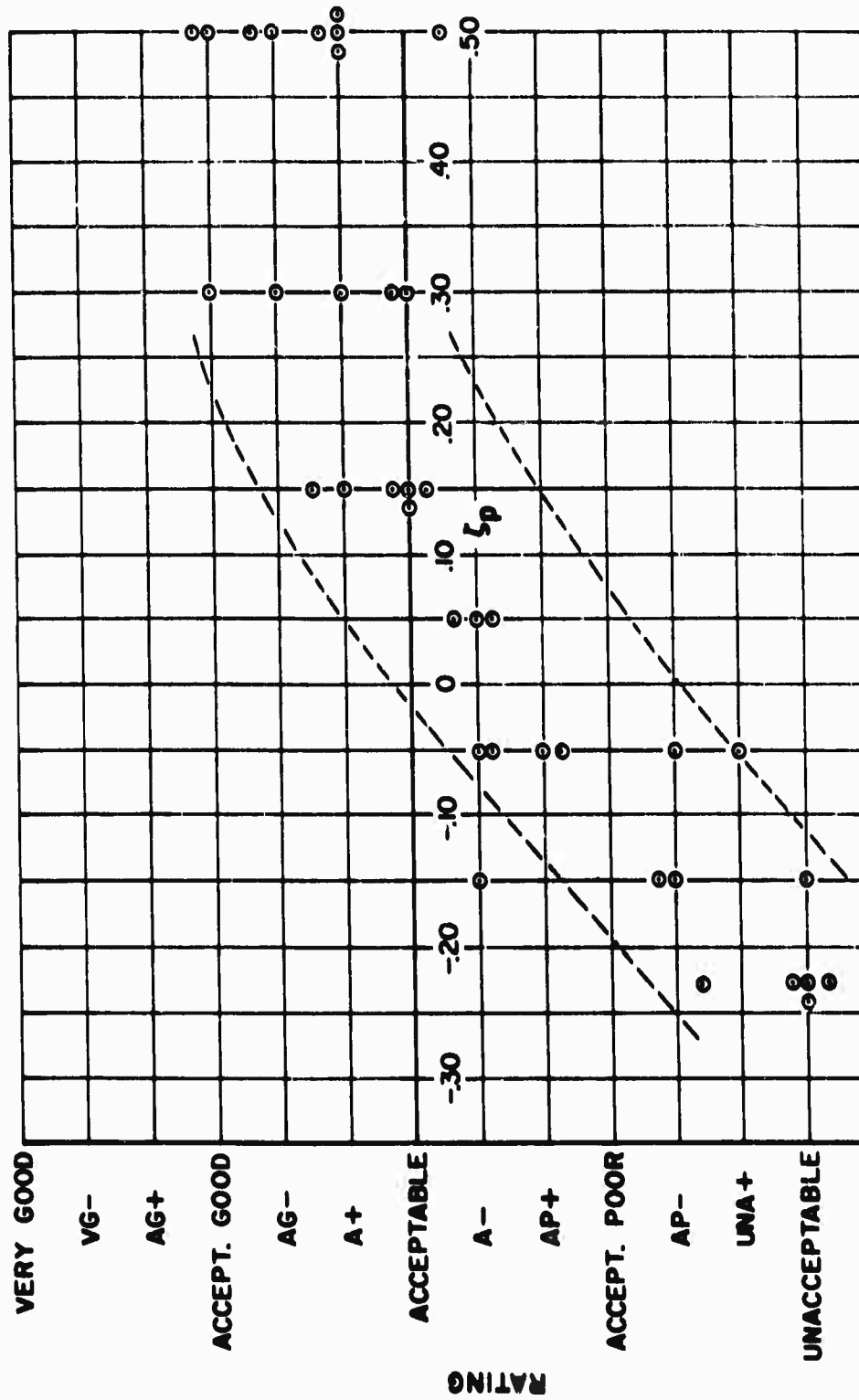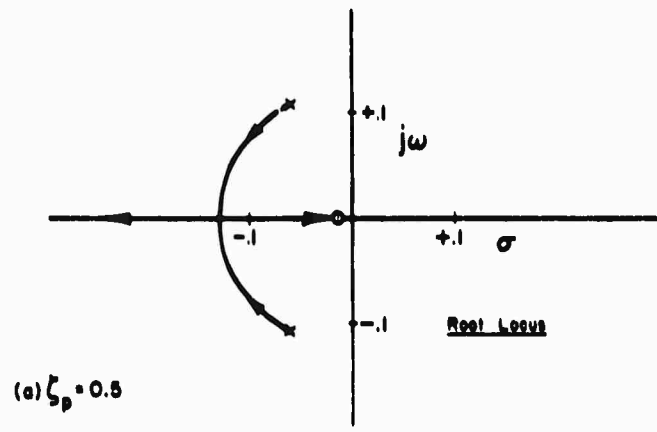
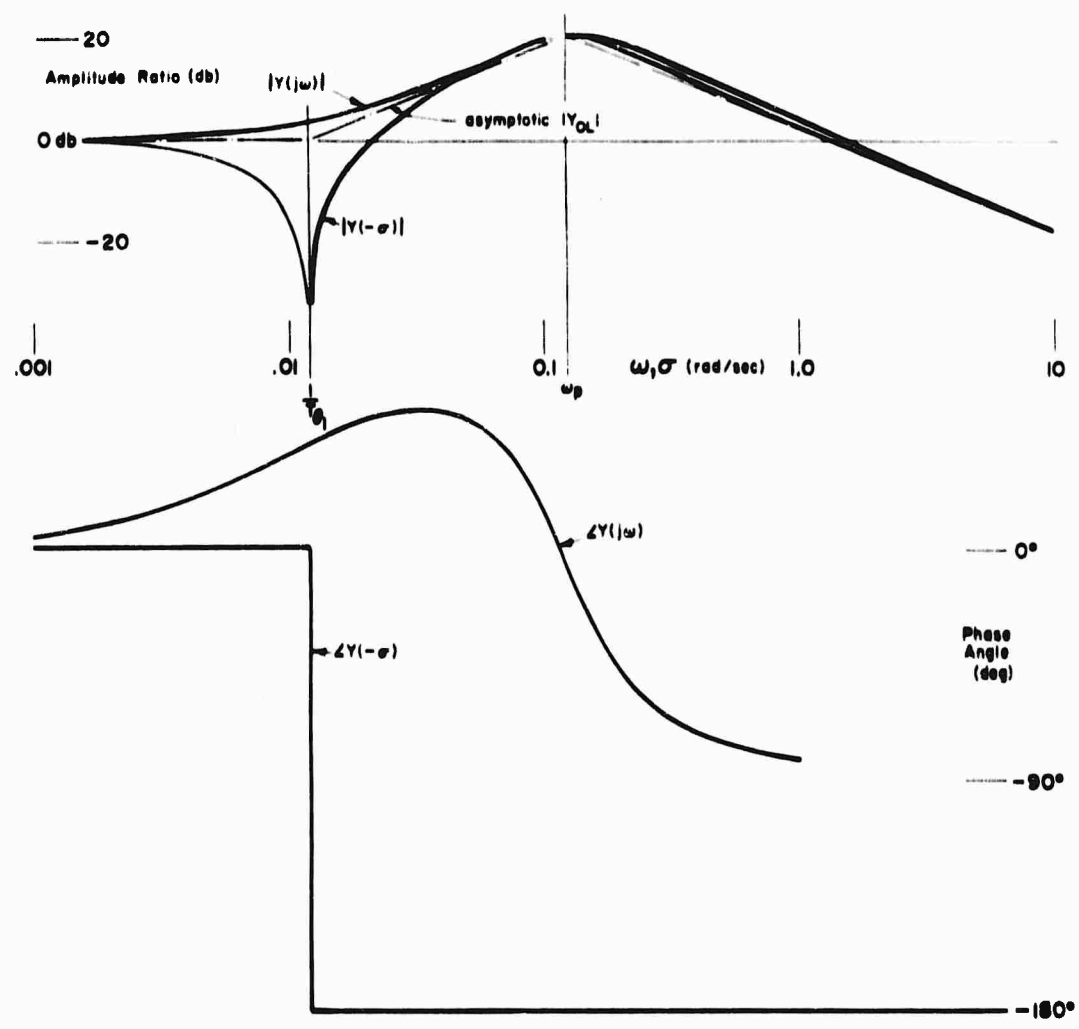FIGURE 40

PILOT OPINION VS. PHUGOID DAMPING RATIO

(a) $\zeta_p = 0.5$

FIGURE 41

SYSTEM SURVEYS OF POSITIVELY-DAMPED PHUGOID MODES
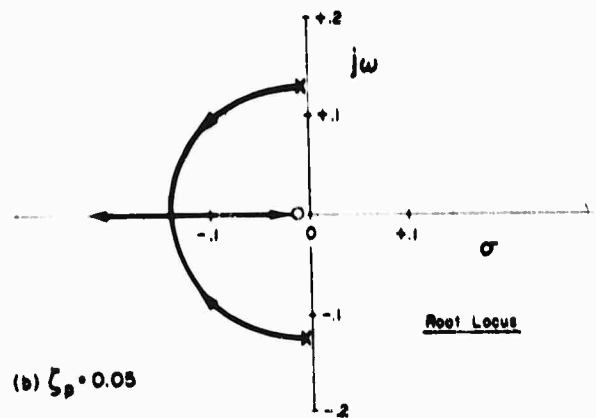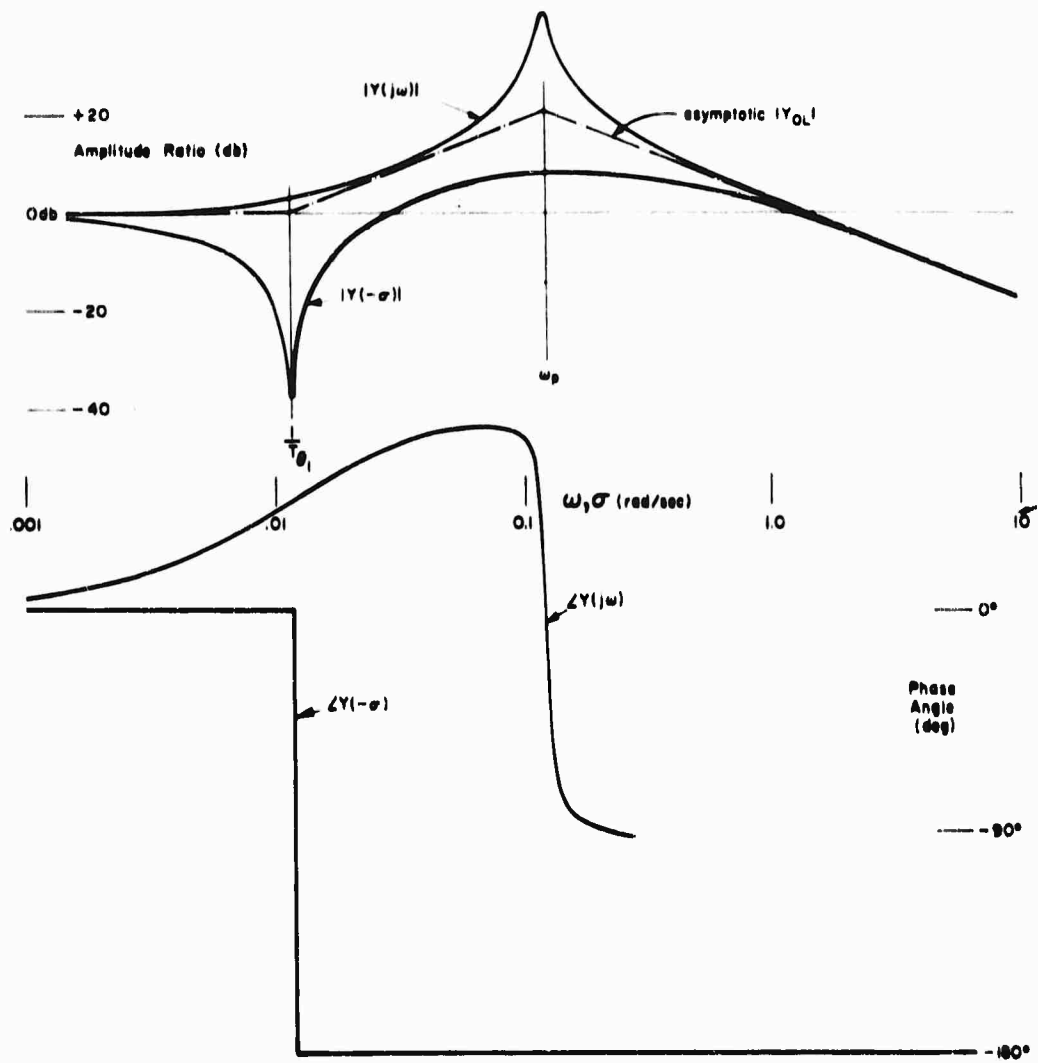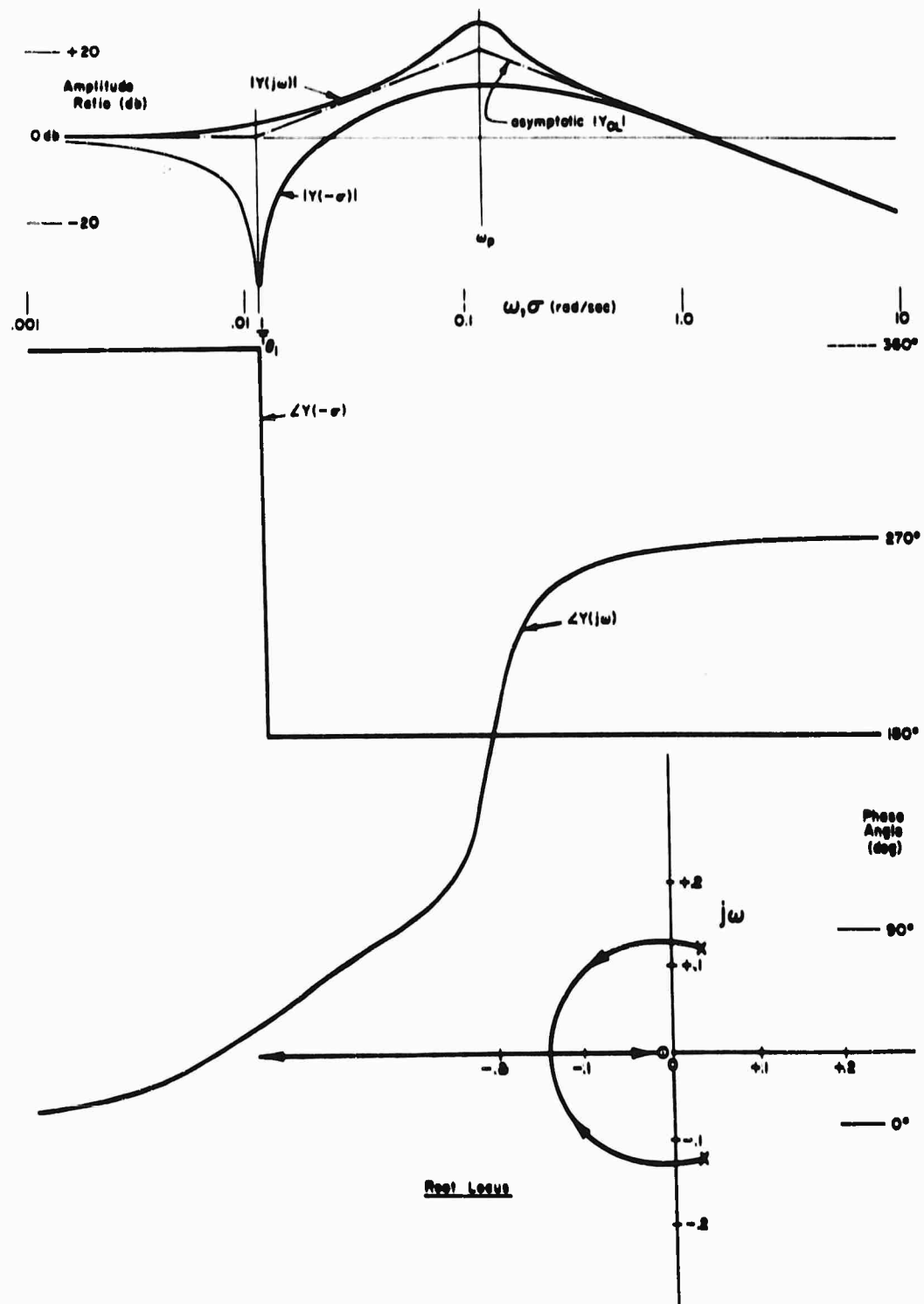
(b) $\zeta_p = 0.05$

FIGURE 41 (CONCLUDED)

FIGURE 42
SYSTEM SURVEY OF PHUGOID MODE WITH $\zeta_p = -0.22$

B. "TUCK" MODE

An airframe having a long time-constant divergence ("tuck") has the phugoid transfer form

$$Y_c = \frac{-K_c(T_{\theta_1}s + 1)}{(T_{p_1}s + 1)(-T_{p_2}s + 1)} \tag{30}$$

where, in general, $1/T_{\theta_1} = 1/T_{p_1} - 1/T_{p_2}$ and $1/T_{p_1} \doteq 1/T_{p_2}$ so that $1/T_{\theta_1}$ is very small with respect to either $1/T_{p_1}$ or $1/T_{p_2}$ (see the Appendix). A generic plot of a system having this form and these relative values of the time constants is shown in Figure 43. As in the preceding case, the stability criterion requires a gain greater than unity at 180 degrees of phase so a minimum value of (pure) pilot gain is required to stabilize the system ($K_pK_c \geq 1$). Because this minimum gain is much higher than that for the negatively damped phugoid case, it may become critical with regard to possible interference with the gains desired for good short period performance. The divergent "tuck" characteristic can therefore adversely influence short period performance by imposing gain restrictions; the nature of these restrictions will be explored in the following section. In the meantime it is pertinent to observe that, as in the phugoid cases, the pilot can easily control the "tuck" mode provided he gives it a large percentage of his attention. Presumably his opinion will deteriorate as the divergent time constant decreases and requires increasing attention on his part.

C. INTERACTION OF LOW FREQUENCY AND SHORT PERIOD MODES

The possible interference of the low frequency mode with the gains desired for good short period closures, although most apparent for the "tuck" case, exists in general for all cases. Consider the asymptotic amplitude Bodes of Figure 44 for the complete θ/δ_e transfer function. (For simplicity a nonequalized pilot is assumed.) Short period stability always requires that the gain be less than one (zero db) at $\omega \doteq \omega_{sp}$, which imposes a maximum allowable limit. As noted in the preceding section, unstable phugoids or "tucks" impose a minimum limit on the gain consistent with stabilizing such divergent low frequency modes. Additionally, considering the cardinal adjustment "rule" that requires good low frequency performance, the minimum total open loop gain at frequencies approaching zero must be at least one to insure adequate crossover, regardless of the period and damping of the low frequency mode. The resulting regions of probable gain are shown in Figure 44.

The maximum width of these regions, considering a minimum gain of unity and a maximum gain corresponding to crossover at ω_{sp} (see also Figure 45, Chapter VI), is given by (in linear rather than decibel measure)

$$\text{For } \frac{1}{T_{\theta_2}} < \omega_{sp} \; ; \; \frac{T_{\theta_1}T_{\theta_2}}{T_{p_1}T_{p_2}} \text{ or } T_{\theta_1}T_{\theta_2}\omega_p^2$$

$$\text{For } \frac{1}{T_{\theta_2}} > \omega_{sp} \; ; \; \frac{T_{\theta_1}}{T_{p_1}T_{p_2}\omega_{sp}} \text{ or } \frac{T_{\theta_1}}{\omega_{sp}}\omega_p^2$$
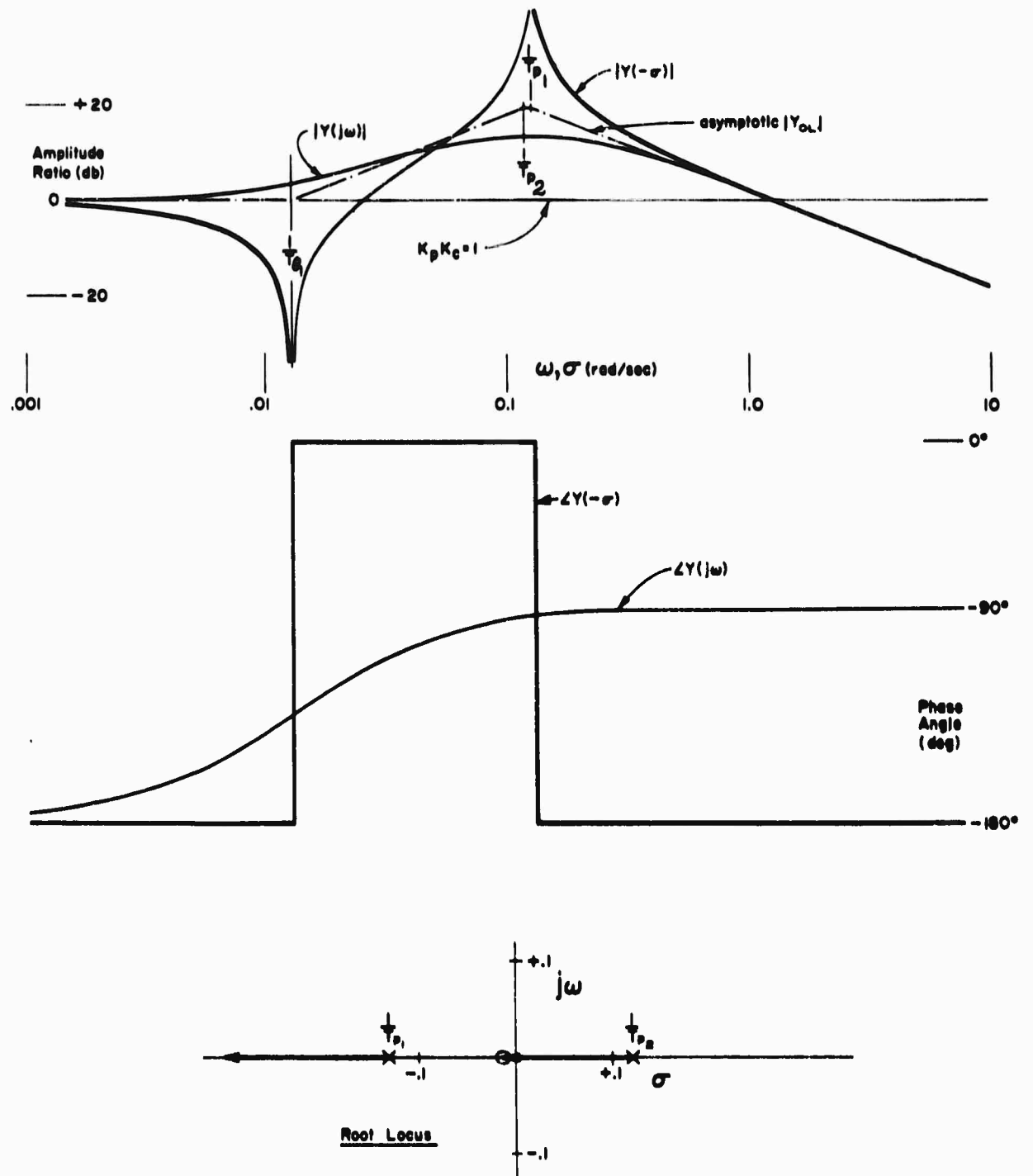
FIGURE 43
SYSTEM SURVEY OF DIVERGENT TUCK MODE

and a finite gain region requires that the absolute value of these ratios be less than one. Note that the second ratio is equal to the first multiplied by $1/T_{\theta_2}\omega_{sp}$ and that, when the second ratio applies, the value of this multiplicative factor is by definition greater than unity. The basic criterion is therefore that for $1/T_{\theta_2} < \omega_{sp}$ which becomes, in terms of the approximate relationships given in the Appendix,

$$\left| \frac{g}{U_o} \frac{Z_u - \dfrac{M_u Z_w}{M_w}}{\left(1 - \dfrac{Z_w M_q}{M_\alpha}\right)\left(Z_w X_u - X_w Z_u + \dfrac{Z_\delta}{M_\delta} X_w M_u\right)} \right| < 1 \tag{31}$$

It is simple to show that this required inequality may not be realized in quite common flight situations. In particular, if $C_{L_u} = C_{M_u} = 0$, implying that there are no power-on or Mach number effects influencing lift or pitching moments, Eq. (31) becomes, in terms of the aerodynamic derivatives,

$$\frac{1}{\left(1 + \dfrac{\rho S c C_{M_q} C_{L_\alpha}}{4mC_{M_\alpha}}\right)\left[\dfrac{C_{L_\alpha}}{C_L^2}\left(C_{D_o} - \dfrac{\partial C_D}{\partial C_L^2} C_L^2\right) + 1\right]} < 1 \tag{32}$$

Noting that for reasonable static margins, the second term in the first bracket is small with respect to one, it is clear that the criterion will not be met for conditions where, approximately,

$$\frac{\partial C_D}{\partial C_L^2} C_L^2 > C_{D_o} \tag{33}$$

This situation has previously been noted in Reference 17 as corresponding to a "performance reversal," i.e., dD/dU negative.
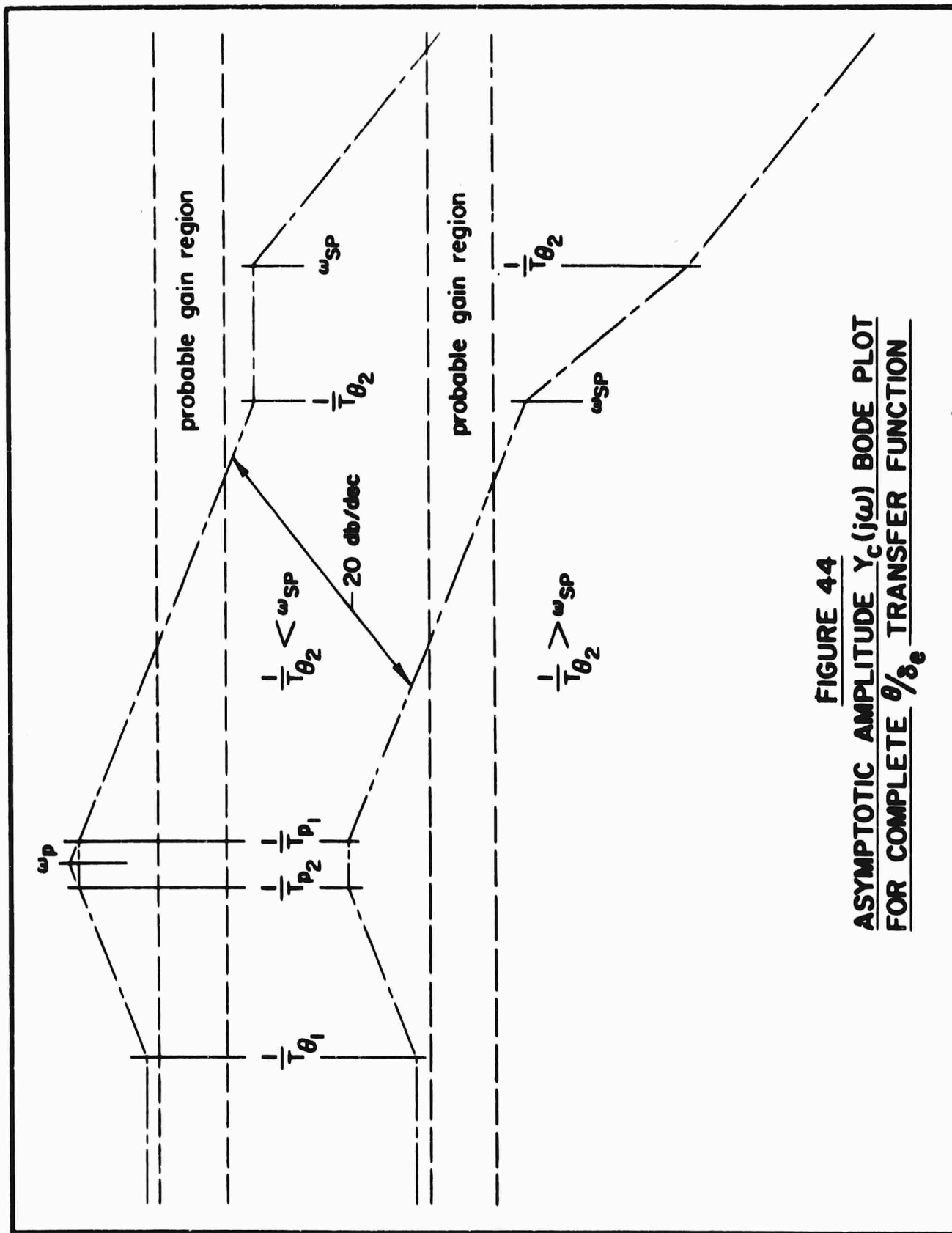
FIGURE 44

ASYMPTOTIC AMPLITUDE $Y_c(j\omega)$ BODE PLOT FOR COMPLETE θ/δ_e TRANSFER FUNCTION

CHAPTER VI

CONCLUSIONS

The analyses and correlations shown in this report combine previously unconnected research results into a unified longitudinal handling qualities theory for vehicles operating within the atmosphere. The total effort can be conveniently summarized under three major headings: (1) Description of the pilot as an opinion-generating (vocal) adaptive controller; (2) Establishment of a handling quality theory based upon vehicle-pilot system studies; and (3) Delineation of significant longitudinal handling quality parameters. Conclusions of this report relating to these topics are summarized in outline or tabular form below.

A. CONNECTION OF PILOT OPINION WITH PILOT MODEL

Recognizing that the term "pilot model" relates to the mathematical description of the pilot's dynamic behavior in closed loop control of a vehicle, it is clear that those factors which affect his opinion are also, strictly speaking, part of the pilot model. That is, the influences noted here can be considered to supplement the general rules regarding pilot adaptation and adjustment. As such they <u>are</u> a part of the pilot model. They are, however, separated here for convenience and emphasis.

1. Effect of Closed Loop Dynamics on Opinion

   a. For systems where a first or second order mode is an adequate approximate description of the closed loop dynamics, a necessary, but not sufficient, requirement for good opinion is

$$\omega_c > \omega_{co}$$

   b. For systems where first <u>and</u> second order modes are required to adequately approximate the dominant closed loop dynamics, an additional necessary, but not sufficient, requirement for good opinion is

$$\zeta_{CL} > .35$$

   c. Conditions where ω_c cannot be made greater than ω_{co} are associated with extreme efforts on the part of the pilot to overcome this deficiency, and with exceptionally nonlinear pilot response.

2. Effect of Pilot-Adopted Form on Opinion

   a. Best opinion, for a given open loop gain, always occurs when no pilot equalization is required (i.e., when $Y_p \doteq K_p e^{-\tau s}/T_N s + 1$). A well defined, although fairly broad, "best opinion" region exists for these nonequalized cases. This optimum region is a function of the manipulative device (restraining forces), muscle group used by the pilot, etc.

b. Configurations where pilot lead is required suffer a differential opinion change (from the nonequalized pilot case) proportional to T_L $dA/d\mu$.

c. Configurations where pilot lag is required result in a differential opinion degradation from the nonequalized pilot case.

B. ESTABLISHMENT OF A HANDLING QUALITIES THEORY

A complete, albeit rudimentary, theory for closed loop handling qualities has been formulated, and critically examined in the light of available experimental data. While all checks so far made indicate that the theory has a wide area of applicability, the actual limits of validity and/or modifications required for special circumstances have not yet been defined. Predictions based upon the theory have been made for conditions not yet examined in flight or simulator.

Typical steps involved in the analytical prediction of handling qualities for a new configuration involve:

1. Determination of the effective controlled element dynamics.

2. Estimation of the pilot-adopted describing function form.

3. Adjustment of parameters in the pilot describing function form consistent with all loop closure rules.

4. Estimation of the closed loop system dynamics, including the compatibility of $\omega_c > \omega_{co}$.

5. Estimation of differential opinion degradation from nonequalized pilot situations.

C. SIGNIFICANT LONGITUDINAL HANDLING QUALITIES PARAMETERS

Application of the theory to a variety of configurations has resulted in a fairly complete understanding of the vehicle parameters which are important in manual longitudinal control of "conventional" (i.e., not rotary wing, VTOL, etc.) aircraft. All of these parameters are connected directly with the vehicle transfer functions. In the longitudinal axis three equivalent-airframe transfer functions are required to characterize the controlled element for various closed loop tasks. These are θ/δ_e for attitude control, a_z/δ_e for situations where normal acceleration is controlled (e.g., fire control tracking and constant load factor pullups) and u/δ_e for control of long period trim or airspeed. Generic asymptotic Bode diagrams, which illustrate many of the parameters, for these three transfer functions are shown in Figures 45-47.

A summary of longitudinal handling quality parameters derived from considerations of the three equivalent-airframe transfer functions is given in Table VI. Most of these parameters have been discussed in this report, although a few items not discussed have been added to make the table complete.

FIGURE 45

GENERIC BODE DIAGRAM OF COMPLETE PITCH ATTITUDE TRANSFER FUNCTION FOR CONVENTIONAL AIRFRAME
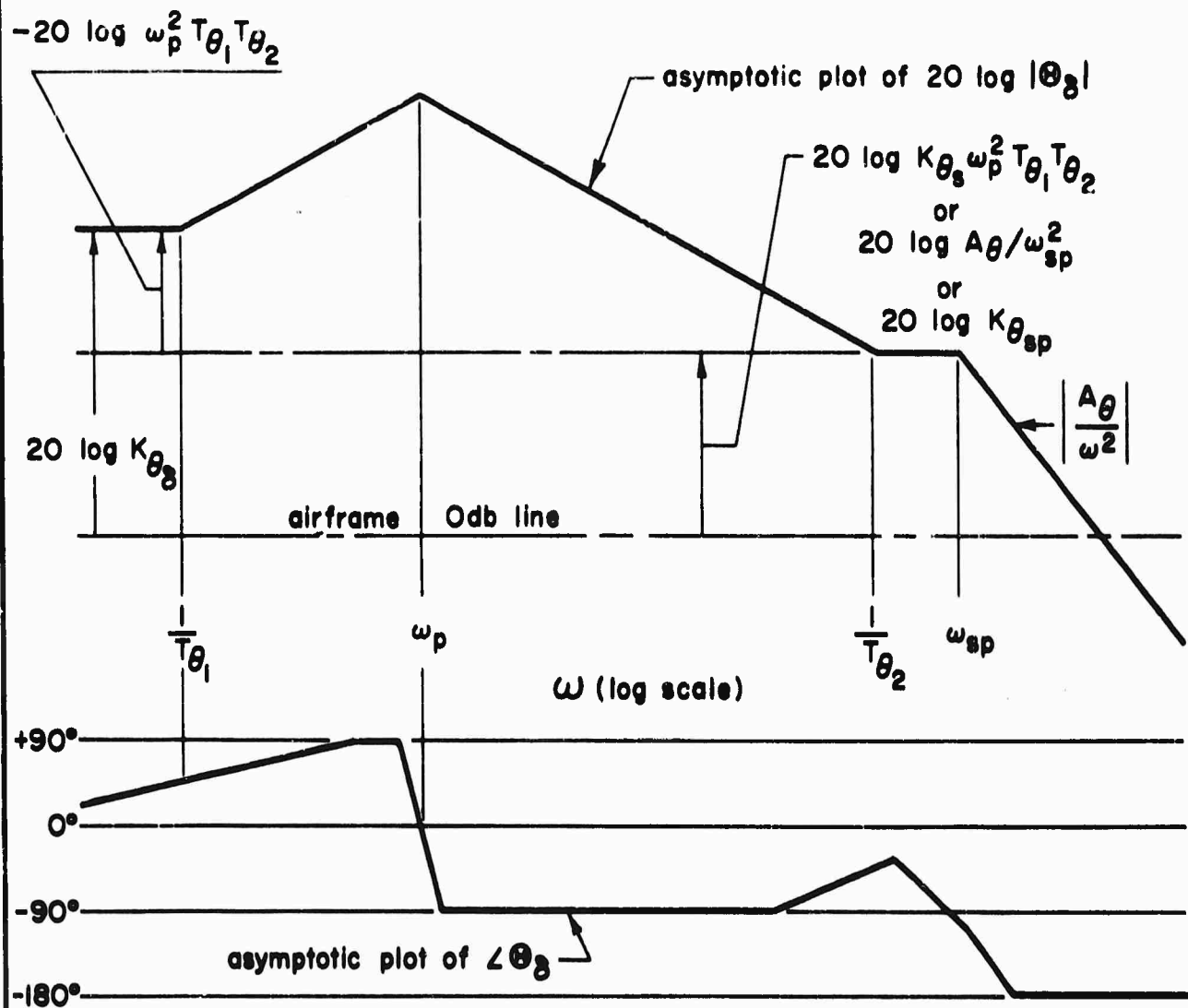
$$\Theta_\delta = \frac{\theta}{\delta_e} = \frac{A_\theta s^2 + B_\theta s + C_\theta}{(s^2 + 2\zeta_p \omega_p s + \omega_p^2)(s^2 + 2\zeta_{sp}\omega_{sp}s + \omega_{sp}^2)}$$

$$= \frac{K_{\theta_\delta}(T_{\theta_1}s + 1)(T_{\theta_2}s + 1)}{\left[\left(\frac{s}{\omega_p}\right)^2 + \frac{2\zeta_p s}{\omega_p} + 1\right]\left[\left(\frac{s}{\omega_{sp}}\right)^2 + \frac{2\zeta_{sp}s}{\omega_{sp}} + 1\right]}$$

FIGURE 46
GENERIC BODE DIAGRAM OF SHORT PERIOD NORMAL
ACCELERATION TRANSFER FUNCTION
FOR CONVENTIONAL AIRFRAME

$$A_{z\delta} = \frac{a_z}{\delta_e} = \frac{K_h (T_{h_2}s + 1)(-T_{h_3}s + 1)}{\left[\left(\frac{s}{\omega_{sp}}\right)^2 + \frac{2\zeta_{sp}s}{\omega_{sp}} + 1\right]}$$

$$K_h = \frac{A_h}{T_{h_2}T_{h_3}\omega_{sp}^2}$$

$$\omega_h = \sqrt{\frac{1}{T_{h_2}T_{h_3}}}$$

$$U_\delta = \frac{u}{\delta_e} = \frac{K_u' (T_{u_1} s + 1)}{\left[\left(\frac{s}{\omega_p}\right)^2 + \frac{2\zeta_p s}{\omega_p} + 1\right]}$$

FIGURE 47
GENERIC BODE DIAGRAM OF LONG PERIOD SPEED
TRANSFER FUNCTION FOR CONVENTIONAL AIRFRAME
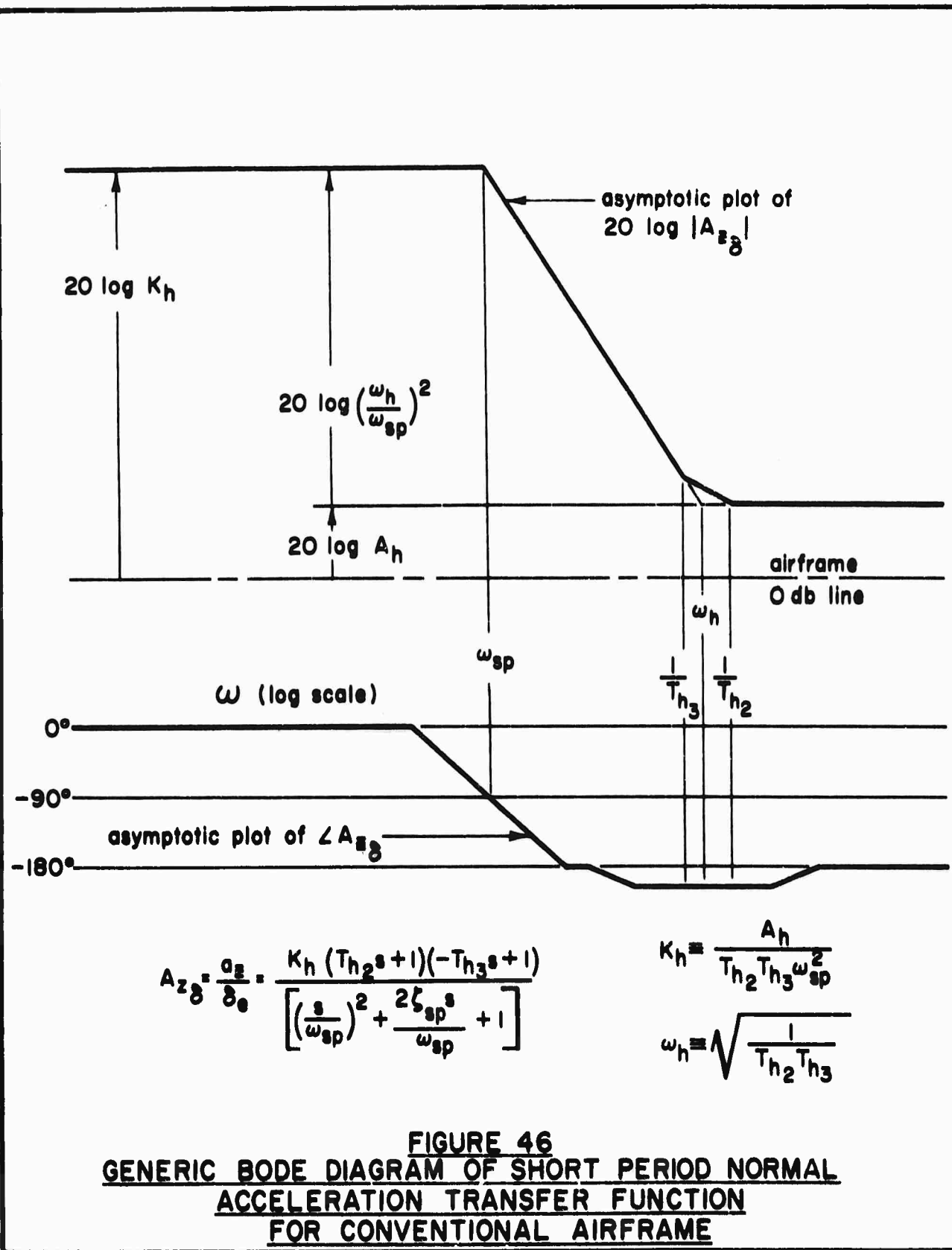
TABLE VI

SUMMARY OF SIGNIFICANT LONGITUDINAL DYNAMIC HANDLING QUALITY PARAMETERS

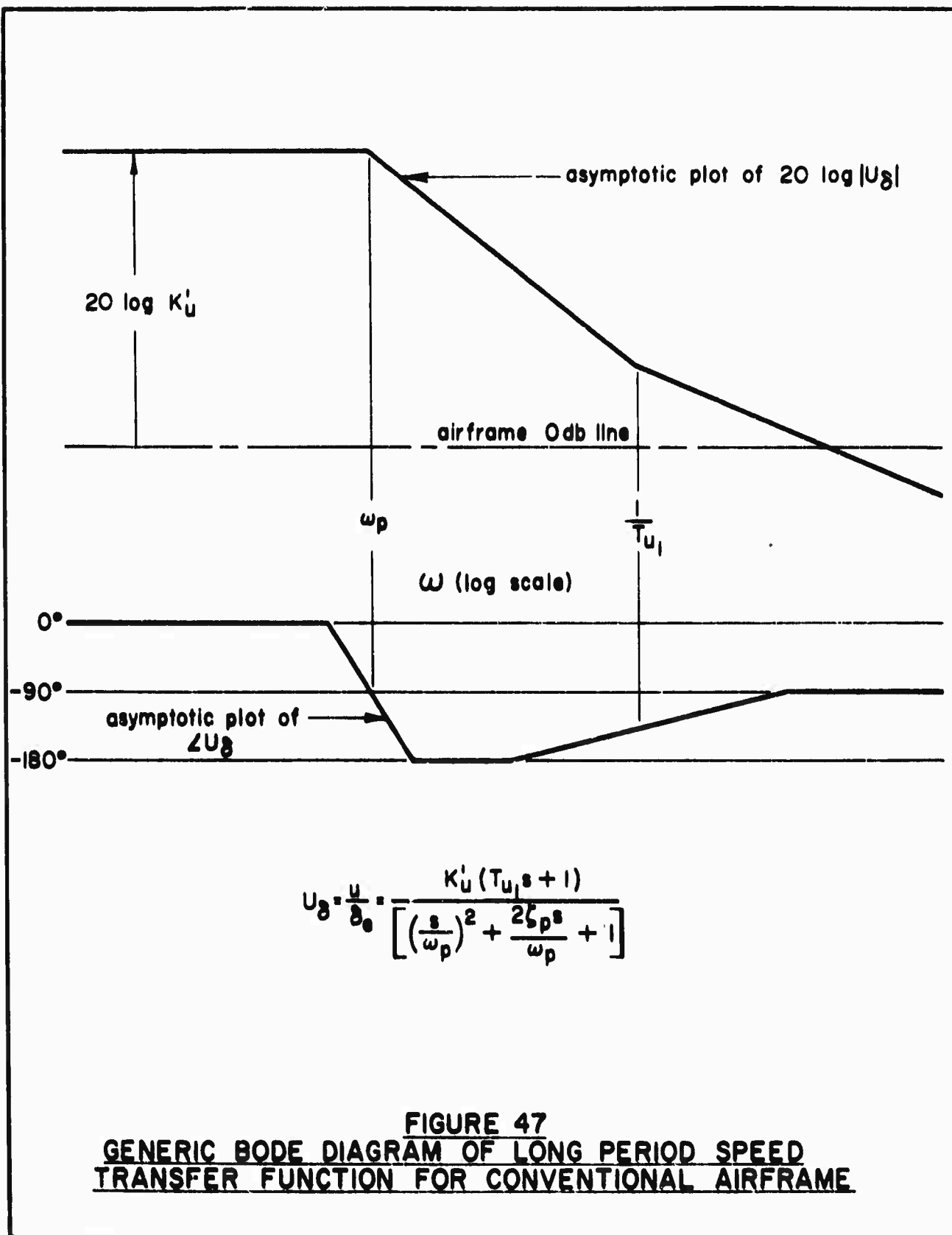|	Parameter	Approx. Value in Terms of Transfer Func. Quan.	Approximate Value in Terms of Stability Derivatives
Characteristic quantities derivable from homogeneous equations of motion	① Short period damping	ζ_{sp}	$\dfrac{-(M_q + M_{\dot\alpha} + Z_w)}{2\sqrt{M_q Z_w - M_\alpha}}$
	② Short period natural frequency	ω_{sp}	$\sqrt{M_q Z_w - M_\alpha}$
	③ Phugoid natural frequency	ω_p	$\sqrt{\dfrac{g}{U_o}\left[\dfrac{M_u}{M_w} Z_w - Z_u\right]}$
	④ Longitudinal divergence	$\dfrac{1}{T_{p_1}}$ $\dfrac{1}{T_{s_1}}$	$\dfrac{1}{T_{p_1}} - \dfrac{1}{T_{p2}} \doteq -X_u + \dfrac{M_u}{M_\alpha}(X_\alpha - g);$ $-\dfrac{1}{T_{p_1}T_{p_2}} \doteq -\dfrac{g}{U_o}\left(Z_u - \dfrac{M_u Z_w}{M_w}\right)$ $-\dfrac{1}{T_{s_1}} + \dfrac{1}{T_{s_2}} \doteq -(M_q + M_{\dot\alpha} + Z_w);$ $-\dfrac{1}{T_{s_1}T_{s_2}} \doteq M_q Z_w - M_\alpha$
Quan. derivable from complete eqs. of motion in attitude control tasks	⑤ Short period lead	$\dfrac{1}{T_{\theta_2}}$	$-Z_w + \dfrac{Z_\delta}{M_\delta} M_w \doteq -Z_w$
	⑥ Gain at short period break point	$\left(\dfrac{\partial\delta_e}{\partial F_s}\right)K_{\theta_{sp}}$	$\dfrac{\partial\delta_e}{\partial F_s}\dfrac{M_\delta}{\omega_{sp}^2} = -\dfrac{g/U_o}{\dfrac{\partial F_s}{\partial n}\left(Z_w - \dfrac{Z_\delta}{M_\delta}M_w\right)}$
	⑦ Static gain relative to gain at short period	$\dfrac{1}{\omega_p^2 T_{\theta_1} T_{\theta_2}}$	
Quan. derivable from short period eqs. of motion in load factor control tasks	⑧ Stick force per g $\partial F_s/\partial n$	$g\dfrac{\partial F_s}{\partial\delta_e}\left[\dfrac{\delta_e}{a_z}(s)\right]_{s=0}$	$-\dfrac{\partial F_s}{\partial\delta_e}\dfrac{\omega_{sp}^2}{M_\delta}\dfrac{g/U_o}{\left(Z_w - \dfrac{Z_\delta}{M_\delta}M_w\right)}$
	⑨ Z_δ effect	$\left(\dfrac{\omega_h}{\omega_{sp}}\right)^2$	$\dfrac{1 - \dfrac{M_\delta Z_\alpha}{Z_\delta M_\alpha}}{1 - \dfrac{M_q Z_w}{M_\alpha}}$
Quan. deriv. from long period eqs. of motion in speed tasks	⑩ Stick force per knot $\partial F_s/\partial u_k$		$1.69\dfrac{\partial F_s}{\partial\delta_e}\dfrac{U_o\omega_p^2}{gZ_\delta}\dfrac{1}{\left(1 - \dfrac{M_\delta Z_\alpha}{Z_\delta M_\alpha}\right)}$

General Effect(s) Measured	Remarks
	ζ_{sp} and ω_{sp} (with $\partial F_s/\partial n$ and $1/T_{\theta_2}$ fixed) are primary opinion quantities in short period control. ω_{sp} values limited by open loop response and controllability factors. ζ_{sp} is sole determinant of general time character of short period response. Influence of these two quantities on opinion, controllability, response, etc., has been thoroughly covered by flight, simulator, and analysis. Boundaries are well known and factors in opinion are well understood. Preferred values for "good" airframes are $\zeta \doteq 1/\sqrt{2}$ and $\omega_{sp} \doteq \pi$. These values are 'good' only when $1/T_{\theta_2}$ is near ω_{sp}.
	For normal vehicles ($\omega_p^2 > 0$, $\omega_p/\omega_{sp} < 1/20$) the factor is of little importance in handling qualities. When $\omega_p/\omega_{sp} > 1/20$, can create troublesome control difficulties. Has been thoroughly investigated in flight and by analysis.
	When C_{m_u} is principal cause of divergence, the mode is $1/T_{p_1}$, called "tuck." When C_{m_α} is principal cause of divergence, the mode is $1/T_{s_1}$, called "pitch-up." Maximum value is critical controllability parameter in longitudinal control. Preliminary analyses have been made. Flight and simulator studies are currently in process at NASA and CAL.
Lag between normal acceleration and pitching velocity in short period motions.	Has always been in a nearly optimum location to aid short period attitude control. In future aircraft, as Z_W becomes smaller, two effects will become dominant: (a) Pitching velocity and load factor responses will differ drastically. (b) Pilot behavior will be modified to avoid a "droop" characteristic. Also influences control of short time-constant divergence (Item 4). Essentially no coverage in either flight or simulator. Needs considerable effort, including investigation of the effects of positive Z_W (negative C_{L_α}).
Effective airframe sensitivity for attitude control.	Key factor in pitch attitude control by pilot. On normal airframe is usually satisfactory if $\partial F_s/\partial n$ is suitable. May be critical at low C_L's and on tailless configurations. Has not been studied directly in either flight or simulator.
Deg. of static attitude control available (d.c. gain for crossovers between $1/T_{\theta_2}$ and ω_{sp}).	Has not been recognized as a critical parameter in the past. Low speed situations (ω_p relatively large) will be most sensitive in this regard. Has not been studied in either flight or simulator. Better understanding is very desirable.
Effective airframe sensitivity	Fundamental short period control parameter. Has been thoroughly studied in flight and simulator. For center-stick fighters "good" values cluster about 8 lb/g.
Degree of dynamic load factor control available.	Values have been large in the past with no attendant problems except a minor one in open loop response. On future craft, with smaller Z_W and M_δ/Z_δ ratios, may become exceedingly important. Has not been studied. Needs considerable effort for special future configurations.
"Speed trim" sensitivity	Has been considered a key factor, both steady state (trim) and dynamic (tuck) for years. Detailed effects have not, however, been thoroughly studied.

The basic parameters are given both in terms of their approximate values as transfer function quantities and as stability derivative combinations (see the Appendix). The remarks column summarizes various points derived from analysis and/or flight test, and also indicates those items where future work is recommended.

Some of these parameters, for example Items 1, 2, 3, 8, and 10, may be considered classical. Others, such as Items 5 and 6, had values on past aircraft which were satisfactory if the classical items were satisfactory (although this same state of affairs may not be true in the future). Still others, such as Items 4 and 9, have been recognized as quantities which require attention, although little experimental work has been accomplished which show their detailed effects. Finally, parameters such as Items 7 and 9 (in the ω_h/ω_{sp} form) have not previously been considered.

REFERENCES

1. Krendel, E. S., and G. H. Barnes, Interim Report on Human Frequency Response Studies, WADC Technical Report 54-370, June 1954.

2. McRuer, D. T., and E. S. Krendel, Dynamic Response of Human Operators, WADC Technical Report 56-524, October 1957.

3. Hall, I. A. M., Effect of Controlled Element on the Human Pilot, WADC Technical Report 57-509, August 1958.

4. Seckel, E., I. A. M. Hall, D. T. McRuer, and D. H. Weir, Human Pilot Dynamic Response in Flight and Simulator, WADC Technical Report 57-520, October 1957.

5. Ashkenas, I. L., and D. T. McRuer, The Determination of Lateral Handling Quality Requirements from Airframe Human-Pilot System Studies, WADC Technical Report 59-135, June 1959.

6. Rathert, George A., Jr., Brent Y. Creer, and Joseph G. Douvillier, Jr., Use of Flight Simulators for Pilot-Control Problems, NASA Memorandum 3-6-59A, February 1959.

7. Brown, John L., and C. C. Collins, "Air-to-Air Tracking During Closed-Loop Centrifuge Operation," Aviation Medicine, November 1958, pp. 794-804.

8. Tustin, A., An Investigation of the Operator's Response to Manual Control of a Power Driven Gun, C. S. Memorandum No. 169, Metropolitan-Vickers Electrical Co., Ltd., Attercliffe Common Works, Sheffield, England, August 22, 1944.

9. Tustin, A., Notes on Manual Control of Guns Further to C. S. 169 and C. S. 184, C. S. Memorandum No. 203, Metropolitan-Vickers Electrical Co., Ltd., Attercliffe Common Works, Sheffield, England, April 4, 1945.

10. Tustin, A., The Choice of Response Characteristics for Controllers for Power Driven Guns, C. S. Memorandum No. 184, Metropolitan-Vickers Electrical Co., Ltd., Attercliffe Common Works, Sheffield, England, October 10, 1944.

11. Tustin, A., "The Nature of the Operator's Response in Manual Control and Its Implications for Controller Design," Journal of the I.E.E., Vol. 94, Part IIA, No. 2, 1947.

12. Russell, L., Characteristics of the Human as a Linear Servo-Element, M. S. Thesis, Massachusetts Institute of Technology, May 18, 1951.

13. Human Dynamic Study, Goodyear Aircraft Corporation, Report No. GER-4750, April 8, 1952.

14. Investigation of Control "Feel" Effects on the Dynamics of a Piloted Aircraft System, Goodyear Aircraft Corporation, Report No. GER-6726, April 25, 1955.

15. Elkind, J. I., *Characteristics of Simple Manual Control Systems*, Massachusetts Institute of Technology, Lincoln Laboratory, Report No. 111, April 6, 1956.

16. McRuer, D. T., and E. S. Krendel, "The Human Operator as a Servo System Element," *Journal of the Franklin Institute*, Vol. 267, Nos. 5 and 6, May and June 1959.

17. Ashkenas, I. L., and D. T. McRuer, *Approximate Airframe Transfer Functions and Application to Single Sensor Control Systems*, WADC Technical Report 58-82, June 1958.

18. Newell, F., and G. Campbell, *Flight Evaluations of Variable Short-Period and Phugoid Characteristics in a B-26*, WADC Technical Report 54-594, December 1954.

19. Harper, R. P., Jr., *Flight Evaluations of Various Longitudinal Handling Qualities in a Variable-Stability Jet Fighter*, WADC Technical Report 55-299, July 1955.

20. Chalk, C. R., *Additional Flight Evaluations of Various Longitudinal Handling Qualities in a Variable-Stability Jet Fighter*, WADC Technical Report 57-719, Part II, July 1958.

21. Cooper, G. E., "Understanding and Interpreting Pilot Opinion," *Aeronautical Engineering Review*, Vol. 16, No. 3, March 1957.

22. Newell, F., and D. W. Rhoads, *Flight Evaluation of Variable Phugoid Damping in a JTB-26B Airplane*, WADC Technical Report 56-223, December 1956.

AIRFRAME TRANSFER FUNCTIONS

As shown in Reference 17, the longitudinal dynamic characteristics of an airframe can be represented adequately by two separate sets of simplified equations of motion. The first of these, involving predominantly attitude and normal acceleration changes, is the classical two-degree-of-freedom short period set of equations. The longer period phenomena, which include both the classical phugoid oscillation and the more novel tuck divergence, require the consideration of a simplified three-degree-of-freedom set of equations. Consequently, the airframe motions of importance in long period phenomena include changes in forward speed in addition to attitude and normal acceleration. Most piloting tasks of interest for longitudinal control involve stabilization of vehicle attitude and velocity. In special circumstances, such as constant load factor pullups and fire control tracking (with certain types of fire control systems), the closed loop system can also involve direct control of normal acceleration. Each of these motion quantities is either inherently or especially presented to the pilot in display form so that visual modality can be of paramount interest in their control.

The controlled element transfer function characteristics of general interest to the longitudinal control problem are summarized (from Reference 17) as to form and relative pole-zero values as follows.

A. SHORT PERIOD — Basic Assumption: Forward speed remains constant, i.e., $u = 0$

   1. Attitude Transfer Function

$$\frac{\theta}{\delta_e} = \frac{A_\theta}{T_{\theta_2}\omega_{sp}^2} \frac{(T_{\theta_2}s + 1)}{s\left(\frac{s^2}{\omega_{sp}^2} + \frac{2\zeta_{sp}}{\omega_{sp}}s + 1\right)}$$

$$\text{or} \qquad\qquad\qquad\qquad\qquad\qquad\qquad (A-1)$$

$$\frac{A_\theta}{T_{\theta_2}\left(-\frac{1}{T_{s_1}T_{s_2}}\right)} \frac{(T_{\theta_2}s + 1)}{s(-T_{s_1}s + 1)(T_{s_2}s + 1)}$$

In terms of stability derivatives:

$$A_\theta = M_\delta + M_{\dot{w}}Z_\delta \doteq M_\delta \qquad\qquad\qquad ; \text{ assumes } |M_{\dot{w}}Z_\delta| \ll |M_\delta|$$

$$\frac{1}{T_{\theta_2}} \doteq \frac{M_w Z_\delta - M_\delta Z_w}{M_\delta + M_{\dot{w}}Z_\delta} \doteq -Z_w + \frac{Z_\delta}{M_\delta}M_w \quad ; \text{ assumes } |M_{\dot{w}}Z_\delta| \ll |M_\delta|$$

$$\qquad\qquad \doteq -Z_w \qquad\qquad\qquad\qquad ; \text{ assumes } \left|\frac{Z_\delta}{M_\delta}M_w\right| \ll |Z_w|$$

$$\omega_{sp}^2 = -\frac{1}{T_{s_1}}\frac{1}{T_{s_2}} \doteq M_q Z_w - M_\alpha \qquad\qquad\qquad (A-2)$$

$$2(\zeta\omega)_{sp} = -\frac{1}{T_{s_1}} + \frac{1}{T_{s_2}} \doteq -(M_q + M_{\dot{\alpha}} + Z_w)$$

$$K_\theta \equiv \frac{A_\theta}{T_{\theta_2}\omega_{sp}^2} \equiv -\frac{A_\theta T_{s_1}T_{s_2}}{T_{\theta_2}} \doteq \frac{M_w Z_\delta - M_\delta Z_w}{M_q Z_w - M_\alpha}$$

2. Vertical Acceleration Transfer Function

$$\frac{a_z}{\delta_e} = -\frac{A_h \omega_h^2}{\omega_{sp}^2} \frac{\left(\dfrac{s^2}{\omega_h^2} + \dfrac{2\zeta_h}{\omega_h} s + 1\right)}{\left(\dfrac{s^2}{\omega_{sp}^2} + \dfrac{2\zeta_{sp}}{\omega_{sp}} s + 1\right)} \qquad \text{for forward control}^*$$

or   (A-3)

$$\frac{A_h}{T_{h_2} T_{h_3} \omega_{sp}^2} \frac{(T_{h_2}s + 1)(-T_{h_3}s + 1)}{\left(\dfrac{s^2}{\omega_{sp}^2} + \dfrac{2\zeta_{sp}}{\omega_{sp}} s + 1\right)} \qquad \text{for aft control}^*$$

In terms of stability derivatives:

$$A_h = -Z_\delta$$

$$\omega_h^2 = -\frac{1}{T_{h_2}} \frac{1}{T_{h_3}} \doteq -M_\alpha + \frac{Z_\alpha}{Z_\delta} M_\delta \doteq \frac{Z_\alpha}{Z_\delta} M_\delta \; ; \; \text{assumes} \left|\frac{Z_\delta}{M_\delta} M_w\right| \ll \left|Z_w\right|$$

(A-4)

$$2(\zeta\omega)_h = \frac{1}{T_{h_2}} - \frac{1}{T_{h_3}} \doteq -(M_q + M_{\dot\alpha})$$

$$K_h \equiv -\frac{A_h \omega_h^2}{\omega_{sp}^2} \equiv \frac{A_h}{T_{h_2} T_{h_3} \omega_{sp}^2} \doteq \frac{M_\delta Z_\alpha - M_\alpha Z_\delta}{M_q Z_w - M_\alpha}$$

Additionally, for aft control:

$$\frac{1}{T_{h_2}} \doteq -\frac{(M_q + M_{\dot\alpha})}{2} + \sqrt{-\frac{Z_\alpha}{Z_\delta} M_\delta}$$

(A-5)

$$\left|\frac{1}{T_{h_3}}\right| \doteq +\frac{(M_q + M_{\dot\alpha})}{2} + \sqrt{-\frac{Z_\alpha}{Z_\delta} M_\delta}$$

---

*Both denominators can also assume the second form shown for θ/δ_e.

3. Relative Pole-Zero Values

$$\frac{1}{T_{\theta 2}} < 2(\zeta\omega)_{sp}, \text{ from Eqs. (A-2)}$$

$$< \omega_{sp} \text{ for } \zeta < 0.5$$

$$\frac{\omega_h^2}{\omega_{sp}^2} \doteq - \frac{Z_\alpha M_\delta}{Z_\delta M_\alpha}, \text{ from Eqs. (A-2) and (A-4); assumes } |M_q Z_w| \ll |M_\alpha|$$

$$\doteq - \frac{C_{L\alpha}}{C_{M\alpha}} \frac{C_{M\delta}}{C_{L\delta}} \doteq - \frac{x_t}{x_{ac}}$$ where tail length, x_t, and distance to aerodynamic center, x_{ac}, are both measured from the c.g. positive forward; for static stability $x_{ac} < 0$. Accordingly,

$$\omega_h > \omega_{sp} \quad \text{or alternatively} \quad \frac{1}{T_{h2}} > \frac{1}{T_{h3}} \gg \omega_{sp}$$

4. Pitching Velocity: Vertical Acceleration Transfer Function

$$\frac{\dot{\theta}}{a_z} = \frac{A_\theta(s + \frac{1}{T_{\theta 2}})}{\underbrace{-A_h(s^2 + 2\zeta_h\omega_h s + \omega_h^2)}}$$

or   (A-6)

$$(s + \frac{1}{T_{h2}})(s - \frac{1}{T_{h3}})$$

From the general relative pole-zero values noted above, it is clear that for frequencies of the order of short period the denominator dynamics will be negligible, i.e., $|s^2 + 2\zeta_h\omega_h s|_{s=j\omega_{sp}} \ll \omega_h^2$ or $|s|_{s=j\omega_{sp}} \ll 1/T_{h2}, 1/T_{h3}$. Then,

$$\frac{\dot{\theta}}{a_z} \doteq \frac{A_\theta \frac{1}{T_{\theta 2}} (T_{\theta 2}s + 1)}{\underbrace{-A_h\omega_h^2}}$$

or   (A-7)

$$A_h \frac{1}{T_{h2}T_{h3}}$$

or, substituting the derivative expressions,

$$\frac{\dot{\theta}}{a_z} \; : \; \frac{-M_\delta Z_w(T_{\theta_2}s + 1)}{Z_\delta \dfrac{U_o Z_w}{Z_\delta} M_\delta} \; : \; -\frac{T_{\theta_2}s + 1}{U_o} \tag{A-8}$$

5. Stick Force Per g in Steady Maneuvers

The steady state stick force per g, considering only the short period mode, is

$$\frac{\partial F_s}{\partial n} \; = \; g\,\frac{\partial F_s}{\partial \delta_e}\left[\frac{\delta_e(s)}{a_z(s)}\right]_{s=0} \; = -\frac{\partial F_s}{\partial \delta_e}\frac{g\,\omega_{sp}^2}{M_\delta\left(Z_\alpha - \dfrac{Z_\delta M_\alpha}{M_\delta}\right)} \tag{A-9}$$

Relating this to the attitude gain at short period, $K_{\theta_{sp}} = M_\delta/\omega_{sp}^2$, discussed in Chapter IV, Section D,

$$\frac{\partial F_s}{\partial n} \; = -\frac{\partial F_s}{\partial \delta_e}\frac{g}{K_{\theta_{sp}}}\frac{1}{\left(Z_\alpha - \dfrac{Z_\delta M_\alpha}{M_\delta}\right)}$$

or, in terms of the basic aerodynamic parameters,

$$: \; \frac{\dfrac{\partial F_s}{\partial \delta_e}}{K_{\theta_{sp}}}\left(\frac{C_L}{C_{L_\alpha} - \dfrac{C_{M_\alpha}}{C_{M_\delta}}C_{L_\delta}}\right) \tag{A-10}$$

For conventional airplanes with "constant" stick force per g, $\partial F_s/\partial\delta_e$ is proportional to the dynamic pressure, C_L is of course inversely proportional to dynamic pressure, and the remaining aerodynamic parameters are constant. Thus, $\partial F_s/\partial n$ = constant/$K_{\theta_{sp}}$ and a constant stick force per g also implies then a constant effective attitude control gain, $K_{\theta_{sp}}$. In turn, a constant $K_{\theta_{sp}}$ will (exclusive of other dynamic effects) call for a fixed pilot gain, K_p. Thus, a "good" stick force per g, a "good" $K_{\theta_{sp}}$, and a "good" K_p are all different ways of saying the same thing.

B. LONG PERIOD — Basic Assumption: $\left|(s - M_q)q\right| \ll \left|M_\alpha\alpha + M_u u\right|$

   1. Attitude Transfer Function (for frequencies $\ll 1/T_{\theta_2}$)

$$\frac{\theta}{\delta_e} = \frac{A_\theta'}{T_{\theta_1}\omega_p^2} \frac{(T_{\theta_1}s + 1)}{\left(\dfrac{s^2}{\omega_p^2} + \dfrac{2\zeta_p}{\omega_p}s + 1\right)}$$

or   (A-11)

$$\frac{A_\theta'}{T_{\theta_1}\left(-\dfrac{1}{T_{p_1}T_{p_2}}\right)} \frac{(T_{\theta_1}s + 1)}{(-T_{p_1}s + 1)(T_{p_2}s + 1)}$$

In terms of stability derivatives:

$$A_\theta' \doteq \frac{M_\delta Z_w}{M_\alpha}$$

$$\frac{1}{T_{\theta_1}} \doteq -X_u + X_w\left(\frac{Z_\delta M_u - M_\delta Z_u}{Z_\delta M_w - M_\delta Z_w}\right)$$

$$\doteq -X_u - \frac{X_w}{Z_w}\frac{Z_\delta}{M_\delta}\left(M_u - \frac{M_\delta}{Z_\delta}Z_u\right) ; \quad \text{assumes } \left|\frac{Z_\delta}{M_\delta}M_w\right| \ll \left|Z_w\right| \tag{A-12}$$

$$\omega_p^2 = -\frac{1}{T_{p_1}}\frac{1}{T_{p_2}} \doteq -\frac{g}{U_o}\left(Z_u - \frac{M_u Z_w}{M_w}\right) \doteq -\frac{\dfrac{g}{U_o}\left(Z_u - \dfrac{M_u Z_w}{M_w}\right)}{1 - \dfrac{Z_w M_q}{M_\alpha}}\left(\begin{matrix}\text{More general}\\\text{approximation}\end{matrix}\right)$$

$$2(\zeta\omega)_p = \frac{1}{T_{p_1}} - \frac{1}{T_{p_2}} \doteq -X_u + \frac{M_u}{M_\alpha}(X_\alpha - g)$$

$$K_\theta' \equiv \frac{A_\theta'}{T_{\theta_1}\omega_p^2} \equiv -\frac{A_\theta'T_{p_1}T_{p_2}}{T_{\theta_1}} \doteq \frac{M_\delta(X_u Z_w - X_w Z_u) + Z_\delta X_w M_u}{g(M_w Z_u - M_u Z_w)}$$

2. Velocity Transfer Function

$$\frac{u}{\delta_e} = \frac{A_u'}{T_{u_1}\omega_p^2} \frac{(T_{u_1}s + 1)}{\left(\frac{s^2}{\omega_p^2} + \frac{2\zeta_p}{\omega_p} s + 1\right)}$$

or   (A-13)

$$\frac{-A_u'}{T_{u_1}\left(\frac{1}{T_{p_1}T_{p_2}}\right)} \frac{(T_{u_1}s + 1)}{(-T_{p_1}s + 1)(T_{p_2}s + 1)}$$

In terms of stability derivatives:

$$A_u' \doteq -\frac{M_\delta(X_\alpha - g)}{M_\alpha}$$

$$\frac{1}{T_{u_1}} \doteq -\frac{gZ_\delta\left(M_w - \frac{M_\delta}{Z_\delta} Z_w\right)}{M_\delta(X_\alpha - g)}$$

(A-14)

$$\doteq \frac{gZ_w}{(X_\alpha - g)} \quad ; \quad \text{assumes} \left|\frac{Z_\delta}{M_\delta} M_w\right| \ll |Z_w|$$

$$K_u' \equiv \frac{A_u'}{T_{u_1}\omega_p^2} \equiv -\frac{A_u'T_{p_1}T_{p_2}}{T_{u_1}} \doteq \frac{M_\delta Z_w}{M_w Z_u - M_u Z_w}$$

3. Relative Pole-Zero Values

$\frac{1}{T_{\theta_1}}$ Of same order of magnitude as $2(\zeta\omega)_p$ or $\frac{1}{T_{p_1}} - \frac{1}{T_{p_2}}$; can be larger or smaller

$\frac{1}{T_{u_1}}$ Always roughly the same as $(\zeta\omega)_{sp}$; can be larger or smaller